

S

Protective Equipment

Studies and Research Projects



REPORT R-753



Needlestick Resistance of Protective Gloves

Development of a Test Method

*Toan Vu-Khanh
Patricia Dolez
C. Thang Nguyen
Chantal Gauvin
Jaime Lara*





Established in Québec since 1980, the Institut de recherche Robert-Sauvé en santé et en sécurité du travail (IRSST) is a scientific research organization known for the quality of its work and the expertise of its personnel.

OUR RESEARCH *is working for you !*

Mission

To contribute, through research, to the prevention of industrial accidents and occupational diseases as well as to the rehabilitation of affected workers.

To offer the laboratory services and expertise necessary for the activities of the public occupational health and safety prevention network.

To disseminate knowledge, and to act as scientific benchmark and expert.

Funded by the Commission de la santé et de la sécurité du travail, the IRSST has a board of directors made up of an equal number of employer and worker representatives.

To find out more

Visit our Web site for complete up-to-date information about the IRSST. All our publications can be downloaded at no charge.

www.irsst.qc.ca

To obtain the latest information on the research carried out or funded by the IRSST, subscribe to *Prévention au travail*, the free magazine published jointly by the IRSST and the CSST.

Subscription: 1-877-221-7046

Legal Deposit

Bibliothèque et Archives nationales du Québec
2012

ISBN: 978-2-89631-638-0 (PDF)

ISSN: 0820-8395

IRSST – Communications and Knowledge
Transfer Division
505 De Maisonneuve Blvd. West
Montréal, Québec
H3A 3C2

Phone: 514 288-1551

Fax: 514 288-7636

publications@irsst.qc.ca

www.irsst.qc.ca

© Institut de recherche Robert-Sauvé
en santé et en sécurité du travail,
October 2012

Protective Equipment

Studies and Research Projects

REPORT R-753

Needlestick Resistance of Protective Gloves Development of a Test Method

Disclaimer

The IRSST makes no guarantee regarding the accuracy, reliability or completeness of the information contained in this document. Under no circumstances shall the IRSST be held liable for any physical or psychological injury or material damage resulting from the use of this information.

Note that the content of the documents is protected by Canadian intellectual property legislation.

*Toan Vu-Khanh, Patricia Dolez, C. Thang Nguyen
École de technologie supérieure*

*Chantal Gauvin
Mechanical and Physical Risk Prevention, IRSST*

*Jaime Lara
IRSST*

Clic Research
www.irsst.qc.ca



This publication is available free of charge on the Web site.

This study was financed by the IRSST. The conclusions and recommendations are those of the authors.
This publication has been translated; only the original version (R-711) is authoritative.

IN CONFORMITY WITH THE IRSST'S POLICIES

The results of the research work published
in this document have been peer-reviewed.

ACKNOWLEDGMENTS

This study would not have been possible without the active participation of the members of the monitoring committee, including (in alphabetical order) Serge Bourgon, Louis Bousquet, Pierre Brassard, H el ene Brochu, Denis C ot e, Diane C ot e, St ephane Gauthier, Paul Imbeault, Sylvain Lallier, Lizette Larouche, Christiane Leblond, St ephane Lemaire, Michel Martin, Marc Ouellet, Charles Plante, Denis Poissant, Sylvie Poulin, S ebastien Talbot, Beno t Traversy, Denise Truchon and Claude Vaudreuil. Thank you all for your enthusiasm, your questions, your comments and your suggestions.

We also benefited from substantial support from glove manufacturers and distributors, who supplied us free of charge with the samples we needed for testing: in alphabetical order, Ansell, Best Glove Manufacturing, Hakson Gloves & Safety Wears Inc., Hatch Corporation, HexArmor, Marigold Industrial, Masley Enterprises Inc., North Safety Products, Seattle Marine and Fishing Supply Co., Superior Glove Works and Warwick Mills. Many thanks for your continued support for our research.

Lastly, the authors wish to underscore the involvement and contributions of the following people to the findings presented here: IRSSST technician Pierre Drouin, IRSSST trainees Jean-Fran ois Bernard and Daniel Robinson, and  ETS students Gbeuli Guero and AbdelKarim Kazan.

ABSTRACT

Needlestick injury is a hazard faced by a growing number of workers. In addition to other hazard-reduction strategies, including engineering technology initiatives and administrative measures, protective clothing, especially needlestick-resistant gloves, must be made available to these workers.

This study was conducted in response to joint requests to identify gloves that afford adequate needlestick protection. The requests were made by two sector-based associations—the APSAM (municipal affairs) and the APSSAP (provincial affairs)—and three associations whose members are exposed to needlestick hazards—police officers, correctional services officers and blue-collar workers. The lack of standard test methods for characterizing the needlestick resistance of gloves makes it very difficult to identify the best gloves available. The National Institute of Justice (NIJ), which issues recommendations on protective gloves for correctional services officers and police officers in the United States, and Committee F-23 of the American Society for Testing and Materials (ASTM), have made this question one of their priorities. The objective of this study was to continue the work on puncture resistance begun in an earlier project and to develop a test method for characterizing needlestick resistance. Preliminary work was also done to assess puncture resistance that takes the effect of the hand wearing the glove into consideration. Lastly, the effect on dexterity, tactile sensitivity and comfort of the most needlestick-resistant gloves was examined in the occupational groups considered in this study. Those results will be presented in another research report.

The study confirmed that needlesticks are different from punctures by standard probes, with respect both to fracture mechanism and force levels measured. While puncture by standard probes is governed by the maximum rate of strain of the material, needlesticks include a large measure of cutting and friction because of the cutting edge at the tip of the needle. The influence of needle characteristics (dimensional tolerances, wear, diameter, tip angle and number of facets), test material properties (thickness, type and hardness) and experimental conditions (probe velocity, angle of attack, temperature and humidity) on the force measuring needlestick resistance was studied for a series of materials representative of different types of protective gloves (elastomers, coated fabrics, SuperFabric[®] and TurtleSkin[®]).

Based on these results, a method for measuring the needlestick resistance of glove materials was developed and used to test a series of commercially available protective gloves. This report includes recommendations regarding the best gloves to use for a given purpose.

CONTENTS

ACKNOWLEDGMENTS	I
ABSTRACT	III
1. INTRODUCTION	1
1.1 Importance.....	1
1.2 Origin of Occupational Health and Safety Problem.....	2
1.3 Scientific and Technical Importance of Study	3
1.4 Goal and Specific Objectives of Study	6
2. EXPERIMENTAL METHODS.....	7
2.1 Materials	7
2.2 Measurement of Needlestick Resistance of Glove Materials.....	8
2.2.1 Free-Form Deformation Test Setup	9
2.2.2 FFD Test Setup with Prestressed Material	9
2.2.3 Test Setup with Support Blocks	10
2.2.4 Standard Needles and Probes	11
2.2.5 Operating Conditions for Testing Protective Materials	12
2.2.6 Measurement Method Used to Characterize Needlestick Resistance of Protective Gloves	13
2.3 Puncture Resistance Measurement	15
2.4 Cut Resistance Measurement.....	15
3. RESULTS	17
3.1 Analysis of Fracture Mechanism Involved in Needlesticks.....	17
3.1.1 Comparison of Puncture by Standard Probes and Needlesticks.....	17
3.1.2 Description of Needlestick Process	18
3.1.3 Parameters Governing Needlestick Mechanism.....	20
3.1.4 Calculation of Fracture Energy of Rubber Associated with Needlesticks	21
3.2 Effect of Needle Characteristics.....	22
3.2.1 Effect of Variability in Needle Manufacture.....	22
3.2.2 Effect of Needle Wear	24
3.2.3 Effect of Needle Diameter.....	27
3.2.4 Effect of Needle Tip Angle	30
3.2.5 Effect of Number of Facets	31

3.3	Effect of Sample	32
3.3.1	Effect of Type of Material.....	33
3.3.2	Effect of Size of Hole of Sample Holder	35
3.3.3	Effect of Sample Thickness.....	36
3.3.4	Effect of Material Hardness	37
3.4	Effect of Experimental Conditions	38
3.4.1	Effect of Probe Velocity.....	38
3.4.2	Effect of Angle of Attack.....	42
3.4.3	Effect of Temperature	46
3.4.4	Effect of Humidity.....	50
3.4.5	Effect of Lubricants.....	52
3.5	Effect of Prestress.....	54
3.6	Effect of Support Simulating a Hand	56
3.7	Glove Performance	59
3.7.1	Needlestick Resistance	59
3.7.2	Puncture Resistance.....	61
3.7.3	Cut Resistance	63
4.	DISCUSSION	65
4.1	Comparison of Glove Resistance Measured Using Hypodermic Needle Test Method and Standard Puncture and Cutting Test Methods	65
4.2	Analysis of Behaviour of Materials with Respect to Needlesticks	66
4.3	Selecting Gloves for Protection Against Needlesticks.....	67
5.	CONCLUSION.....	69
6.	RECOMMENDATIONS	71
	BIBLIOGRAPHY.....	73
	APPENDIX A: GLOVE MODELS TESTED	79
	APPENDIX B: PARAMETERS GOVERNING NEEDLESTICK MECHANISM	81
	APPENDIX C: CALCULATION OF NEEDLESTICK FRACTURE ENERGY	85
C.1	Principle of Approach	85
C.2	Calculation of Prestretch Energy.....	87
C.3	Needlestick Fracture Energy	91
	APPENDIX D: GLOVE TEST RESULTS.....	95

TABLES

Table 1 – Characteristics of medical needles used	12
Table 2 – Conditions of measurement method used to characterize needlestick resistance of protective gloves	14
Table 3 – Maximum force and displacement values for puncture by conical probe A of ASTM standard F1342-05 and by a 23G needle, for three thicknesses of neoprene, at a probe velocity of 100 mm/min (standard deviation in parentheses).....	18
Table 4 – Fracture energy values associated with puncture by 23G medical needles, cutting and tearing of neoprene and nitrile	22
Table 5 – Puncture force values and dimensions of 21G needles used to test variability associated with needle manufacturing tolerances, L : total length of bevel, l : thickness of needle wall at tip, and D and d , respectively: outside and inside diameter at transition between facets (SD: standard deviation; CV: coefficient of variation).....	23
Table 6 – Effect of needle tip angle on maximum puncture force for four protective glove materials, with single-facet 25G needles travelling at 13 mm/min (standard deviation in parentheses) and ANOVA with 95% confidence interval	31
Table 7 – Effect of number of needle facets on maximum puncture force for four protective materials, with 25G needles travelling at 13 mm/min (standard deviation in parentheses) and ANOVA with 95% confidence interval	32
Table 8 – Maximum puncture force (F) and displacement (d) values of 25G needles with two diameters of sample-holder hole D_h (13.5 and 38.0 mm) for different materials, with a needle velocity of 13 mm/min (standard deviation in parentheses).....	36
Table 9 – Summary of effect of parameters related to characteristics of needles and samples, experimental conditions, prestress and presence of a support simulating a hand, on maximum puncture force F for different protective materials (NT: not tested; NS: not significant; NA: not applicable).....	66
Table 10 – Resistance to mechanical hazards for 12 models of glove. NIJ Protocol 99-114 ratings are given in parentheses.	68
Table 11 – List of 58 glove models tested	79
Table 12 – Needlestick fracture energy extrapolated for three gauges (diameters) of three-facet needle (23G, 25G and 28G) and two thicknesses of neoprene (0.4 and 1.6 mm), with a probe velocity of 50 mm/min, standard deviation in parentheses	84
Table 13 – Needlestick fracture energy extrapolated for three gauges (diameters) of three-facet needle (23G, 25G and 28G), both with and without lubricant, and two elastomers (1.6 mm neoprene and 0.8 mm nitrile glove), with a probe velocity of 50 mm/min, standard deviation in parentheses	84
Table 14 – Results of testing of protective glove needlestick resistance, using method described in Section 2.2.6	95

Table 15 – Results of testing of protective glove puncture resistance, using method described in Section 2.3	97
Table 16 – Results of testing of protective glove cut resistance, using method described in Section 2.4.....	99

FIGURES

Figure 1 – Schematic diagram of how SuperFabric [®] provides needlestick resistance	8
Figure 2 – Free-form deformation measurement device.....	9
Figure 3 – Diagram of prestress application device.....	10
Figure 4 – Diagram of setup configuration with support block.....	10
Figure 5 – Medical needles: (a) single-facet (front view); (b) three-facet (front view); (c) three-facet (side view: D = diameter, α = tip angle).....	12
Figure 6 – Setup for needle puncture.....	14
Figure 7 – Probe A from ASTM standard F1342-05 used to measure the puncture resistance of protective clothing materials	15
Figure 8 – Sample-mounting device designed to hold multilayered samples in place while measuring cut resistance	16
Figure 9 – Typical force-versus-displacement curves for (a) a round-tip probe (probe A of ASTM standard F1342-05) and (b) a 25G medical needle for a sheet of 0.8 mm neoprene.....	17
Figure 10 – Change in force as a function of 21G needle displacement for 3.2 mm neoprene, at a probe velocity of 50 mm/min. 0, I, X, T, M and F indicate the stages in the puncture process.....	20
Figure 11 – Optical microscopic image of surface of neoprene sample pierced by a medical needle (x20)	21
Figure 12 – Dimensions L , D , l and d of medical needles, L : total length of bevel, l : thickness of wall of needle at tip, and D and d , respectively: outside and inside diameter at transition between facets.....	24
Figure 13 – Change in maximum puncture force as a function of outside diameter of needle at transition between facets for 15 measurements with 0.4 mm neoprene and 21G needles travelling at 13 mm/min.....	24
Figure 14 – Effect of needle wear on penetration of fabric-backed nitrile with 21G and 27G needles travelling at 13 mm/min.....	25
Figure 15 – Effect of needle wear on penetration of neoprene-coated fabric having a rough, hard-particle finish, with 21G and 27G needles travelling at 13 mm/min.....	26
Figure 16 – Effect of needle wear on penetration with 21G and 27G needles of three superimposed layers of SuperFabric [®] , with the middle layer at 90° (0/90/0) to the other two (needle velocity of 13 mm/min).....	27
Figure 17 – Change in maximum penetration force as a function of needle diameter for a 0.8 mm sheet of nitrile and a 1.6 mm sheet of neoprene (needle velocity of 50 mm/min for neoprene and 13 mm/min for nitrile).....	28

Figure 18 – Change in maximum puncture force as a function of needle diameter for neoprene-coated interlock knit cotton (Scorpio [®] gloves, wrist area), with a needle velocity of 13 mm/min	29
Figure 19 – Change in maximum puncture force as a function of needle diameter for a triple-layer configuration of SuperFabric [®] (middle layer at 90° to the other two) and for samples from Hercules One gloves (needle velocity of 13 mm/min)	29
Figure 20 – Change in maximum puncture force as a function of needle diameter for TurtleSkin [®] (samples S 002-b and D 006b), with a needle velocity of 26 mm/min	30
Figure 21 – Comparison of maximum puncture force values for different protective materials, with a 25G needle travelling at 13 mm/min.....	33
Figure 22 – Optical microscopic image of interaction between needle tip and liner yarn on penetration of neoprene-coated interlock knit sample	34
Figure 23 – Optical microscopic image of puncture site of a SuperFabric [®] sample, showing where a needle caused a brittle fracture of the hard plate	34
Figure 24 – Three examples of change in force as a function of 25G needle displacement, for a three-layer sample of SuperFabric [®]	35
Figure 25 – Optical microscopic image of interaction between needle tip and yarn of woven liner on penetration of sample of TurtleSkin [®] D 006-a (woven lining with polymer coating)	35
Figure 26 – Change in maximum puncture force as a function of sample thickness for neoprene (50 Shore A) and nitrile (70 Shore A), with 25G needles travelling at 13 mm/min	37
Figure 27 – Change in maximum puncture force as a function of number of layers of SuperFabric [®] , with 25G needles travelling at 13 mm/min	37
Figure 28 – Change in maximum puncture force as a function of material hardness for a 1.6 mm sheet of neoprene and a 0.8 mm sheet of nitrile, with 25G needles travelling at 13 mm/min.....	38
Figure 29 – Change in maximum puncture force as a function of probe velocity for a 1.6 mm sheet of neoprene and 21G, 25G and 28G needles	39
Figure 30 – Change in maximum puncture force as a function of probe velocity on a semilogarithmic scale, for a 1.6 mm sheet of neoprene and 25G needles	40
Figure 31 – Change in maximum puncture force as a function of probe velocity on a semilogarithmic scale, for neoprene-coated knit cotton (Scorpio [®] glove, wrist area) and 25G needles.....	40
Figure 32 – Change in maximum puncture force as a function of probe velocity on a semilogarithmic scale, for a three-layer stack of SuperFabric [®] and two types of TurtleSkin [®] samples (S 002-b and D 006-b), with 25G needles	41
Figure 33 – Needle configuration in relation to surface of protective glove at puncture	42

Figure 34 – Change in maximum puncture force as a function of the needle’s angle of attack, for two thicknesses of neoprene (0.8 and 1.6 mm), with 21G needles travelling at 13 mm/min	43
Figure 35 – Diagram of needle penetrating material at an angle other than 90°	43
Figure 36 – Change in maximum puncture force as a function of total distance travelled by needle, for three thicknesses of neoprene (0.8, 1.6 and 3.2 mm), four angles of attack (30°, 45°, 60° and 90°) and 21G needles travelling at 13 mm/min	44
Figure 37 – Change in maximum puncture force as a function of needle’s angle of attack, for knit cotton fabric and neoprene-coated knit cotton fabric (Scorpio [®] glove, wrist area), 25G needles travelling at 13 mm/min	45
Figure 38 – Change in maximum puncture force as a function of needle’s angle of attack, for one, two and three layers of SuperFabric [®] , with 25G needles travelling at 13 mm/min	45
Figure 39 – Change in maximum puncture force as a function of needle’s angle of attack, for TurtleSkin [®] samples S 002-a, S 002-b, D 006-a and D 006-b, with 25G needles travelling at 13 mm/min (error bars omitted for easier reading)	46
Figure 40 – Influence of temperature on maximum puncture force for a 0.8 mm sheet of neoprene, 23G needles and several needle velocity v values.....	47
Figure 41 – Time-temperature superposition of maximum puncture force values for 0.8 mm neoprene, a 23G needle and several temperature T and probe velocity v values..	48
Figure 42 – Change in maximum puncture force as a function of temperature for sheets of neoprene (1.6 mm) and nitrile (0.8 mm), with a 25G needle travelling at 13 mm/min	49
Figure 43 – Change in maximum puncture force as a function of temperature for a 1.6 mm sheet of fabric-backed nitrile and a layer of SuperFabric [®] , with a 25G needle travelling at 13 mm/min	49
Figure 44 – Change in maximum puncture force as a function of humidity after conditioning, for a 1.6 mm sheet of neoprene and a 0.8 mm sheet of nitrile, with a 25G needle travelling at 13 mm/min	51
Figure 45 – Change in maximum puncture force as a function of humidity after conditioning, for a 1.6 mm fabric-backed sheet of nitrile, neoprene-coated knit material (Scorpio [®] glove, wrist area) and a layer of SuperFabric [®] , with a 25G needle travelling at 13 mm/min	51
Figure 46 – Change in maximum puncture force as a function of needle diameter, with and without lubricant (silicone grease) for a 3.2 mm sheet of neoprene, with a probe velocity of 50 mm/min.....	52
Figure 47 – Change in reduction of maximum puncture force by application of a lubricant (silicone grease) as a function of needle diameter for a 3.2 mm sheet of neoprene, with a probe velocity of 50 mm/min	53

Figure 48 – Effect of liquid soap lubrication on maximum puncture force, at different probe velocities, for a 3.2 mm sheet of neoprene and 23G needles.....	54
Figure 49 – Photograph of a glove under strain.....	55
Figure 50 – Force-versus-displacement curves for different degrees of strain associated with prestress applied to a 0.8 mm sheet of neoprene, with 23G needles travelling at 50 mm/min.....	55
Figure 51 – Change in maximum puncture force as a function of prestress value, for a 1.6 mm sheet of neoprene and a 0.8 mm sheet of nitrile, with a 25G needle travelling at 13 mm/min.....	56
Figure 52 – Effect of hardness of rubber block simulating a hand on maximum puncture force, for a 1.6 mm sheet of neoprene, a 0.8 mm sheet of nitrile of hardness 70 Shore A, and a neoprene-coated knit cotton fabric (Scorpio [®] glove, wrist area), with 25G needles travelling at 13 mm/min.....	57
Figure 53 – Diagram showing (a) needlestick process and (b) puncture by round-tip probe, in configuration with support block.....	58
Figure 54 – Effect of hardness of rubber block simulating a hand on maximum puncture force for three layers of SuperFabric [®] and TurtleSkin [®] samples S 002-a, D 006-a, S 002-b and D 006-b, with 25G needles travelling at 13 mm/min (error bars omitted for easier reading).....	59
Figure 55 – Sample force-versus-displacement curves plotted from needlestick resistance values of HexArmor 8030 gloves.....	60
Figure 56 – Maximum puncture force measured for protective gloves, with 25G needles travelling at 500 mm/min (method described in Section 2.2.6).....	61
Figure 57 – Samples of force-versus-displacement curves obtained with type A puncture probe of ASTM Standard F1342-05 [34] for Hakson 9000C gloves.....	62
Figure 58 – Maximum puncture force measured for protective gloves, using the method described in Section 2.3, and rated according to NIJ Test Protocol 99-114.....	63
Figure 59 – Protective glove cut resistance, measured using the method described in Section 2.4, and rated according to NIJ Test Protocol 99-114.....	64
Figure 60 – Comparison of maximum puncture force values measured with 25G hypodermic needles, as described in Section 2.2.6, and those measured with probe A of ASTM Standard F1342-05, for 58 models of glove.....	65
Figure 61 – Change in force applied as a function of crack depth, for three thicknesses of neoprene (0.4, 0.8 and 1.6 mm), with 25G needles travelling at 50 mm/min.....	81
Figure 62 – Change in force required to initiate crack (position I in Figure 10, p. 20) as a function of neoprene thickness, with 25G needles travelling at 50 mm/min.....	82
Figure 63 – Method of determining change in strain energy corresponding to different needlestick depths.....	83
Figure 64 – Change in puncture energy as a function of crack depth, for three thicknesses of neoprene, with a 23G needle travelling at 50 mm/min.....	83

Figure 65 – Sample-holder setup devised for prestretching samples in preparation for needlesticks	85
Figure 66 – Typical force-versus-displacement curves for different degrees of prestretching applied to neoprene, for 23G needles travelling at 50 mm/min.....	86
Figure 67 – Change in puncture energy as a function of crack depth, for different degrees of prestretching applied to a 1.6 mm sheet of neoprene, with 23G needles travelling at 50 mm/min.....	87
Figure 68 – Cut geometries (a) corresponding to the description of Rivlin and Thomas, (b) corresponding to needlestick.....	88
Figure 69 – Change in prestretch energy T as a function of extension, for a 1.6 mm sheet of neoprene ($C_1 = 172$ kPa, $C_2 = 443$ kPa), calculated using Equation 10	89
Figure 70 – Comparison of calculations of prestretch energy using Equation 10 (method based on formalism of Rivlin and Thomas) and Equation 18 (extension of LEFM to rubber), for a 1.6 mm sheet of neoprene.....	91
Figure 71 – Change in puncture energy as a function of prestretch energy calculated using Equation 10 (method based on formalism of Rivlin and Thomas) and Equation 18 (extension of LEFM to rubber), for a 1.6 mm sheet of neoprene punctured by 23G medical needles travelling at 50 mm/min	92
Figure 72 – Change in puncture energy as a function of prestretch energy, for 0.8 mm nitrile punctured by 23G medical needles, with and without lubricant, travelling at 50 mm/min.....	93

1. INTRODUCTION

1.1 Importance

Hand injuries account for approximately 19% of all injuries compensated by the CSST, Quebec's occupational health and safety board, with slightly over CAN\$264 million being paid out for the years 2003–2005 [1]. In some industries, such as metal machining, the proportion can even exceed 30% of CSST-compensated injuries [1,2]. Of this 30%, over half are cuts or puncture wounds [1].

The health care sector has been dealing with the problem of needlestick injuries for a long time. For instance, 15% of cuts and injuries suffered by surgical operating staff are caused by needles [3]. Of this percentage, up to 77% of incidents are caused by suture needles [3] and around 13% by hollow-bore needles [4]. However, hollow-bore needles are associated with a much higher risk of infection transmission, as the volume of blood transferred through an injury is approximately twice that for suture needles [5].

The risk of contracting an infection through a needlestick injury is far from negligible: contact with the blood of someone who has tested positive for the hepatitis B virus (HBV) has been associated with an estimated transmission risk of between 6% and 30% for non-immunized individuals [6,7]. The human immunodeficiency virus (HIV), HBV and the hepatitis C virus (HCV) can survive outside the human body for several weeks [8]. As a result, the U.S. Occupational Safety and Health Administration (OSHA) has estimated that 5.6 million health care and related workers are at risk of professional exposure to blood-borne diseases, including HIV, HBV and HCV [9]. In Quebec, 1,885 people were tested between March 1999 and October 2002 by the postexposure prophylaxis referral centre at St. Luc Hospital (part of the Centre hospitalier universitaire de Montréal, or CHUM) [8]. A review of 202 files of patients who had been to the referral centre between March 1 and December 31, 1999, showed that over 50% of cases of accidental exposure to blood and other body fluids were caused by needles [10].

Other occupational groups are also increasingly facing the problem of needlestick injury. Examples abound: police officers who search suspects or vehicles; correctional services officers who frisk inmates and search through their personal effects and cells; and garbage collectors and park maintenance workers. One study of New York City police officers identified 121 cases of transcutaneous exposure in 1992, including 15 cases due to needles [11]. Given that around 60% of the men arrested on the Island of Manhattan over that same period were intravenous drug users, and that 30% to 60% of the intravenous drug users enrolled in drug treatment programs were HIV positive, these officers are running a high risk of contracting infectious diseases through transcutaneous exposure. Among emergency services workers, it has been found that the most common percutaneous injuries occur as a result of accidental contact needlesticks [12]. These injuries are also the cause of most cases of occupational HIV infection. Another study identified 43 cases of occupational exposure to blood through needles, representing 36% of all cases of needlestick injury analysed [13]. The non-medical occupational categories at the greatest risk of needlestick injury appear to be housekeeping staff (37% of cases) and police officers (35% of cases). It is also important to note that 21% of these cases of occupational needlestick injury are non-accidental, meaning that they are the result of criminal assault with blood-filled syringes or needles. Lastly, Quebec's Institut national de santé publique reported 17

cases of community-acquired needlestick injury between 1996 and 1998 [8]. Most of these cases occurred in parks, school yards or public washrooms, or while handling garbage. The main sources of needles left in inappropriate places are intravenous drug users and diabetics, the vast majority of whom throw their used syringes in the household trash.

1.2 Origin of Occupational Health and Safety Problem

Wearing suitable protective gloves is recommended as a means of preventing hand injuries, especially where needles are concerned. For instance, the 1999 standard of the National Fire Protection Association (NFPA) specifies requirements for gloves to be worn by emergency medical services workers [14]. A list of protective gloves for law enforcement and correctional services officers exposed to the hazard of hypodermic needles has also been proposed by the National Law Enforcement and Corrections Technology Center (NLECTC) of the National Institute of Justice (NIJ) in the U.S.A. [15]. Wearing protective gloves can considerably lower the risk of infectious disease transmission, with a 52% reduction, for instance, in the volume of blood transferred when a gloved hand is pricked by a hollow-bore needle, compared with an ungloved hand [16]. However, very high rates of glove failure, i.e., accidental puncture, have been recorded, especially in health care. In cardiothoracic surgery, the rate can reach 61% [17] and increases with the length of the procedure. Most cases of glove failure during surgery occur when a needle punctures the non-dominant hand (usually the left). In the case of emergency services workers, the lowest rate of glove failure recorded (10.4% per pair of gloves) may in part be due to the shorter length of time the gloves are worn [18]. Note, however, that 58% of cases of glove failure go unnoticed [19]. The situation is worse in the case of needlesticks, in comparison with cuts and tears, simply because they are so difficult to detect [17].

A number of different strategies have been developed to address the problem of hard-to-detect accidental puncture of protective gloves [20,21]. The first is double gloving, which involves wearing one pair of gloves on top of another. Double gloving is especially recommended for high-risk surgical procedures [22]. A significant reduction in the puncture rate of the inner glove has been found [20,21]. This technique has led to a reduction in the risk of exposure to patient blood in the operating theatre of as much as 87% when the outer glove is punctured [3] and a tenfold reduction in contamination rates among surgeons [20]. Nevertheless, some workers are reluctant to adopt the practice of double gloving because of lower tactile sensitivity and dexterity [3,23]. Note that in the case of hollow-bore needles, double gloving was not found to have any effect on the amount of blood transferred when puncture occurred [16]. Another way to address the problem is to wear two gloves of contrasting colours so that a different colour will become visible at the puncture site [19,24,25]. For the system to work properly, however, the gloves must first be immersed in a solution [24], which may be impractical for some applications [20,23]. Other proposals in the literature include wearing fibre knit glove liners that afford good cut resistance [20,26,27], the cotton sandwich technique, which involves wearing a knit cotton glove between two latex gloves [20], adding local adhesive reinforcements [26] and incorporating an intermediate layer containing a disinfectant liquid into the structure of the glove [16]. New materials have also been developed to provide greater needlestick protection. These include SuperFabric[®], with tiny hard plates adhering to a fabric surface [28], and TurtleSkin[®], which is a cut-resistant, tightly woven, aramid fabric [29].

Nonetheless, one major problem with the development of needlestick-resistant protective gloves is that the standard methods for testing the puncture resistance of protective clothing are inadequate [30]. The resistance values measured for hypodermic needles, which are reported as being the leading cause of needlestick injury in hospitals [31], are significantly lower than those found using the probes proposed in the standards, whether probes with pointed tips [30] or rounded tips [32,33]. The methods used to guide workers exposed to medical needles in the selection of protective gloves are based on existing standard methods for measuring puncture resistance. These methods, like standard ASTM F1342 [34], use pointed-tip or round-tip probes, but not hypodermic needles. The needlestick resistance of these gloves is therefore overestimated, which can give glove wearers a false sense of security. This is the case, for instance, of the method given in NIJ Protocol 99-114 [35] for characterizing and comparing the puncture resistance of gloves intended for use by law enforcement and correctional services officers. It is also the case of the methods used to compare the gloves worn by emergency medical services workers [14,36]. Furthermore, it has been reported, on the basis of a study of four models of latex and nitrile gloves, that there is no correlation between glove puncture resistance measured with standard probes and with hypodermic needles [30].

Two requests for expert assessments were submitted to the IRSST by a Montreal detention centre and the correctional services branch of Quebec's Ministère de la sécurité publique. They were filed when two detention centre officers assigned to go through inmates' personal effects refused to perform their tasks on finding a used needle, and following recommendations made by the CSST occupational health and safety board inspector assigned to the case. The IRSST's support was needed to identify a glove providing adequate protection—especially against needlestick injury, cuts and body fluids—for workers assigned to searches. The request also received the backing of the City of Longueuil, Quebec's École nationale de police and its research centre, the Fédération des policiers et policières municipaux du Québec, the Association des directeurs de police du Québec, the Fraternité des policiers et policières de la ville de Québec, the Association sectorielle paritaire pour la santé et la sécurité du travail – secteur administration provinciale (APSSAP), and the Association sectorielle paritaire pour la santé et la sécurité du travail – secteur affaires municipales (APSAM). The general request concerned gloves designed to protect against needlestick while still providing the dexterity needed to perform required tasks. The occupational groups affected by the various requests included public works blue-collar employees, municipal police officers and correctional services officers assigned to searches.

1.3 Scientific and Technical Importance of Study

Significant progress has been made in recent years, in part thanks to the leadership of the IRSST, in establishing appropriate standard methods for measuring the resistance of protective clothing against mechanical hazards. Research has also helped to improve our understanding of the phenomena involved. Nonetheless, there is still very little in the scientific literature on the subject of needlestick injuries.

The IRSST's work has led to the development of a new test method for cut resistance [37], which has been adopted in the current versions of the ASTM and ISO standards for measuring the cut resistance of protective clothing (ASTM F1790-05 [38] and ISO 13997 [39]). Research

has also revealed that for elastomers, most of the energy expended in a sliding cut is absorbed by the friction between the blade and the test piece [32,40]. The friction factor consists of two components, one related to the rubbing of the lateral surfaces of the blade against the material being cut, and the other to the friction of the actual cutting edge, which have opposite effects on cut resistance. A model linking the friction force to the normal load applied has also been established [41].

The biggest improvements with respect to puncture testing concern the use of probes of a size and shape that more closely match the hazards in question [42]. In particular, the current version of the ASTM standard for testing the puncture resistance of protective clothing (ASTM F1342-05 [34]) proposes two 2 mm diameter conical tip probes, with probe A having a tip radius of 0.25 mm and probe C a tip radius of 0.50 mm, and a hemispherical tip probe (B) with a diameter of 1 mm. It has also been shown that for rubber membranes, the geometry of the probe tip has a major influence on the maximum puncture force, which depends on the contact surface between the membrane and the probe [32,33]. Puncture appears to be controlled by the material's maximum rate of strain, which is one of its intrinsic parameters. Good correlations have been obtained between the experimental puncture data and a model based on Mooney's formalism [43,44].

Preliminary research on needlestick injury conducted as part of Project 099-101 (Protective Gloves: Study of the Resistance of Gloves to Multiple Mechanical Hazards) showed for the first time, with elastomer membranes, the existence of major differences in mechanism between puncture with the round-tip probes used in the standards and puncture by medical needles with a cutting edge [32,33]. It was found, for instance, that needles penetrate the material gradually, whereas puncture by the standard probes occurs abruptly when the strain in the membrane under the probe tip reaches the material's failure threshold. It was also found that the maximum puncture forces of medical needles are much lower than those recorded with round-tip probes. The same phenomenon has also been reported in studies of protective gloves that compared hypodermic needles [30] and dental needles [45,46] with standard pointed-tip probes, as well as reverse cutting suture needles with taper point suture needles [26]. A significant effect of needle tip shape on maximum puncture force has also been noted in the case of experiments on beef liver [47]. The force increased with the change from a triangular tip to a bevelled tip and then to a tapered tip. The lower puncture force for medical needles and the fact that they penetrate the material gradually have been attributed to the cutting edge at the needle tip [32,33]. There has also been a preliminary suggestion that the needlestick process involves a significant cutting component and that it is related to the fracture energy of the material.

The methods that researchers use to study the needlestick resistance of protective gloves can be divided into two major categories. In most cases, they are based on the setup proposed in standard ASTM F1342 for testing the puncture resistance of protective clothing [34] and use a straight needle as a puncture probe [12,25,30,32,33,45]. The needle is attached to the upper part of a standard mechanical testing machine by means of a load cell, while the test piece is held horizontally between two pierced plates that constitute a base secured to the lower part of the testing machine. The compression load measurement is taken at constant velocity. If a curved needle is used as a probe, an alternative system is used: the test piece is attached to a platform equipped with load cells, and rotational movement is applied to the needle [19,26]. In all cases,

the change in force as a function of time or of probe displacement is recorded. The maximum force is extracted from the data.

A few studies of needlestick resistance of gloves were found in the literature. In some cases, the studies assessed the performance of new materials. It has been shown, for instance, that the maximum puncture force for a cutting-edge needle is ten times higher in glove areas reinforced by specially tanned leather or by Spectra[®] than in latex or Kevlar[®] and Lycra[®] fibre knit gloves [26]. In other studies, the seriousness of the risk of transmission associated with being pricked by a hollow-bore needle was evaluated by measuring the volume of blood transferred through the glove [16]: an 81% reduction in the contamination potential was measured for a glove that included an intermediate layer containing a disinfectant liquid in comparison with a latex glove, whereas no difference was noted between single and double gloving.

Other studies have compared different materials: for instance, it has been shown that nitrile gloves were more resistant to needlesticks than latex gloves when 1.26 mm diameter hypodermic needles were used, even though the nitrile gloves were much thinner [30]. On the other hand, the values reported for nitrile gloves were significantly lower for 0.45 mm diameter dental needles [45,46]. These findings should nevertheless be treated with caution, as the two studies produced contradictory results for the comparison of puncture resistance based on the standard method for the two types of material. In addition, the maximum puncture force increased with needle diameter and with the hardening of the material due to thermo-oxidative aging of the neoprene [32]. Note that a slight effect of the wear of the needle tip from reuse as a puncture probe was observed with the neoprene. In a study of latex and nitrile dental gloves, it was also reported that the least needlestick-resistant part of the glove is the palm [45]. This finding confirms that the glove palm is a valid choice as a sampling area for measuring glove resistance to mechanical hazards in the various standards on protective clothing.

A few researchers have also explored modelling the penetration of needles into soft solids, especially for medical applications [47]. They have shown that the axial force corresponding to the insertion of the needle into the skin and the internal tissue can be expressed as the sum of three components: stiffness force, frictional force and cutting force. The first component only applies before the initial puncture of the surface by the needle and has been associated with the elastic properties of the skin (or the capsule, for internal organs) and internal tissues. The frictional force between the surface of the needle and the surface of the hole made in the tissue, like the cutting force required to slice through the tissue, does not come into play until after the initial puncturing of the surface. It has also been suggested that the asymmetrical distribution of forces in the punctured material at the crack tip, which is related to the bevelled shape of medical needles, can cause the needle to bend. Lastly, a model developed with flat-bottomed and pointed probes used a single-term Ogden strain-energy function to describe the mechanical behaviour of soft solids [48]. A fairly good match was noted with experimental results obtained with silicone rubber and with skin.

1.4 Goal and Specific Objectives of Study

The main goal of this project was to develop a standardizable test method for measuring the needlestick resistance of protective glove materials, in cooperation with ASTM Committee F-23, which could be used to rate the resistance of the materials. In addition to this main goal, the research plan included starting work that would take into account the support function played by the hand in the glove. Another objective was to learn more about the material fracture mechanisms associated with needlesticks in order to help manufacturers to develop better protective gloves. Lastly, commercially available gloves were rated to help workers and employers make an informed choice according to the level of protection required against mechanical hazards. The gloves rated highest for needlestick resistance were also evaluated with workers for dexterity and tactile sensitivity, but those results are presented in a separate report [49].

In short, the specific research project objectives covered by this report were to

1. Study and compare the behaviour of different materials used to make gloves that afford protection against mechanical hazards when the gloves are punctured by a medical needle or by a standard probe.
2. Analyse the influence of different parameters of the needles, the materials and the experimental conditions.
3. Conduct a preliminary study of how a hand in a glove affects needlestick resistance.
4. Propose a method for measuring needlestick resistance that takes the above points into account and can provide a basis for the development of a test standard.
5. Characterize the needlestick resistance of commercially available protective gloves.
6. Make recommendations about which gloves offer the best protection against needlestick injury.

Since this study was initiated in response to requests for an expert assessment, the research focused on three occupational groups: police officers, correctional services officers and blue-collar workers (gardeners and garbage collectors). Representatives from the three groups took an active role throughout the project. The research results could be applied to other occupational categories and other types of work.

2. EXPERIMENTAL METHODS

2.1 Materials

The inventory of protective gloves for this study was drawn up with the help of users and manufacturers. The professional sector associations (the APSAM and the APSSAP) representing the occupational groups involved in the project (police officers, correctional services officers and blue-collar workers) conducted a survey to determine which models of gloves are currently being used by their members.

Protective glove manufacturers' print and online catalogues were reviewed to identify models described as being puncture- or needlestick-resistant. A list of approximately 120 models of gloves made by North American manufacturers and 21 made by European or Asian manufacturers was compiled. A list of 25 models of gloves that could potentially be used by police and correctional services officers was also found on the Justnet website; it was compiled for the purposes of a testing program conducted by the National Law Enforcement and Corrections Technology Center of the National Institute of Justice in the United States [50].

On the basis of this information, 24 manufacturers were contacted and 11 of them agreed to provide gloves for the study. The list of 58 models of gloves of which samples were obtained is given in Appendix A (p. 79). These gloves were characterized in terms of puncture resistance under the current ASTM standard (see Section 2.3) and needlestick resistance using the free-form deformation method developed for this project (see Section 2.2.6). For the 12 most puncture-resistant models of glove, cut resistance was also measured according to the current ASTM standard (see Section 2.4).

Representative model materials of the different types of protective gloves used to guard against mechanical hazards were selected for a more fundamental study of needlesticks and the effects of the different experimental parameters. For unlined gloves, two types of elastomer, neoprene and nitrile, were tested in the form of homogeneous sheets of constant thickness in order to limit variability. Sheets of neoprene 0.4, 0.8, 1.6 and 3.2 mm thick were procured from Fairprene Industrial Products of Fairfield, Connecticut, and sheets of nitrile 0.8, 1.6, 2.4 and 3.2 mm thick from McMaster Carr of Atlanta, Georgia. Nitrile samples were also cut out of 0.8 mm thick nitrile gloves (Sol-Vex 37-165 made by Ansell). Sheets of different hardnesses of neoprene (30, 50 and 70 Shore A) and nitrile (50, 60 and 70 Shore A) were also obtained from McMaster Carr.

Two types of protective materials representative of lined gloves were used. Sheets of fabric-backed nitrile (two thicknesses: 1.6 and 4.2 mm) were obtained from McMaster Carr. Although this material is too stiff to be used for gloves, it provides a sample of a fabric immersed in a polymer matrix. At the same time, samples were taken from the palm and wrist areas of neoprene-coated knit cotton gloves (Scorpio 8-352 made by Ansell, 1.3 mm thick). These gloves have a rough finish designed to provide a better grip on wet and slippery surfaces. The rough finish is produced in part by adding small hard particles to the neoprene coating that protrude above the glove surface. In view of the fact that the hard particles in the palm area of the glove increase the variability of results enormously, samples from the wrist area, which has a similar structure, but without any particles, were taken to examine the effect of the different experimental parameters. Some measurements were also taken for the fabric liner of the gloves.

Two types of material designed specially to provide protection against mechanical hazards were also included in the study. SuperFabric[®] is a new material developed by HDM to provide a high degree of cut, puncture and abrasion resistance [28]. It consists of tiny hard plates attached to a fabric surface (Figure 1). When needlestick protection is required, at least two layers of material are superimposed so that the spaces between the plates on one layer are covered by the plates of the other layers (Figure 1). This material has been tested both individually and in the form of superimposed layers, with each layer being aligned 90° to the preceding layer, in accordance with the manufacturer's instructions; testing was also done on samples taken from the palm of Hercules One gloves (model 4042) made by HexArmor[®]. These gloves have four layers: a liner, two layers of SuperFabric[®] and an outer layer of synthetic leather.

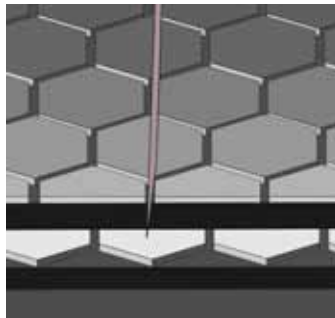


Figure 1 – Schematic diagram of how SuperFabric[®] provides needlestick resistance

TurtleSkin[®], made by Warwick Mills, is the other material that was tested. According to the manufacturer, its tightly-woven aramid fibres (Kevlar[®]) provide outstanding cut, puncture, abrasion and needlestick resistance without sacrificing dexterity and tactile sensitivity [29]. Four types of materials used in two models of glove (Search 002 and Duty 006) were tested. Sample S 002-a, with a thickness of 0.4 mm, consisted of a thin black coated fabric with a rough finish. Sample S 002-b, 0.35 mm thick, had a thin woven yellow liner and a smooth coating. Sample D 006-a, 1.35 mm thick, had a woven yellow liner and a thick black coating. And finally, sample D 006-b consisted of the thick woven yellow liner found in sample D 006-a (thickness of 0.35 mm).

2.2 Measurement of Needlestick Resistance of Glove Materials

A significant part of the project concerned the development of a method for measuring the needlestick resistance of glove materials under conditions that simulate the wearing of gloves. In this respect, the setup developed for the purposes of an earlier project on a method of assessing the puncture resistance of protective gloves [42] and adopted in the corresponding ASTM standard [34] provided a basis for the free-form deformation methods, with prestressed material and a support, that are described in this section. In the following pages, the term “probe” refers to both needles and to standard probes.

2.2.1 Free-Form Deformation Test Setup

The free-form deformation (FFD) test setup consisted of a base holding the sample in position and a probe that applied a compression force to the centre of the sample. As shown in Figure 2, the sample was mounted between two pierced steel plates equipped with a compressed-air closure system. The edges of the hole in the lower plate were rounded to prevent stress concentration in the sample. Two dimensions for the diameter D_h of the hole in the sample-holder plates were available, 13.5 mm and 38 mm. The base was positioned in a universal test machine (Instron 1137 or MTS Insight), and the probe was secured by a dowelling chuck in a 50 lb (222 N) load cell.

This setup can be placed in an oven to expose the sample to higher-than-ambient temperatures. It can also be inclined in relation to the axis of movement of the probe in order to vary the angle of incidence between probe and sample.

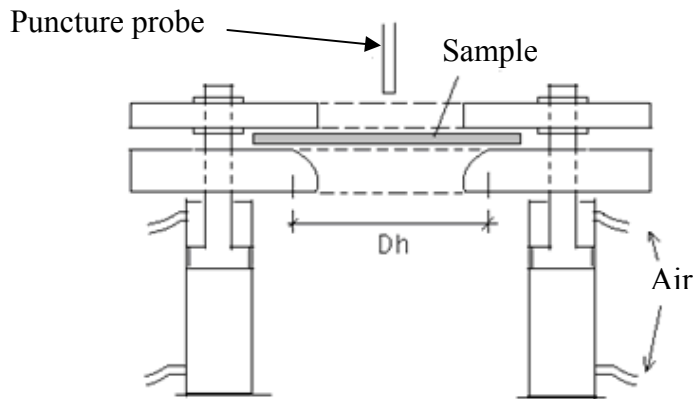


Figure 2 – Free-form deformation measurement device

2.2.2 FFD Test Setup with Prestressed Material

When worn, gloves can get stretched, at the finger joints, for instance, when the hand flexes repeatedly or if the glove is very tight-fitting. This prestressing of the glove material may affect its needlestick resistance. To examine this phenomenon, an equibiaxial prestress application system was adapted to the FFD test setup. As shown in Figure 3, the prestress was applied by means of a hollow copper cylinder placed under the sample and raised up using a laboratory jack.

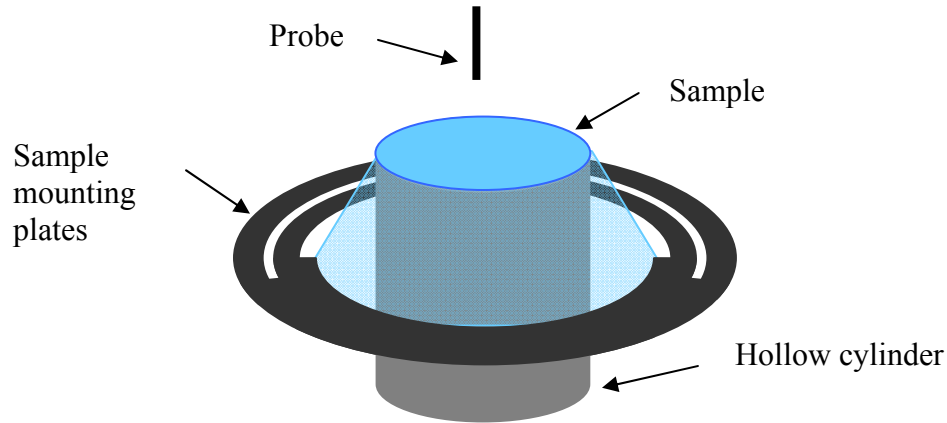


Figure 3 – Diagram of prestress application device

Once the prestress was applied, marks were pencilled on the diameter of the hollow cylinder. The biaxial deformation applied was calculated by measuring the diameter of the stretched surface indicated by the marks after eliminating the prestress. This setup made it possible to apply prestresses corresponding to deformations greater than 100% to the elastomer membranes, which have high extensibility.

2.2.3 Test Setup with Support Blocks

To assess what effect the underneath elastic pressure exerted by the hand wearing the glove has on the glove's needlestick resistance, preliminary testing of the effect of a support simulating the stiffness of underneath hand in a glove was also conducted in this project. The FFD setup was used in combination with rubber blocks of different hardnesses placed under the test piece. As shown in Figure 4, the system was devised so that the rubber blocks merely provided a support for the sample: a piece of aluminum foil connected to the probe by means of an electric circuit was positioned between the test piece and the rubber support, directly beneath the needle, to detect the precise moment when the underside of the test piece was punctured.

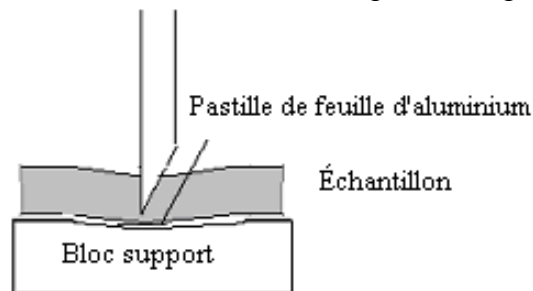


Figure 4 – Diagram of setup configuration with support block

Different types of neoprene in the form of 2.5 cm-thick sheets with hardness values between 20 and 100 Shore A (McMaster Carr) were used as the support blocks. In comparison, hardness values equivalent to 20 Shore A have been reported for the palmar side of the fingers and of the

hand, whereas the hardness of the dorsal side of the fingers reached values equivalent to 50 Shore A [51]. The hardness values used in this study therefore correspond to the physiology of the hand.

2.2.4 Standard Needles and Probes

As for the gloves, an inventory of needles was taken with the help of both manufacturers and users. The different types of needles available on the market were identified from the online catalogues of a few manufacturers. At the same time, a survey of pharmacists was conducted to determine the models of needles most sold to individuals. Contacts were also established with organizations connected with the drug-using community to identify the needles most often used by that clientele. Information about the types of needles to which are exposed the occupational groups involved in the study was obtained through the monitoring committee. It was determined that the needles to which police officers, correctional services officers and blue-collar workers are most often exposed are mainly 23 to 29 gauge three-facet medical needles. These results are also corroborated by 2008 data from the North American Syringe Exchange Network (NASEN) indicating that 100% of the needles supplied under Syringe Exchange Programs (SEPs) are 25G to 29G. In fact, 96% of them are 27G and 28G [52].

To study the effect of the different characteristics of medical needles (diameter, tip angle and number of facets) on the needlestick resistance of the protective materials, 21G to 29G intramuscular hypodermic needles (between 0.35 mm and 0.8 mm in diameter) and spinal needles (which have only one facet) were used. These stainless-steel needles made by Becton and Dickinson (BD) and by Terumo[®] Medical Corporation are among the most commonly used in Quebec. Table 1 lists their main characteristics, while Figure 5 shows the single-facet (spinal needle) and three-facet (hypodermic needle) configurations. Note that the angle value reported for three-facet needles corresponds to the angle of the facets near the tip (see Figure 5.c). The fine stylet (rod) down the middle of the spinal needles was removed for the testing.

Table 1 – Characteristics of medical needles used

Number of facets	Gauge	Diameter D (mm)	Tip angle α	Use
3	29G	0.32	24°	Intramuscular hypodermic
3	28G	0.35	18°	Intramuscular hypodermic
3	27G	0.40	19°	Intramuscular hypodermic
3	25G	0.50	18°	Intramuscular hypodermic
3	23G	0.65	16°	Intramuscular hypodermic
3	22G	0.70	20°	Intramuscular hypodermic
3	21G	0.80	19°	Intramuscular hypodermic
1	25G	0.50	20°	Spinal
1	25G	0.50	30°	Spinal

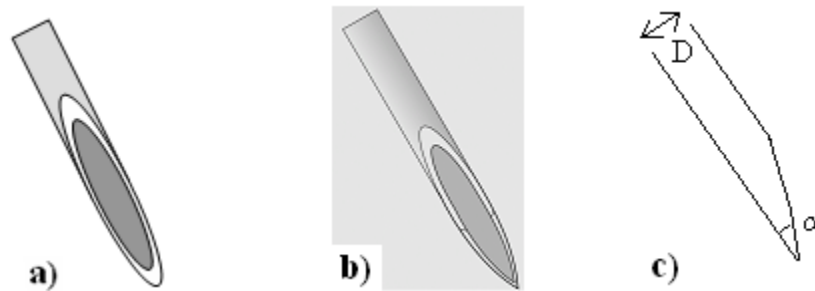


Figure 5 – Medical needles: (a) single-facet (front view); (b) three-facet (front view); (c) three-facet (side view: D = diameter, α = tip angle)

Cylindrical and conical probes were also used in combination with the various setups designed to study needlesticks, with a view to highlighting possible differences in fracture mechanism depending on geometry. These are type A conical-head cylindrical probes (2 mm diameter, cone of angle 26° and ball tip of radius 0.25 mm) and type B hemispheric-head cylindrical probes (1 mm diameter and ball tip of radius 0.5 mm) described in the method for ASTM standard F1342-05 on measuring the puncture resistance of materials used for protective clothing [34]. Some measurements were also taken with stainless-steel, flat-head, 0.5 mm diameter stylets.

2.2.5 Operating Conditions for Testing Protective Materials

The variation in the force applied to the sample by the probe was measured as a function of probe displacement. To improve the resolution of the force-versus-displacement curves, probe

velocities (between 10 and 100 mm/min) lower than the 500 mm/min specified in ASTM standard F1342-05 [34] were used for most of the protective material testing.

Based on the force and displacement data recorded, maximum force and displacement values corresponding to this maximum force were determined. For each condition, the measurement was repeated four times. A distance of at least the diameter of the hole of the sample-mounting plates used was always left between two contiguous puncture sites on a sample.

As a general rule, the needles used as test probes were only used once. The results obtained with some relatively hard protective materials revealed rapid dulling of the needle tip from one test to the next, causing a sharp increase in the puncture force between two successive tests performed with the same needle (see Section 3.2.2). The only exceptions were the study of the effect of needle wear and the tests done on elastomer membranes, for which the needles could be reused up to five times. A previous study showed that, in the case of neoprene, an increase in the puncture force of less than 7% resulted after 10 successive uses of the same needle as a probe [32]. Moreover, unless otherwise specified, the reported results are for ambient temperature conditions with the sample-mounting plates having a 38 mm hole, and a normal angle of incidence of the probe in relation to the sample plane. The tests on the protective materials showed that the diameter of the mounting plate hole had no significant effect on the puncture force of medical needles (see Section 3.3.2). Medical needles used as puncture probes had three facets, unless otherwise specified. Similarly, for the neoprene and nitrile sheets, the hardness was 50 Shore A, unless otherwise specified.

2.2.6 Measurement Method Used to Characterize Needlestick Resistance of Protective Gloves

As part of this project, a method for measuring the needlestick resistance of protective gloves was developed and used to rate the 58 models of glove listed in Appendix A (p. 79).

The method, based on the principle of free-form deformation (FFD) (see Section 2.2.1), is similar to the setup proposed in ASTM standard F1342-05 [34]. It consists in measuring the force required to puncture the sample with a probe—in this case, a 25G intramuscular hypodermic needle. The setup used to hold the sample is like the one illustrated in Figure 2, with a diameter Dh of 13.5 mm. It is placed in a test machine equipped with a 56.2 lb (250 N) load cell (see Figure 6). The conditions under which glove needlestick resistance was measured are summarized in Table 2. The method was similar to that in ASTM standard F1342-05, with two differences: the probe used was a hypodermic needle and a new needle was used for each test.



Figure 6 – Setup for needle puncture measurement

Table 2 – Conditions of measurement method used to characterize needles resistance of protective gloves

Setup	Free-form deformation, 10 mm (internal diameter) sample mounting-plate hole
Probe	25G (0.5 mm) intramuscular hypodermic needle (three facets, regular angle [18°], made by BD Medical), new needle for each test
Sample	Cut from palm of glove, includes all layers of material at palm
Load cell	50 lb
Velocity	500 mm/min
Angle of attack	90°
Temperature	Ambient
Distance between puncture sites on test piece	10 mm minimum

The suggested procedure for ensuring that the variability between gloves of the same model is taken into account satisfactorily includes a minimum of 12 repeat measurements, taken on four different gloves, as proposed in ASTM standard F1342-05 [34]. As the number of glove samples available for the study was limited, however, the number of repeats for the tests on the 58 models of glove was reduced to two sets of five measurements taken on samples from two different gloves, for a total of 10 values.

When the measurements were taken, the applied force and probe displacement data were recorded as the needle penetrated the sample. The puncture force value indicated in the report

corresponds to the maximum of the force-versus-displacement curve. The means and standard deviations were calculated on the basis of the data recorded for the repeat measurements.

2.3 Puncture Resistance Measurement

The 58 models of glove were also tested for puncture resistance, following the method described in ASTM standard F1342-05 [34]. This involved measuring the force required for a probe to puncture a sample of the glove material. The setup used was like the one illustrated in Figure 2, with a diameter Dh of 13.5 mm. It was placed in a test machine equipped with a 250 N load cell. Probe A from the standard, shown in Figure 7, was used. The probe is a 2 mm-diameter stainless-steel rod with a conical head and a round tip having a radius of 0.25 mm. It is equivalent to the one used in NIJ Test Protocol 99-114 [35] for the comparative evaluation of protective gloves for law enforcement and corrections applications [15].

The tests were conducted at ambient temperature with a constant probe velocity of 500 mm/min. The samples were cut from the palm area of the glove and included all the layers of material at the palm. The applied force and probe displacement values were recorded, so that the maximum force value could be determined.

As with the needlestick resistance tests, since the number of glove samples available for the study was limited, the number of repeats was reduced to two sets of five measurements taken on samples from two different gloves, for a total of 10 values. The means and standard deviations for the puncture force were calculated on the basis of the data recorded for the repeat measurements.

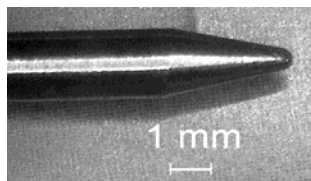


Figure 7 – Probe A from ASTM standard F1342-05 used to measure the puncture resistance of protective clothing materials

2.4 Cut Resistance Measurement

Given that typical working conditions often involve simultaneous exposure to several different types of mechanical hazards, cut resistance measurements were also conducted on the 12 models of glove identified by the occupational groups in question as the most appropriate. With regard to protective materials, two standards, ASTM F1790-05 [38] and ISO 13997 [39], propose a technique for characterizing resistance to cutting by sharps, which is based on work done at the IRSST [36]. The method consists in determining the force required for a blade to travel 20 mm through the thickness of the material being tested. The TDM-100 tomodynamometer (RGI Industrial Products, Saint-Jean-sur-Richelieu, Quebec), designed specifically for the purposes of this kind of characterization and recommended in both standards, was used for the study.

The method follows the instructions of ASTM standard F1790-05 [38]. One difference concerns the cutting-edge calibration process proposed in the standard, which is done with neoprene and involves calculating a correction factor that is then applied to the measurement of the distance travelled during the tests. Given that, when cut, the protective glove materials to be evaluated behave very differently from the standard reference material, i.e., neoprene, no corrective factor was used for the measurements reported here. For the testing of gloves having multiple layers of material, a sample-mounting device designed specially for that purpose (Figure 8) [53] (its introduction into the ASTM standard is currently under discussion) was used to hold the whole test piece in place.

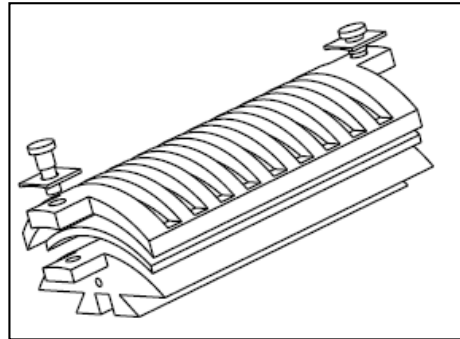


Figure 8 – Sample-mounting device designed to hold multilayered samples in place while measuring cut resistance

3. RESULTS

The main objective of this project was to develop a method of measuring the needlestick resistance of protective glove materials. It required studying how medical needles interact with the different types of materials used to make gloves that provide protection against mechanical hazards, including fracture mechanisms and the effect of different experimental parameters. The study was conducted on materials used in the different glove types, a detailed description of which is provided in Section 2.1 of this report. Sections 3.1 to 3.6 below present the results obtained for these materials. Tests were also run on a series of mechanical hazard protective gloves. The results in terms of needlestick resistance as measured according to the method developed in this project, as well as puncture and cut resistance, are given in Section 3.7.

3.1 Analysis of Fracture Mechanism Involved in Needlesticks

This section offers an analysis of the fracture mechanism involved in needlesticks and draws a comparison with what happens in the case of the round-tip probes used in the ASTM standard method of measuring the puncture resistance of protective clothing [34].

3.1.1 Comparison of Puncture by Standard Probes and Needlesticks

Earlier research had found major differences between puncture by round-tip probes, like those used in ASTM standard F1342-05, and needlesticks [32,33]. The force-versus-displacement curves illustrated in Figure 9 show that the maximum force and the probe displacement at maximum force are much higher for the round-tip probe than for the needle.

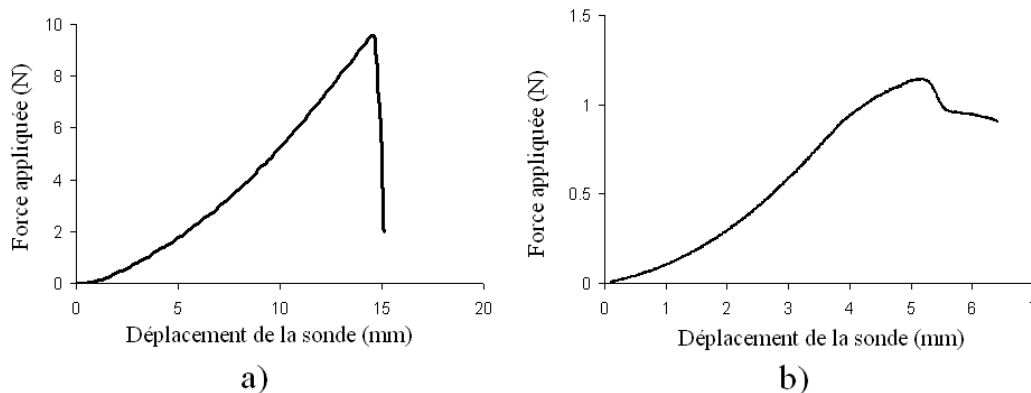


Figure 9 – Typical force-versus-displacement curves for (a) a round-tip probe (probe A of ASTM standard F1342-05) and (b) a 25G medical needle for a sheet of 0.8 mm neoprene

Table 3 shows maximum puncture force values and probe displacement values at maximum force for a sheet of neoprene measured with both conical probe A of ASTM standard F1342-05 (2 mm in diameter, round tip with radius 0.25 mm) and a 23G (0.65 mm diameter) three-facet medical needle. The measurement results were obtained for three different thicknesses of neoprene, under identical experimental conditions, including a probe velocity of 100 mm/min. The maximum force values are lower by around an order of magnitude for the needles, and the

probe displacement values at maximum force are a third lower. For a flat-bottomed cylindrical punch with a diameter of 0.5 mm, the force value recorded for the puncturing of a 0.8 mm sheet of neoprene at a velocity of 100 mm/min is 10.8 N [32], which is comparable to what is obtained with conical probe A, since it has a tip diameter of 0.5 mm, the same as the flat probe. The much lower values obtained for needles therefore cannot be attributed to the difference in probe diameter. These results highlight the fact that a given material's resistance to round-tip probes, like the ones used in puncture testing standards, is very different from its resistance to needlesticks.

Table 3 – Maximum force and displacement values for puncture by conical probe A of ASTM standard F1342-05 and by a 23G needle, for three thicknesses of neoprene, at a probe velocity of 100 mm/min (standard deviation in parentheses)

	Thickness of neoprene (mm)	0.4	0.8	1.6
Conical probe	Maximum puncture force (N)	5.1 (0.2)	10.4 (0.3)	19.2 (0.5)
	Displacement at maximum force (mm)	14.7 (0.2)	14.9 (0.2)	15.3 (0.2)
Medical needle	Maximum puncture force (N)	0.5 (0.04)	1.4 (0.1)	2.2 (0.1)
	Displacement at maximum force (mm)	2.7 (0.2)	3.6 (0.2)	5.3 (0.3)

The data also indicate that round-tip probes and needles have different puncture mechanisms. For round-tip probes, earlier research has shown that elastomer puncture occurs suddenly and without precracking when the deformation of the material under the probe tip reaches its failure threshold [32,33]. As a result, probe displacement, which governs sample deformation, reaches high values at puncture. In contrast, for needles, the cutting edge of the tip quickly creates a crack in the surface of the material. It then progressively widens the crack as it penetrates further into the thickness of the membrane. This whole process occurs without the sample undergoing any significant deformation, which means low needle displacement values at puncture.

The intrinsic properties of the material that govern resistance to puncture by round-tip probes and that govern needlestick resistance are not the same. Earlier work involving round-tip probes has shown that elastomer puncture is related to the tensile strength of the material and its deformation at failure [32,33]. In contrast, for needles, the deformation of the material does not seem to play a major role. Instead, a cutting process appears to be involved. It has been suggested, provisionally, that the needlestick resistance of elastomers is related to the fracture energy of the material [33].

3.1.2 Description of Needlestick Process

The shape of the curve produced in a needlestick test depends on the characteristics of the needle (needle-tip diameter and geometry) and the type of material. Figure 10 shows a force-versus-displacement curve for a 3.2 mm sample of neoprene rubber and a three-facet 21G (0.8 mm) needle. The figure also shows a step-by-step interpretation of the process of the needle piercing

the membrane. At position 0, the needle is in contact with the sample, but has not yet exerted any force on it. Between positions 0 and I, the needle pushes against the membrane and deforms it, but without penetrating it. Position I corresponds to the very start of the penetration of the needle tip into the sample. Between positions I and X, deformation of the membrane increases, while the needle penetrates farther into the material. At position X, the tip of the needle pierces the underside of the sample. At position T, the upper part of the bevelled edge of the needle penetrates into the material, reaching the underside of the sample at position M. This is the point at which the hole reaches its maximum size. The needle can then slide easily into the hole that has been made, with a decrease in the applied force. As the needle continues on its trajectory through the membrane, the only force involved is the friction between the needle and the edges of the hole (position F).

Position I was identified on the basis of microscopic observation of the sample surface. To locate position X, where the tip of the needle pierces the underside of the sample, a thin sheet of aluminum foil was placed under the sample in order to cause an electrical contact with the needle at piercing, following a technique suggested by Hewett [12].

Note that, depending on the test, the maximum of the force-versus-displacement curve can be either the force at X or the force at M. With the exception of larger-diameter needles, the thicker materials tested and the slowest needle velocities, usually only one peak can be seen on a force-versus-displacement curve for rubber. The maximum puncture force results reported here therefore correspond to the maximum value on the force-versus-displacement curve.

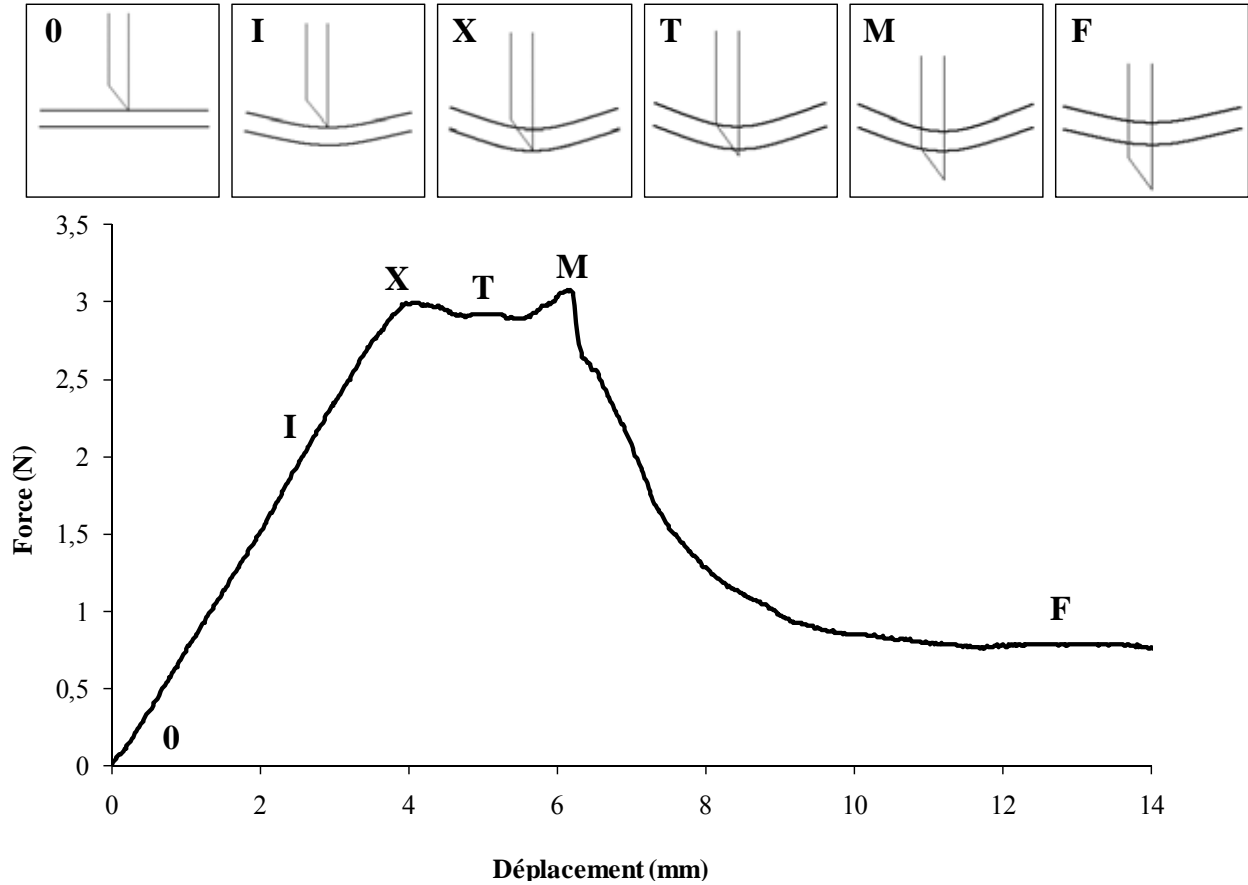


Figure 10 – Change in force as a function of 21G needle displacement for 3.2 mm neoprene, at a probe velocity of 50 mm/min. 0, I, X, T, M and F indicate the stages in the puncture process.

3.1.3 Parameters Governing Needlestick Mechanism

To identify the intrinsic properties of the material that govern the process of needlesticks, a detailed study was conducted of the energy balance between the point where the needle begins to penetrate a sample of neoprene rubber (Figure 10, position I) and the point where the tip of the needle reaches the underside of the sample (Figure 10, position X). This analysis (see Appendix B for details) includes the development of a method for calculating the fracture energy of needlestick. Microscopic observation of the rubber surface pierced by the needle shows the formation of an elliptical crack in the material (Figure 11).

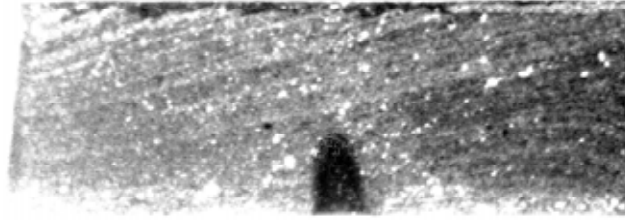


Figure 11 – Optical microscopic image of surface of neoprene sample pierced by a medical needle (x20)

The results given in Appendix B indicate that a needlestick through elastomer involves crack initiation and propagation phenomena that can be characterized by the dissipation of the fracture energy. Friction also plays a significant role.

3.1.4 Calculation of Fracture Energy of Rubber Associated with Needlesticks

In the previous section it was shown that, for rubber, the needlestick mechanism is governed by, among other things, the energy dissipated through crack initiation and propagation. Friction between the needle and the surface of the crack made in the material also plays a significant role in the mechanism. To help calculate the value of the fracture energy associated with needlestick, a technique was used to eliminate the effect of friction on the process.

The technique is based on prestretching the material, in a manner similar to the one that other researchers have used to determine the intrinsic fracture energy for cutting [54,55,56,57]. When the principles proposed by Lake and Yeoh [54,55] are extended to needlesticks following prestretching, the rate of total energy restitution G (per unit of fracture surface) is given by:

$$G = P + T \quad \text{Equation 1}$$

where P is puncture energy and T energy associated with the prestrain. According to what Lake and Yeoh obtained for cutting, G depends solely on the material tested [54]. G should therefore remain constant for low values of T , meaning that an increase in strain energy should correspond to a decrease in puncture energy. At the highest values of T , more complex behaviour is expected because the role played by tearing becomes more significant.

The fracture energy values associated with needlestick were calculated for neoprene and nitrile using the prestrain technique and by extrapolating to zero prestrain, following the method described in Appendix C. The results are given in Table 4, along with the fracture energy values for cutting and tearing obtained for the same neoprene [58] and the same nitrile [59].

Table 4 – Fracture energy values associated with puncture by 23G medical needles, cutting and tearing of neoprene and nitrile

	Neoprene (1.6 mm)	Nitrile (0.8 mm)
Fracture energy for needlestick (kJ/m ²)	1.52	3.54
Fracture energy for cutting (kJ/m ²)	0.7	1.38
Fracture energy for tearing (kJ/m ²)	6.2	9.6

It would appear that the fracture energy of rubber when punctured by a needle is higher than that for cutting, but lower than that for tearing. Thomas's work on rubber fracture may offer an explanation [60]. He showed that the energy release rate during fracture is closely related to the strain energy density at the crack tip (when fracture occurs) and proposed the following relationship for the rate of energy restitution at fracture G :

$$G = W_f d \quad \text{Equation 2}$$

where W_f is the energy density at fracture and d the effective diameter at the crack tip.

The differences between the fracture energy values for needlestick, cutting and tearing obtained for neoprene and nitrile (Table 4) could be due to the differences in the diameters of the crack tips in the three cases: greatest in the case of tearing (0.1–1 mm), intermediary in the case of needles (0.35–0.80 mm) and lowest in the case of cutting (100 nm) [59].

3.2 Effect of Needle Characteristics

In this section, the effect on the maximum puncture force of the various needle characteristics, including variability in manufacture, wear as a result of repeated use as puncture probes, diameter, tip angle and number of facets, was evaluated for the different glove materials.

3.2.1 Effect of Variability in Needle Manufacture

The measurements taken with conical-head puncture probes produced higher puncture force variation values than the measurements with flat-tip or hemispheric-tip probes [61]. This effect has been attributed to greater variability in their geometric characteristics because they are more difficult to manufacture. Since the needles used as probes for measuring glove needlestick resistance are mass-produced, variations in size, geometry and characteristics probably occur, which could also lead to variability in puncture force [12]. As a result, a study was conducted to characterize and identify the source of the variability in puncture force measurements attributable to the use of commercially available medical needles as puncture probes.

For this purpose, tests were conducted on a series of 15 three-facet 21G (0.8 mm) needles taken from the same box of 100 and a sample cut from a sheet of 0.4 mm neoprene. The measurements were taken at a probe velocity of 13 mm/min, with each needle being used once. The results in terms of maximum puncture force for the 15 needles tested are set out in Table 5. The force varies around a mean value of 1.2 N, with a standard deviation of 0.2 N and a coefficient of variation of 17%. Note that variations less than or equal to 1% were seen in the thickness of the sheet of neoprene.

Table 5 – Puncture force values and dimensions of 21G needles used to test variability associated with needle manufacturing tolerances, *L*: total length of bevel, *l*: thickness of needle wall at tip, and *D* and *d*, respectively: outside and inside diameter at transition between facets (SD: standard deviation; CV: coefficient of variation)

Test	Force (N)	<i>D</i> (mm)	<i>d</i> (mm)	<i>L</i> (mm)	<i>l</i> (mm)
1	1.15	0.742	0.478	3.260	0.314
2	1.15	0.740	0.480	3.192	0.291
3	0.96	0.670	0.434	3.340	0.442
4	1.79	0.767	0.427	3.343	0.360
5	1.06	0.684	0.446	3.499	0.369
6	1.40	0.759	0.480	3.366	0.241
7	1.11	0.737	0.470	3.278	0.250
8	1.10	0.722	0.469	3.273	0.298
9	1.09	0.723	0.459	3.143	0.310
10	1.11	0.728	0.364	3.217	0.316
11	1.09	0.703	0.429	3.387	0.316
12	1.20	0.745	0.471	3.300	0.323
13	1.34	0.757	0.472	3.217	0.303
14	1.27	0.750	0.457	3.314	0.293
15	1.19	0.745	0.464	3.160	0.346
Mean	1.20	0.731	0.453	3.290	0.318
SD	0.20	0.027	0.031	0.098	0.049
CV	17%	4%	7%	3%	15%

To identify the cause of the variability, the geometric parameters of the 15 needles used were characterized by optical microscopy. As Figure 12 shows, four dimensions were measured: *L* is the total length of the bevel, *l* the thickness of the needle wall at the tip, and *D* and *d*, respectively the outside and inside diameter of the needle at the transition between the facets. Table 5 gives the measurements for the 15 needles. Variability ranging from 3% to 15% was found in these characteristic dimensions.

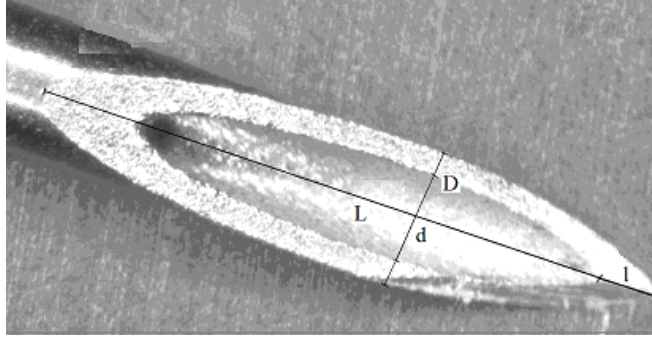


Figure 12 – Dimensions L , D , l and d of medical needles, L : total length of bevel, l : thickness of wall of needle at tip, and D and d , respectively: outside and inside diameter at transition between facets

The maximum puncture force measured in each of the 15 tests was expressed as a function of each characteristic dimension of the needle used in the test. The only size parameter that seems to have an effect on maximum puncture force is D , the outside diameter of the needle at the transition between the facets (Figure 13).

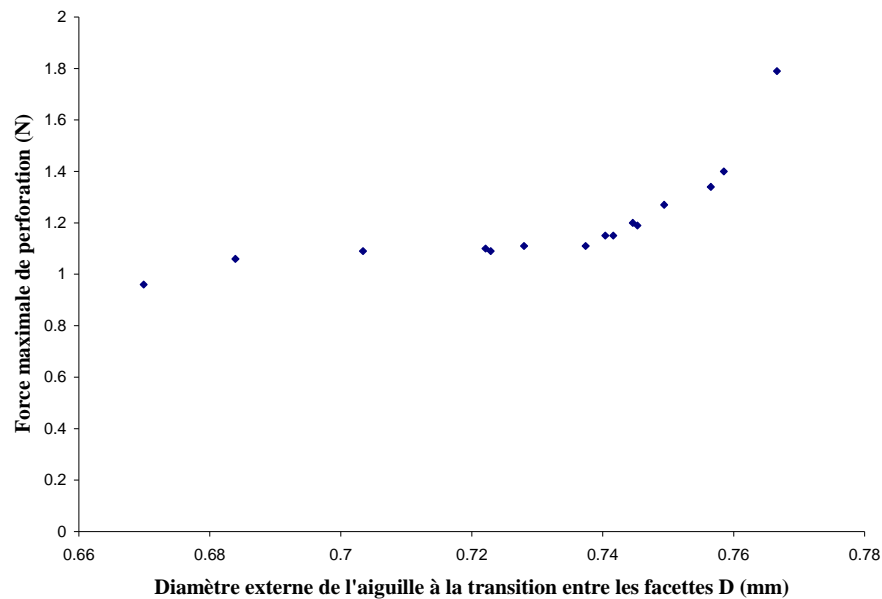


Figure 13 – Change in maximum puncture force as a function of outside diameter of needle at transition between facets for 15 measurements with 0.4 mm neoprene and 21G needles travelling at 13 mm/min

3.2.2 Effect of Needle Wear

A preliminary study of the effect of needle wear was conducted as part of the research project on glove resistance to multiple hazards [32]. It was found that for a 1.6 mm sheet of neoprene and three-facet 23G (0.65 mm) and 28G (0.35 mm) medical needles, the needle tip deteriorated to the same extent, causing an increase in maximum puncture force. The effect was attributed to

progressive dulling of the cutting edge of the needle tip. However, the rate of deterioration, identical for needles of both sizes, was still relatively low, with a variation in maximum puncture force of less than 7% after the same needle had been used 10 times in a row.

However, for materials harder than pure elastomers, greater wear of the cutting tip of the needle can occur and have a significant effect on measurement results. A study was therefore done with sheets of fabric-backed nitrile, samples from neoprene-coated interlock knit gloves with a rough finish (Scorpio® gloves, palm area) and a triple layer of SuperFabric®. Maximum puncture force was measured for each material, reusing the same needle for successive tests, with three-facet 21G (0.8 mm) and 27G (0.4 mm) needles.

A rapid increase in maximum puncture force was seen for two thicknesses (1.6 and 4.2 mm) of a sheet of fabric-backed nitrile with the two sizes of needle (Figure 14). The increase was due to needle wear. For the finer 27G (0.4 mm) needle, only two tests in a row could be done on the two layers of fabric-backed nitrile. During the third test, the needle bent, failing to penetrate the material.

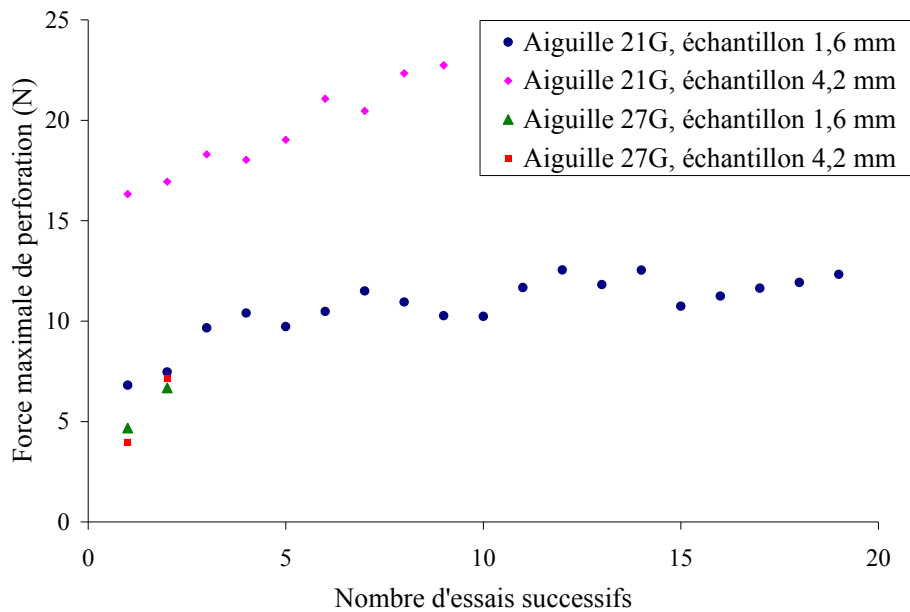


Figure 14 – Effect of needle wear on penetration of fabric-backed nitrile with 21G and 27G needles travelling at 13 mm/min

For the neoprene-coated fabric with a rough finish, the puncture force also increases with successive reuse of the needle (Figure 15). The rate of wear of the cutting tip of the needle is much higher (around 10 times higher), however, than what has been reported for pure neoprene [32]. As a result, when measurements are taken on lined gloves, especially if the finish contains reinforcement particles, a new needle must be used for each measurement.

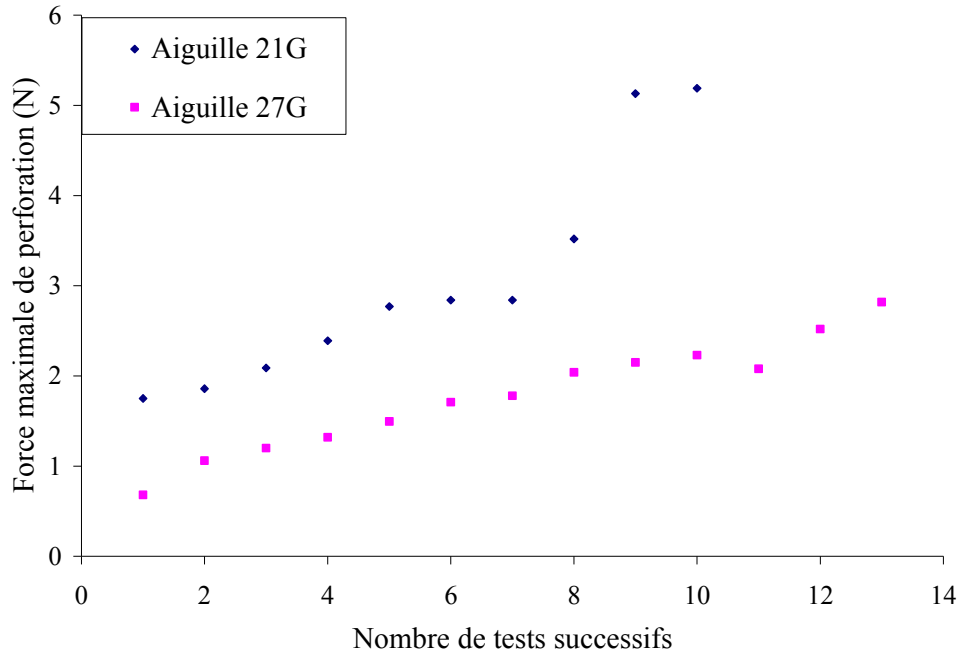


Figure 15 – Effect of needle wear on penetration of neoprene-coated fabric having a rough, hard-particle finish, with 21G and 27G needles travelling at 13 mm/min

The effect of needle wear was also explored with three superimposed layers of SuperFabric[®], with the middle layer at 90° to the top and bottom layers, following the manufacturer's instructions. For the 21G (0.8 mm) needle, Figure 16 shows that maximum puncture force increases significantly with successive use of the needle. When a 27G (0.4 mm) needle was used on a triple layer of SuperFabric[®], the same thing happened as with the fabric-backed nitrile: the needle bent and broke after a few tests. This kind of rapid wear of the needle tip may be due to the nature of SuperFabric[®] and particularly the tiny hard plates attached to the fabric surface. Measuring this kind of material's needlestick resistance therefore requires systematic use of new needles as puncture probes.

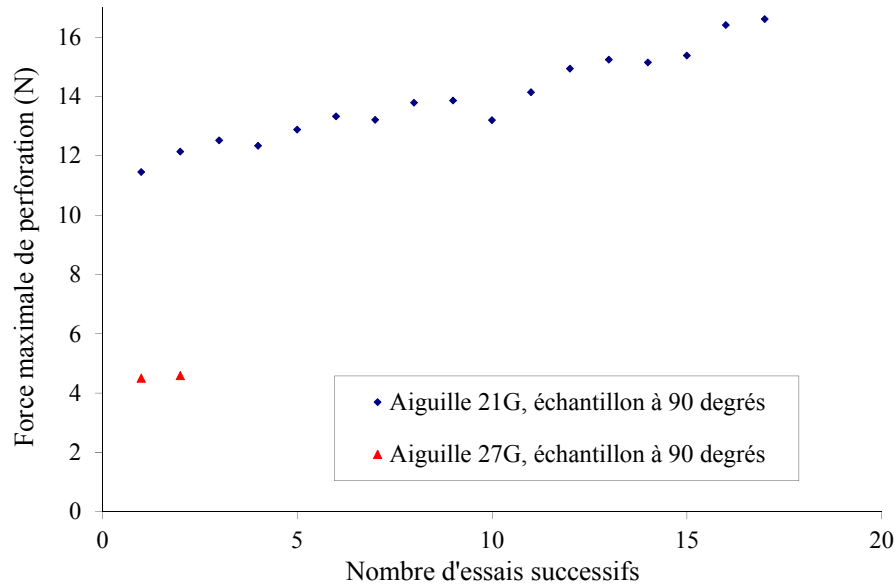


Figure 16 – Effect of needle wear on penetration with 21G and 27G needles of three superimposed layers of SuperFabric[®], with the middle layer at 90° (0/90/0) to the other two (needle velocity of 13 mm/min)

3.2.3 Effect of Needle Diameter

The influence of needle diameter on maximum puncture force was measured using three-facet needles of different diameters between 0.32 and 0.80 mm (29G to 21G) on different types of protective materials.

Figure 17 shows the measurement results for a 0.8 mm sheet of nitrile and a 1.6 mm sheet of neoprene. Note that the probe velocity was 50 mm/min for the neoprene and 13 mm/min for the nitrile. Puncture force increased linearly with needle diameter. For the neoprene, puncture force was proportional to needle diameter, similarly to what was found for round-tip and flat-tip probes [43].

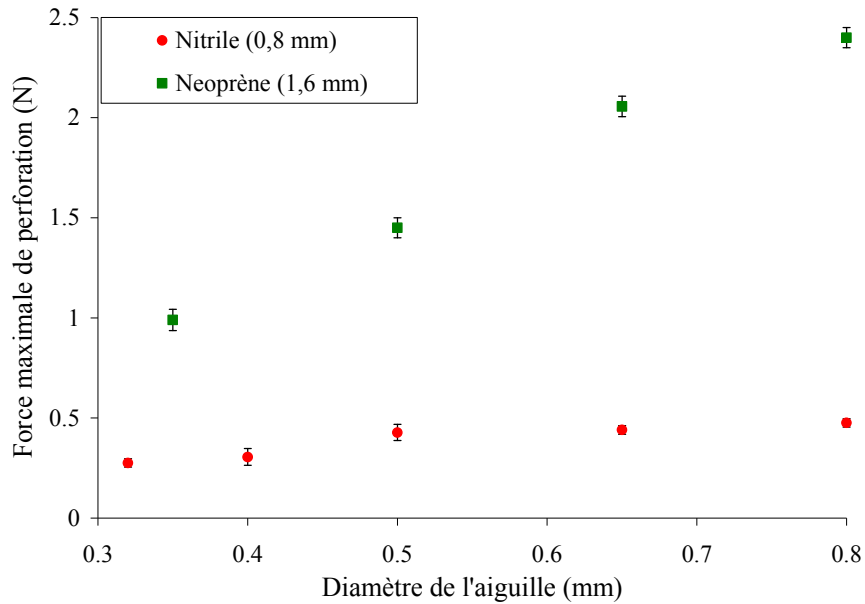


Figure 17 – Change in maximum penetration force as a function of needle diameter for a 0.8 mm sheet of nitrile and a 1.6 mm sheet of neoprene (needle velocity of 50 mm/min for neoprene and 13 mm/min for nitrile)

For the neoprene-coated fabric (Scorpio[®] gloves, samples taken from wrist area), a much higher maximum puncture force value and greater data variability were seen with the largest needle (21G, 0.8 mm) (Figure 18). These higher forces could be caused by greater interaction between the needle and the interlock knit fabric, with the largest needle being unable to slide as easily as the finer needles between the stitches of the fabric. These observations concur with the conclusions of a study on puncture in which the differences in measured force values for lined gloves with two sizes of round-tip probe were attributed to the interaction of the needle tip with the threads of the glove liner [42]. Generally, the relatively significant error bars for this material are due to the inherent lack of homogeneity of the fabric liner: the maximum puncture force values measured differ depending on the position of the puncture site in relation to the stitches of the interlock knit fabric.

For SuperFabric[®], whether the triple-layer configuration or the Hercules One gloves, the maximum puncture force also increases with needle diameter (Figure 19). In addition, for the two materials, no data are available for the finer (29G, 0.32 mm) needles because they break before they can get through the material. Note also that the high variability in the measurement results for SuperFabric[®] may be ascribed to the inherent lack of homogeneity of the material. Indeed, the maximum force value measured depends not just on the position of the puncture site in relation to the tiny hard plates, but also on the relative position of the plates on the different superimposed layers, as Figure 1 shows.

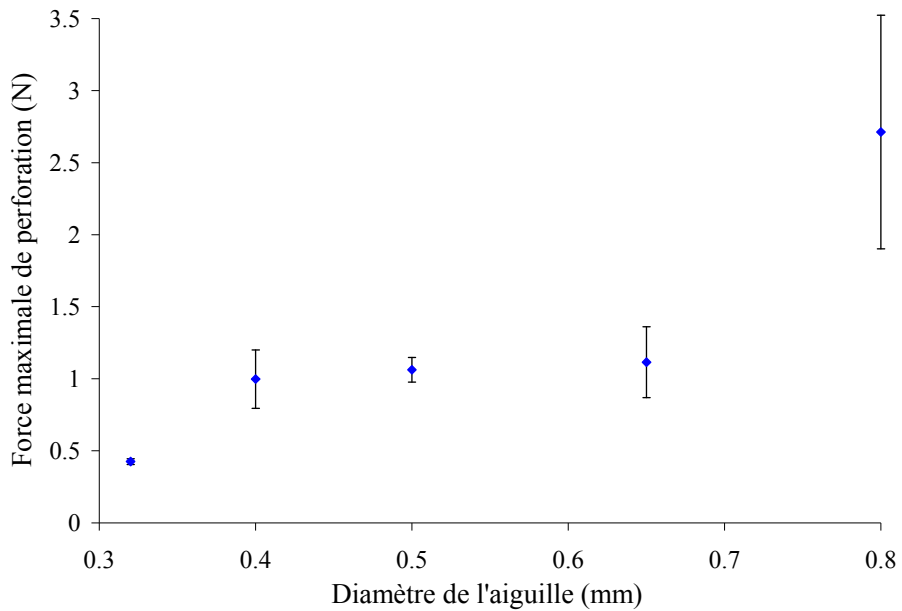


Figure 18 – Change in maximum puncture force as a function of needle diameter for neoprene-coated interlock knit cotton (Scorpio[®] gloves, wrist area), with a needle velocity of 13 mm/min

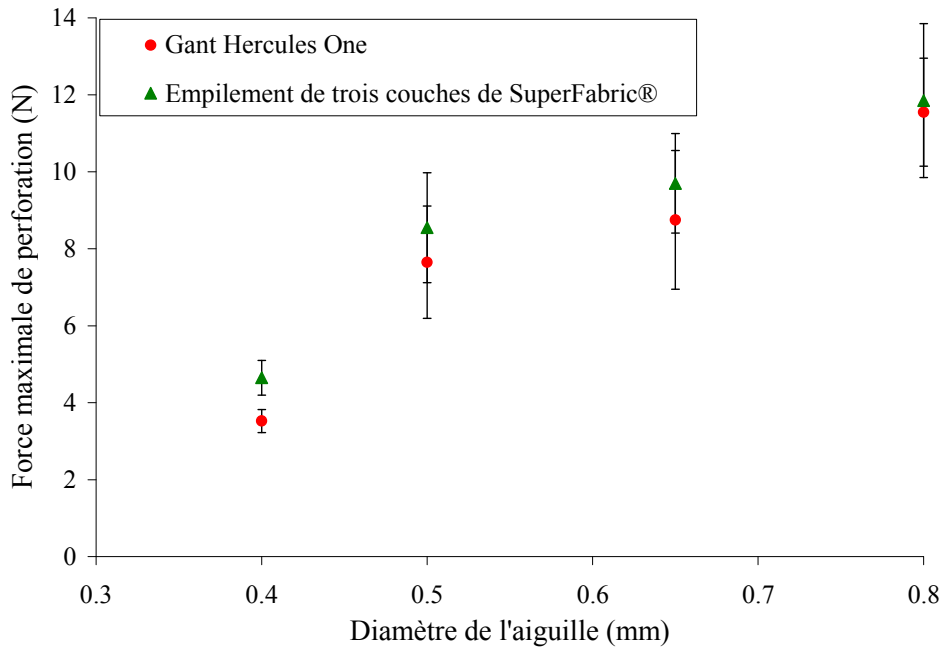


Figure 19 – Change in maximum puncture force as a function of needle diameter for a triple-layer configuration of SuperFabric[®] (middle layer at 90° to the other two) and for samples from Hercules One gloves (needle velocity of 13 mm/min)

Lastly, samples of two types of TurtleSkin[®], S 002-b (thin coated fabric) and D 006-b (thick fabric), were also tested. In both cases, maximum puncture force increased with needle diameter.

The relatively large error bars are related, as in the earlier case, to the lack of homogeneity of the fabric (Figure 20).

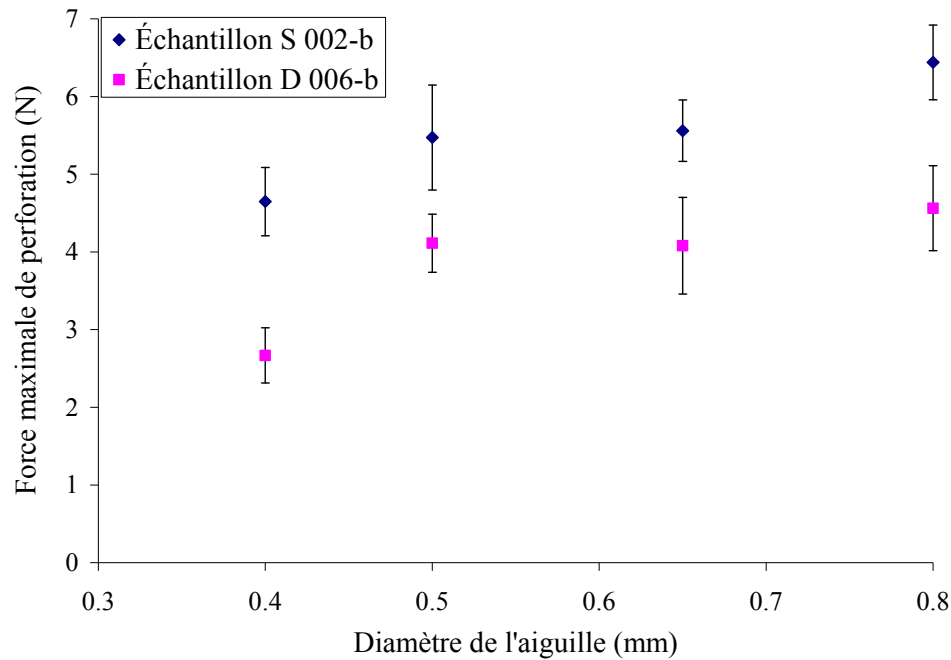


Figure 20 – Change in maximum puncture force as a function of needle diameter for TurtleSkin[®] (samples S 002-b and D 006b), with a needle velocity of 26 mm/min

3.2.4 Effect of Needle Tip Angle

For elastomers, it has been shown that needlesticks involve cutting factors related to the sharp edge of the needle tip. It is therefore important to evaluate the influence of needle tip angle on puncture force. For this purpose, measurements were taken with two models of single-facet, 25G (0.5 mm) needles having different tip angles.

The tests on the effect of needle tip angle on maximum puncture force were conducted on four protective materials: a 1.6 mm sheet of neoprene, a 0.8 mm sheet of nitrile, a neoprene-coated knit cotton material (samples taken from wrist area) and a three-layer stack of SuperFabric[®] (Table 6).

Table 6 – Effect of needle tip angle on maximum puncture force for four protective glove materials, with single-facet 25G needles travelling at 13 mm/min (standard deviation in parentheses) and ANOVA with 95% confidence interval

Materials	Maximum puncture force (N)		ANOVA		
	20° angle	30° angle	<i>F</i>	Result	CCL
Neoprene (1.6 mm)	0.91 (0.03)	0.95 (0.06)	1.1	NS	
Nitrile (0.8 mm)	0.48 (0.02)	0.54 (0.03)	10.3	S	98%
Neoprene-coated knit cotton fabric (wrist)	1.8 (0.3)	2.0 (0.2)	1.9	NS	
Three layers of SuperFabric®	7.0 (1.4)	6.4 (1.4)	0.4	NS	

F: ratio of intergroup and intragroup variances
 Result: S for significant, NS for nonsignificant
 CCL: calculated confidence level

Single-factor analysis of variance (ANOVA) was carried out on the results using Fisher’s *F* distribution to determine the critical value $F_{crit} = 6.0$ corresponding to the desired confidence level of 95% ($\alpha = 0.05$). The homogeneity of variance of the data was tested, as were the normality and independence of the residuals. Statistically significant differences in maximum puncture force values related to the effect of the needle tip angle were found, with a 95% confidence level for nitrile (Table 6): the maximum puncture force is slightly higher for the greater tip angle. Moreover, even if the differences in maximum puncture force were not significant, the same tendency can be seen for the sheet of neoprene and for the neoprene-coated knit gloves. The effect may be due to the fact that a smaller tip angle corresponds to a larger cutting edge, which means the needle tip has greater cutting capacity.

3.2.5 Effect of Number of Facets

The effect of the number of facets on the value of the maximum puncture force was examined with the same four protective materials: the 1.6 mm sheet of neoprene, the 0.8 mm sheet of nitrile, the neoprene-coated knit cotton material (samples taken from wrist area) and the triple-layer stack of SuperFabric® (Table 7). Note that there is a small difference of 2° in the tip angle between the single-facet and the three-facet needles used for these tests. However, in light of the results in the preceding section on the effect of tip angle, the difference may be regarded as negligible.

Table 7 – Effect of number of needle facets on maximum puncture force for four protective materials, with 25G needles travelling at 13 mm/min (standard deviation in parentheses) and ANOVA with 95% confidence interval

Materials	Maximum puncture force (N)		ANOVA		
	Single-facet needle (20° angle)	Three-facet needle (18° angle)	<i>F</i>	Result	CCL
Neoprene (1.6 mm)	0.91 (0.03)	1.13 (0.06)	35.7	S	99.9%
Nitrile (0.8 mm)	0.48 (0.02)	0.46 (0.04)	0.4	NS	
Neoprene-coated knit cotton (wrist)	1.8 (0.3)	1.0 (0.2)	20.7	S	99.6%
Three layers of SuperFabric®	7.0 (1.4)	7.1 (1.2)	0.01	NS	

F: ratio of intergroup and intragroup variances
 Result: S for significant, NS for nonsignificant
 CCL: calculated confidence level

The same ANOVA was done as in the previous section. The homogeneity of variance of the data was tested, as were the normality and independence of the residuals. Statistically significant differences in maximum puncture force values related to the effect of the number of needle facets were found, with a 95% confidence level for neoprene and neoprene-coated knit cotton gloves (Table 8). However, the two materials have contrasting behaviours. For the sheet of neoprene, the maximum puncture force was higher for three-facet than for single-facet needles. For the neoprene-coated knit cotton gloves, in contrast, the maximum puncture force was lower for the three-facet needles.

Further measurements would be required to explain the results obtained. Neoprene and nitrile are two homogeneous types of rubber that generally behave quite similarly. The effect may have been more significant for the neoprene because the samples were thicker (1.6 mm) than the nitrile samples (0.8 mm). For the neoprene-coated knit cotton material, the reduction in maximum puncture force could be due to the tight knit of the lining. The study of the effect of needle diameter on maximum puncture force revealed that the interlock knit liner has a certain influence on the needlestick process (see Figure 18).

3.3 Effect of Sample

This section examines the influence of the type of material, size of the sample-holder hole, membrane thickness and material hardness.

3.3.1 Effect of Type of Material

For the purposes of a quantitative comparison of the needlestick resistance of the different materials, the maximum puncture force values measured under identical conditions, i.e., with a three-facet 25G (0.5 mm) needle and a needle velocity of 13 mm/min, have been combined in Figure 21. Two groups of materials can be identified. First, elastomers and lined elastomers offer very little resistance to needlesticks. Second, the two types of material, i.e., SuperFabric® and TurtleSkin®, developed specially to provide better protection against mechanical hazards score higher in terms of needlestick resistance.

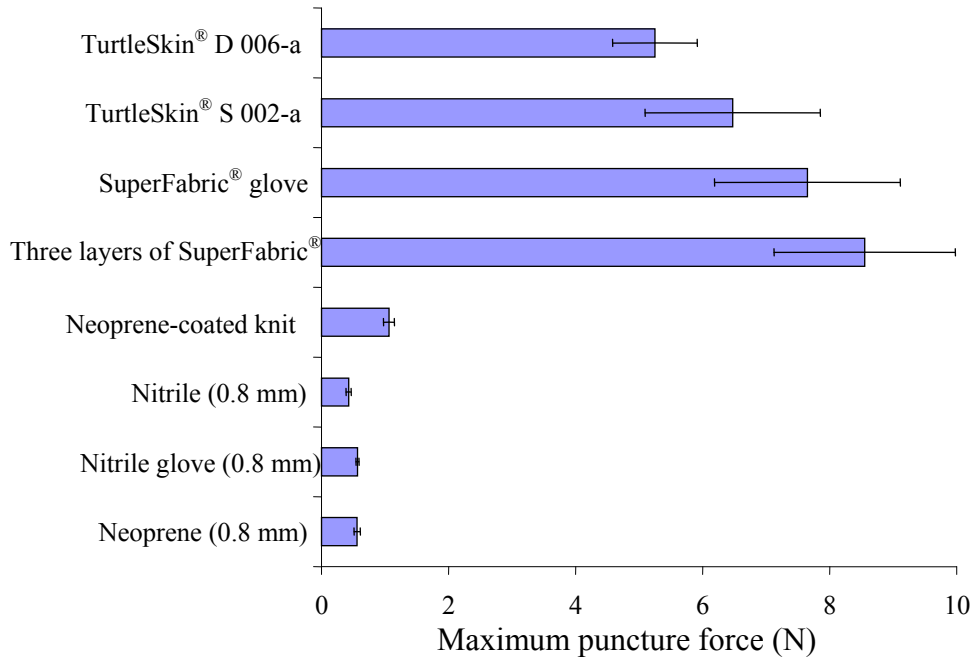


Figure 21 – Comparison of maximum puncture force values for different protective materials, with a 25G needle travelling at 13 mm/min

Microscopically, differences can also be seen in how these different materials behave when punctured by needles. For elastomers, the puncture site is a clean cut, with the diameter of the hole being close to that of the needle (Figure 11, p. 21). For a coated knit material, the needle tip may interact directly with the fabric lining, depending on the position of the puncture site in relation to the stitches (Figure 22). When force-versus-displacement curves are plotted, this may produce several maxima or a broader maximum.

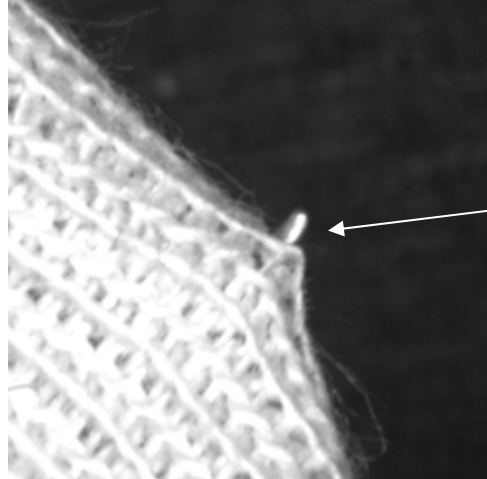


Figure 22 – Optical microscopic image of interaction between needle tip and liner yarn on penetration of neoprene-coated interlock knit sample

In the case of SuperFabric[®], the very different nature of the material, featuring tiny hard plates attached to a fabric backing, means that another mechanism comes into play. When the needle encounters a hard plate, it doesn't result in a cut, but rather a brittle fracture of the plate (Figure 23). On force-versus-displacement curves, a fracture of this kind is reflected in several maxima or a broader maximum (Figure 24). Lastly, there may be an interaction between the needle and the yarn of the woven liner of TurtleSkin[®], as well (Figure 25).

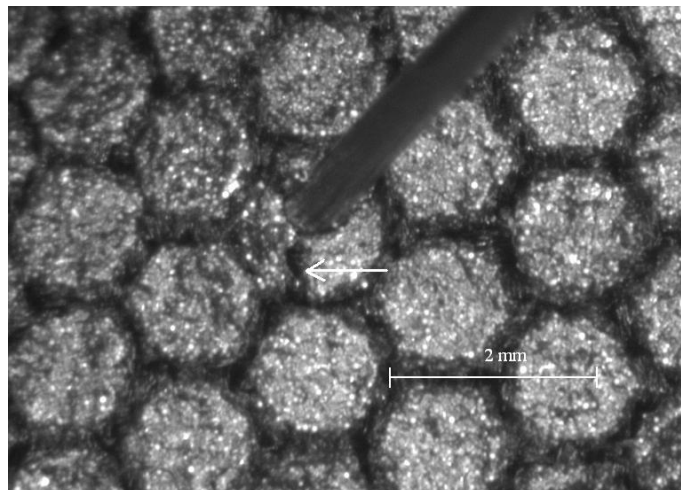


Figure 23 – Optical microscopic image of puncture site of a SuperFabric[®] sample, showing where a needle caused a brittle fracture of the hard plate

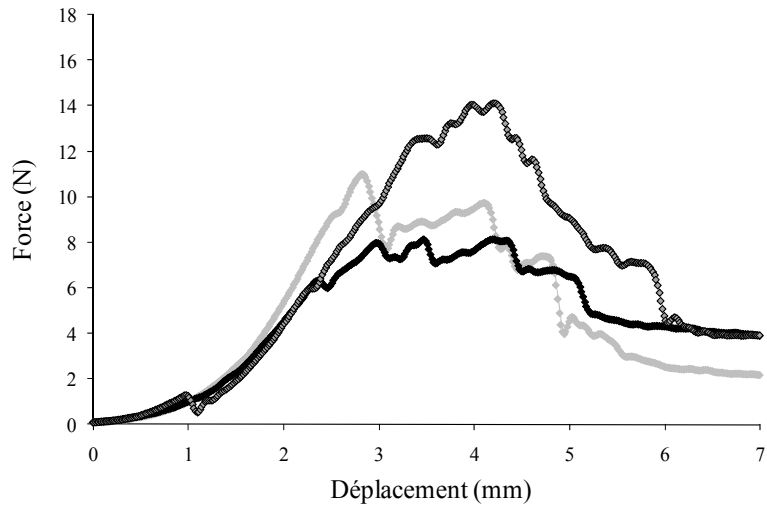


Figure 24 – Three examples of change in force as a function of 25G needle displacement, for a three-layer sample of SuperFabric®

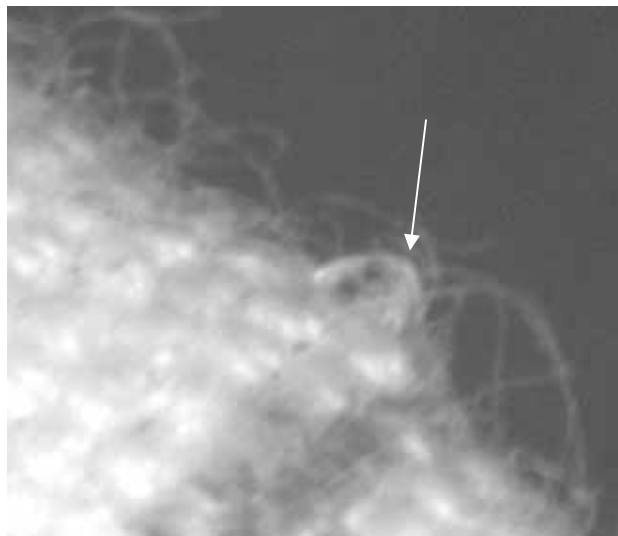


Figure 25 – Optical microscopic image of interaction between needle tip and yarn of woven liner on penetration of sample of TurtleSkin® D 006-a (woven lining with polymer coating)

3.3.2 Effect of Size of Hole of Sample Holder

To examine the influence of the size of the sample-holder hole on needlestick resistance, two diameters were used, 13.5 mm and 38.0 mm. Measurements of maximum puncture force and of needle displacement at maximum force were taken with two different thicknesses of neoprene, nitrile, fabric-backed nitrile and a layer of SuperFabric® (Table 8).

Table 8 – Maximum puncture force (F) and displacement (d) values of 25G needles with two diameters of sample-holder hole D_h (13.5 and 38.0 mm) for different materials, with a needle velocity of 13 mm/min (standard deviation in parentheses)

	$D_h = 13.5$ mm		$D_h = 38.0$ mm	
	F (N)	d (mm)	F (N)	d (mm)
Neoprene (0.8 mm)	0.56 (0.05)	3.1 (0.2)	0.57 (0.05)	5.3 (0.4)
Neoprene (1.6 mm)	1.20 (0.10)	3.2 (0.1)	1.20 (0.10)	5.3 (0.6)
Nitrile (0.8 mm)	0.47 (0.04)	3.2 (0.2)	0.50 (0.04)	5.1 (0.2)
Fabric-backed nitrile (1.6 mm)	5.30 (0.60)	2.8 (0.3)	5.00 (0.70)	3.8 (0.3)
SuperFabric [®] (one layer)	2.80 (1.10)	3.2 (0.6)	2.20 (0.70)	4.4 (0.4)

As expected, the maximum deformation was higher with the larger hole of the sample holder in the case of elastomers. Although a difference can be seen in the deformation rate between the two sizes of sample-holder hole—big for elastomers and small for lined materials and SuperFabric[®]—no significant variation in maximum puncture force values was observed. These results are consistent with what has been reported for round-tip probes [42].

3.3.3 Effect of Sample Thickness

The influence of material thickness on maximum puncture force was examined with two types of elastomer (neoprene and nitrile), as well as with SuperFabric[®], which can be used in several layers in protective gloves. For neoprene and nitrile, sheets of four different thicknesses were used. For both elastomers, a non-linear increase in maximum puncture force as a function of sample thickness was observed (Figure 26).

On the basis of failure mechanics and the development of Equation 6 (Appendix B, p. 82), the total deformation energy of system W can be expressed as follows [33]:

$$W = G_s \cdot A + W_r \quad \text{Equation 3}$$

where G_s represents the energy needed to create a new fracture surface, A is the fracture surface and W_r is the residual deformation energy after puncture. In the case of needlesticks, the fracture surface created is elliptical (Figure 11). The relationship between maximum puncture force and sample thickness for the two elastomers can therefore be attributed to the shape of the fracture surface. In comparison, linear variation in maximum puncture force as a function of sample thickness has been reported for neoprene for cylindrical probes [42].

Figure 27 shows the change in maximum puncture force measured as a function of number of layers of SuperFabric[®]. A regular increase is likewise observed.

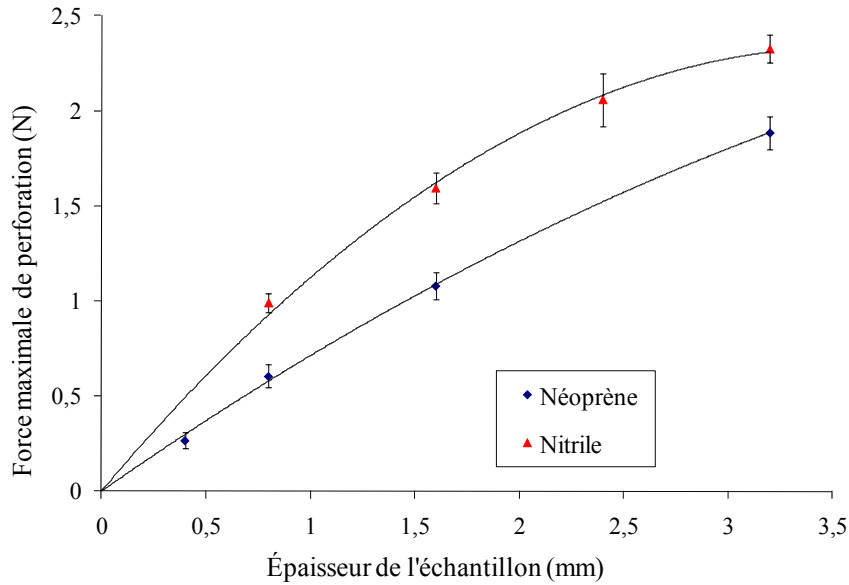


Figure 26 – Change in maximum puncture force as a function of sample thickness for neoprene (50 Shore A) and nitrile (70 Shore A), with 25G needles travelling at 13 mm/min

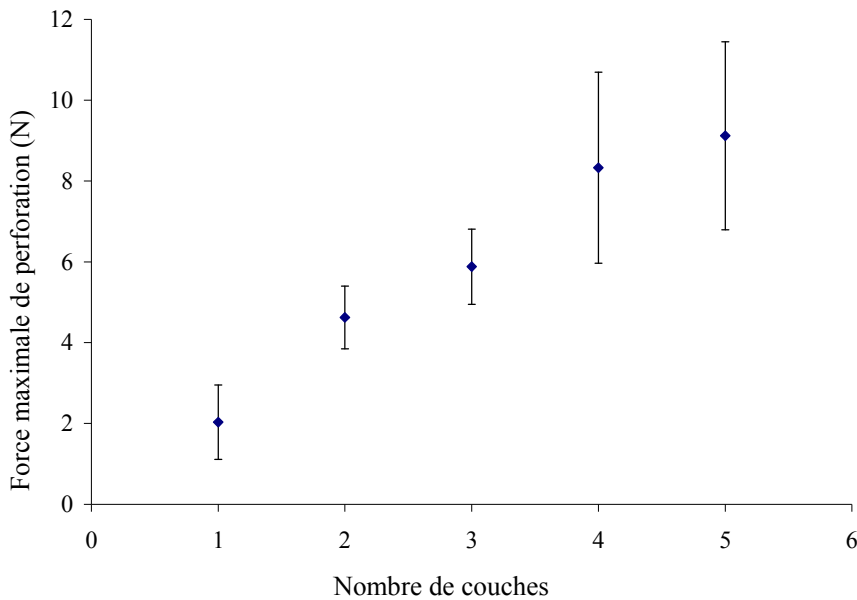


Figure 27 – Change in maximum puncture force as a function of number of layers of SuperFabric[®], with 25G needles travelling at 13 mm/min

3.3.4 Effect of Material Hardness

For neoprene and nitrile, tests were conducted to assess the effect of sample hardness on maximum puncture force. Hardness values were measured using a Shore Instron “A” Scale

IRHD durometer, conforming with ASTM Standard D2240-05 for testing the hardness of rubber [62].

Figure 28 shows change in maximum puncture force as a function of material hardness for a 1.6 mm sheet of neoprene and a 0.8 mm sheet of nitrile, three-facet 25G (0.5 mm) needles and a probe velocity of 13 mm/min. Maximum puncture force can be seen to increase with hardness. Given that needlesticks have been associated with cutting, a parallel could be drawn with the proportionality relationship observed between rubber's cut resistance and its hardness [59].

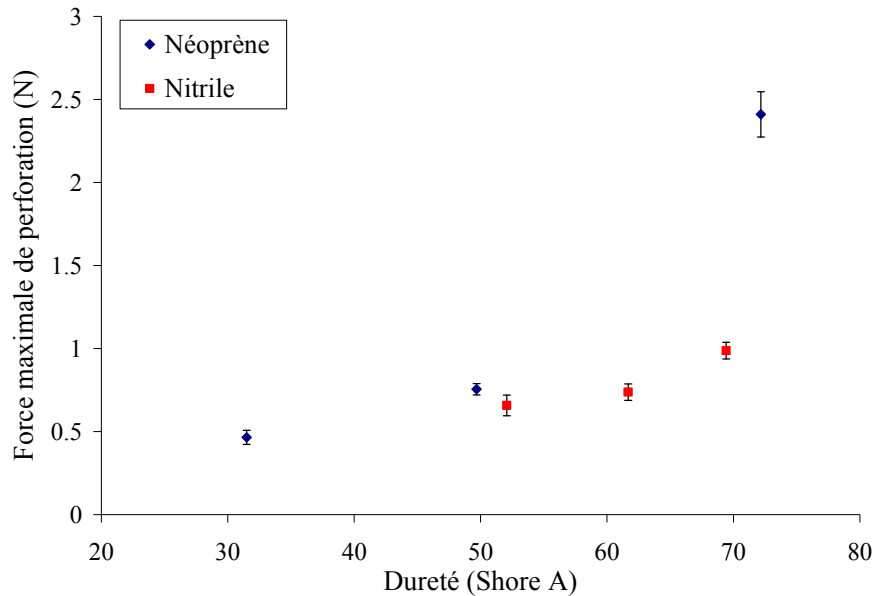


Figure 28 – Change in maximum puncture force as a function of material hardness for a 1.6 mm sheet of neoprene and a 0.8 mm sheet of nitrile, with 25G needles travelling at 13 mm/min

3.4 Effect of Experimental Conditions

This section examines the influence of test conditions on needlestick resistance for the main types of material used to make protective gloves: sheet neoprene and nitrile for unlined gloves; neoprene-coated and uncoated knit cotton and fabric-backed sheet nitrile for lined gloves; and SuperFabric[®] and TurtleSkin[®] materials providing a special structure for sewn gloves. The properties studied were the effect of probe velocity, needle angle of attack in relation to sample, temperature, humidity and presence of a lubricant.

3.4.1 Effect of Probe Velocity

The effect of probe velocity (between 0.2 and 500 mm/min) on maximum puncture force was studied for a variety of materials. For a 1.6 mm sheet of neoprene and three-facet 21G, 25G and 28G (respectively 0.8, 0.5 and 0.35 mm) needles (Figure 29), it can be seen that maximum

puncture force increases with needle velocity between 0.2 and 100 mm/min, then tends to level off beyond 100 mm/min.

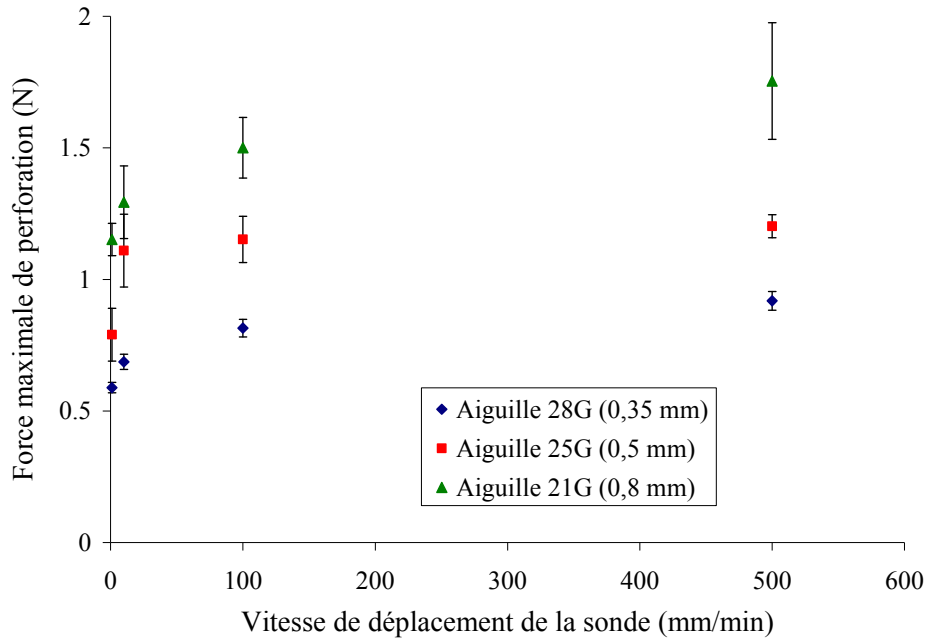


Figure 29 – Change in maximum puncture force as a function of probe velocity for a 1.6 mm sheet of neoprene and 21G, 25G and 28G needles

With respect to developing a measurement method for standardization purposes, this result indicates that small variations in probe velocity around the 500 mm/min mark have a negligible impact on maximum puncture force.

The results obtained with a three-facet 25G (0.5 mm) needle for a sheet of neoprene, a neoprene-coated knit cotton, three layers of SuperFabric[®] and two types of TurtleSkin[®] samples are presented as semilogarithmic plots, in Figure 30, Figure 31 and Figure 32, respectively.

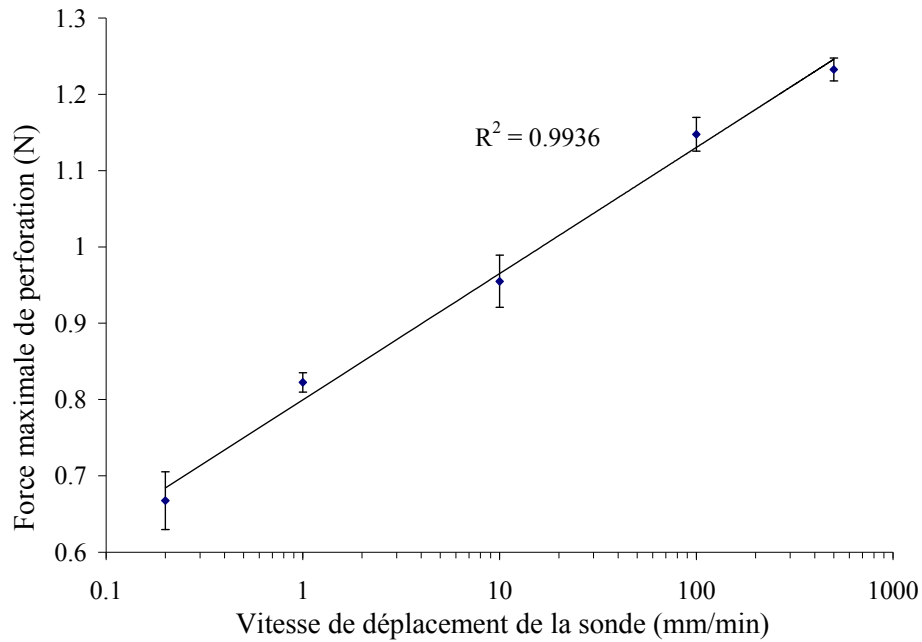


Figure 30 – Change in maximum puncture force as a function of probe velocity on a semilogarithmic scale, for a 1.6 mm sheet of neoprene and 25G needles

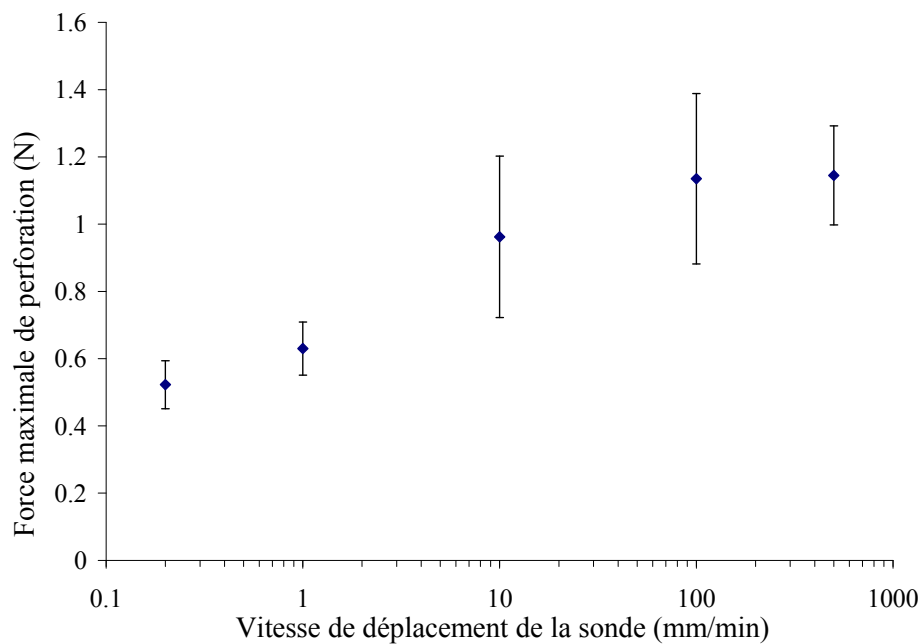


Figure 31 – Change in maximum puncture force as a function of probe velocity on a semilogarithmic scale, for neoprene-coated knit cotton (Scorpio® glove, wrist area) and 25G needles

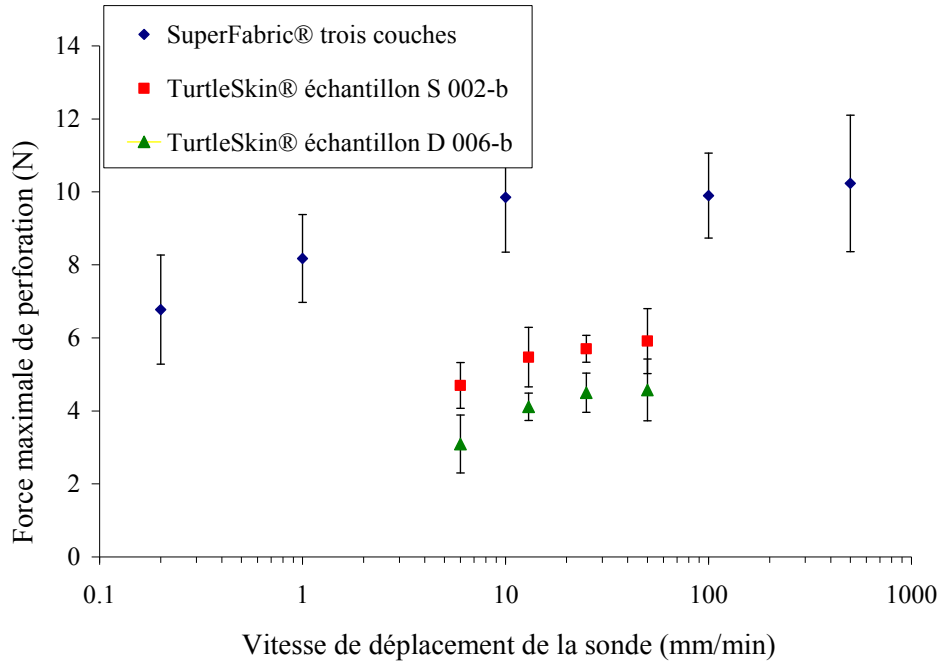


Figure 32 – Change in maximum puncture force as a function of probe velocity on a semilogarithmic scale, for a three-layer stack of SuperFabric® and two types of TurtleSkin® samples (S 002-b and D 006-b), with 25G needles

For all materials, maximum puncture force increases as a function of probe velocity. In addition, for the materials tested, maximum puncture force approximately doubles between 0.2 and 500 mm/min. (Note that in the case of the TurtleSkin® samples, the velocity range was only 6 to 50 mm/min, which is too limited to allow a determination of whether the same rate of change applies.)

For neoprene, a linear rate of change in maximum puncture force as a function of the logarithm of probe velocity can be seen (Figure 30). This behaviour is similar to what was reported for hemispherical- and flat-tipped probes [42]. This monotonic change indicates that the needlestick mechanism for neoprene is identical over the range of probe velocities examined, i.e., between 0.2 and 500 mm/min.

For the other types of material tested—that is, neoprene-coated knit cotton (Figure 31), SuperFabric® and TurtleSkin® (Figure 32)—the large error bars that reflect their intrinsic lack of homogeneity make it impossible to determine accurately the form of the relationship between maximum puncture force and needle velocity. However, the increase in force generally seems to be monotonic. This may indicate that, as for neoprene, a single needlestick mechanism applies for these materials in the range of probe velocities considered.

It should be noted, however, that the probe velocities used in these tests are several orders of magnitude lower than the velocities at which an adult hand can grab something (250 m/min) [63] and much lower again than stabbing velocities (up to 600 m/min) [64]. It may be that the needlestick mechanism highlighted with these moderate probe velocities (see Section 3.1) will

not be the same for impact-type needle velocities. Nonetheless, testing by DuPont [65] has shown that the cut resistance of materials measured at very high blade velocities is similar to that found at moderate velocities. Given that needlesticks can, to a very large degree, be associated with a cutting process, the needlestick resistance of materials under impact velocity conditions may well not differ much from what is measured at moderate velocity.

3.4.2 Effect of Angle of Attack

In actual cases of needlestick injury, angles other than the normal incidence (at a 90° angle) between needle and glove surface at the puncture site can occur (Figure 33). The influence of the needle's angle of penetration into the material, or angle of attack, on the maximum puncture force value was therefore examined. For this purpose, the base of the sample holder was inclined in relation to the needle axis, so that puncture testing could be performed at different angles of attack. The tests were conducted with neoprene, neoprene-coated and uncoated knit cotton fabric, and samples of SuperFabric® and TurtleSkin®. No special attention was given to the relative orientation between the plane of the needle bevel and that of the material being tested.

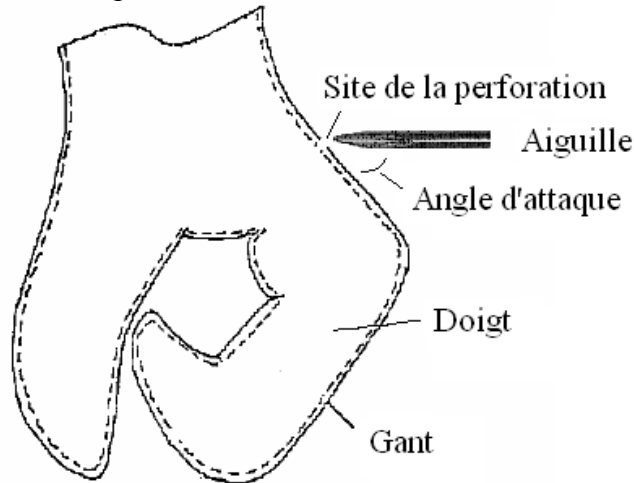


Figure 33 – Needle configuration in relation to surface of protective glove at puncture

Figure 34 shows the change in maximum puncture force as a function of angle of attack of the needle for two thicknesses of neoprene (0.8 and 1.6 mm), three-facet 21G (0.8 mm) needles and a probe velocity of 13 mm/min. It can be seen that the maximum puncture force increases when the angle of attack is less than the normal incidence of 90°.

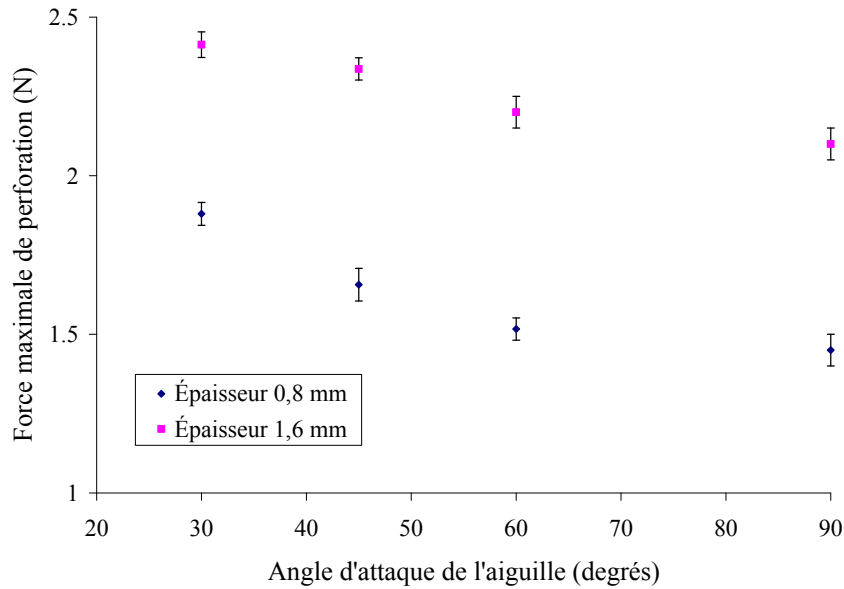


Figure 34 – Change in maximum puncture force as a function of the needle’s angle of attack, for two thicknesses of neoprene (0.8 and 1.6 mm), with 21G needles travelling at 13 mm/min

When the angle of attack differs from 90°, the needle must travel farther to go through the material (Figure 35). The distance actually travelled through the material, h' , may be expressed as a function of the thickness h of the sample and of the angle of attack α of the needle in relation to the plane of the sample, using the following relationship:

$$h' = \frac{h}{\sin \alpha} \tag{Equation 4}$$

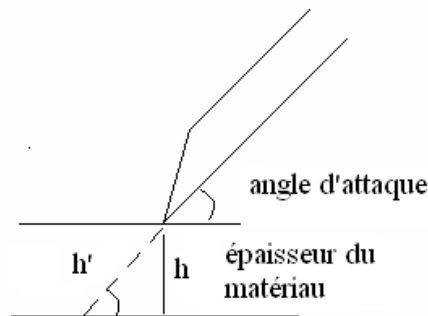


Figure 35 – Diagram of needle penetrating material at an angle other than 90°

The results of Figure 34 were analysed in terms of actual distance h' that the needle travelled through the material (Figure 36). When expressed as a function of h' , the maximum puncture force values for neoprene seem to be superimposed to form a master curve. The results indicate that, for neoprene, the maximum puncture force measured depends on the angle of attack of the needle only in terms of its effect on the thickness of material the needle actually passes through.

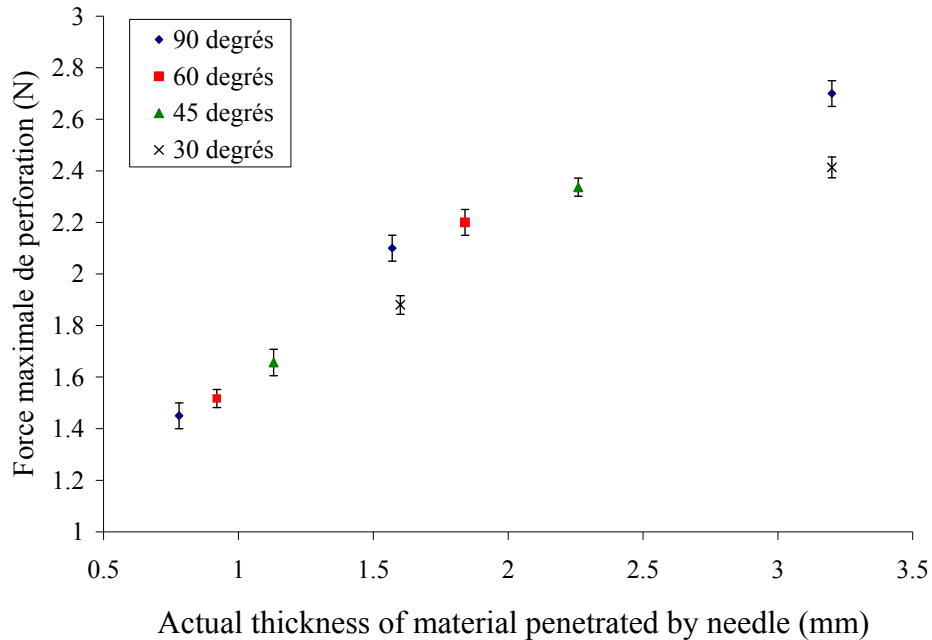


Figure 36 – Change in maximum puncture force as a function of total distance travelled by needle, for three thicknesses of neoprene (0.8, 1.6 and 3.2 mm), four angles of attack (30°, 45°, 60° and 90°) and 21G needles travelling at 13 mm/min

For knit cotton fabric and neoprene-coated knit cotton fabric (Figure 37), as well as for SuperFabric[®] (Figure 38) and TurtleSkin[®] (Figure 39), no significant effect of the angle of attack on the maximum puncture force was observed. For SuperFabric[®], microscopic examination of a puncture site (see Figure 23) shows that the needle makes a brittle fracture in the hard plate. The needlestick process therefore does not seem to depend on the angle of attack of the needle, except in the case of grazing incidence, where the needle can skid across the surface of the plates. For TurtleSkin[®] samples, the lack of effect may be due to the fabric liner.

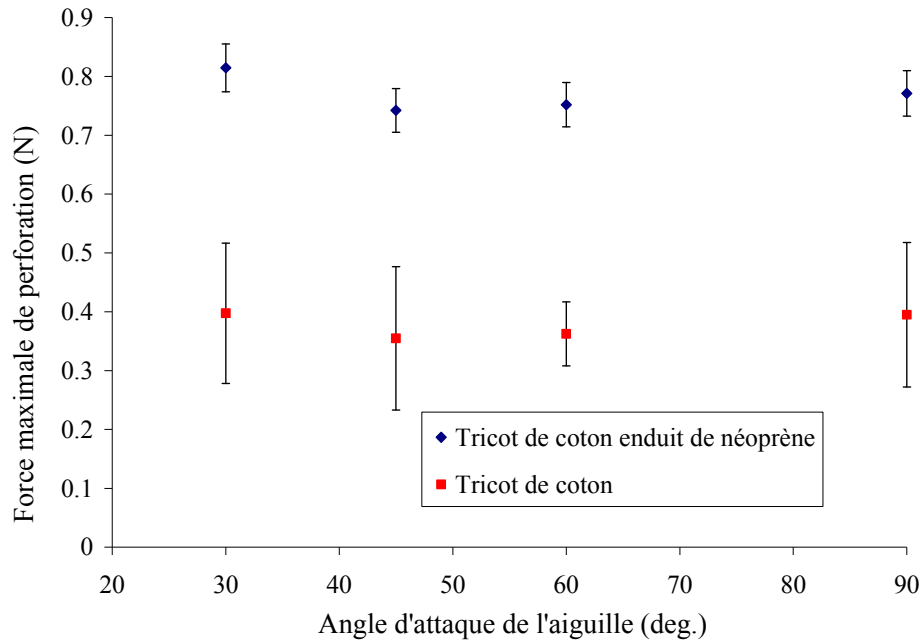


Figure 37 – Change in maximum puncture force as a function of needle’s angle of attack, for knit cotton fabric and neoprene-coated knit cotton fabric (Scorpio[®] glove, wrist area), 25G needles travelling at 13 mm/min

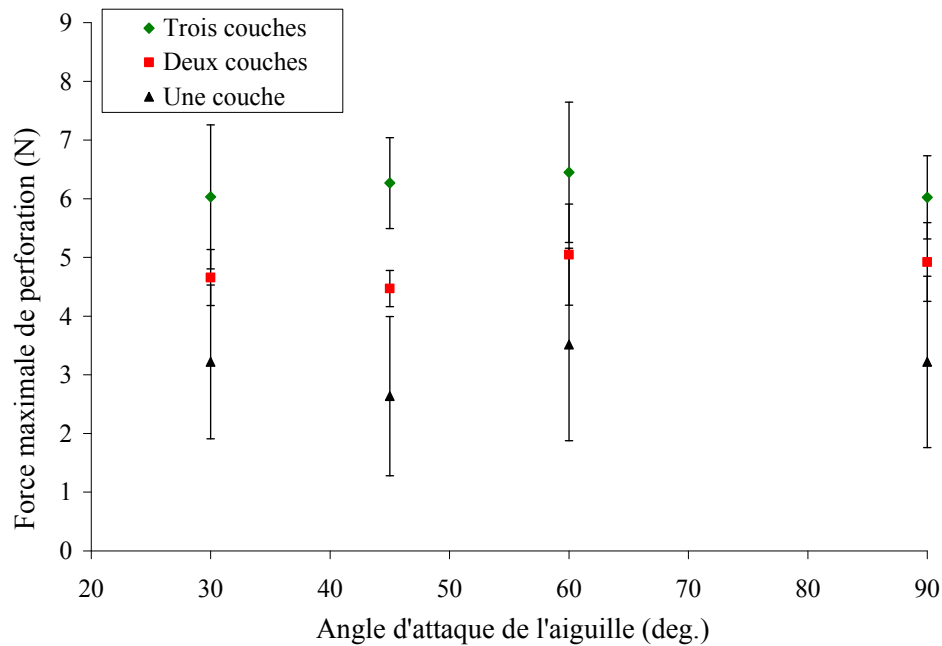


Figure 38 – Change in maximum puncture force as a function of needle’s angle of attack, for one, two and three layers of SuperFabric[®], with 25G needles travelling at 13 mm/min

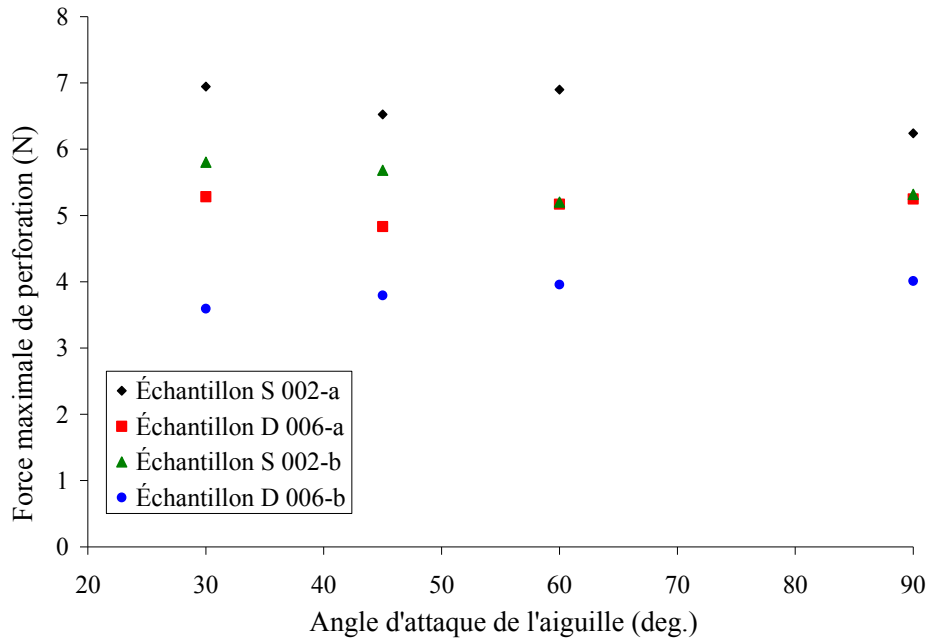


Figure 39 – Change in maximum puncture force as a function of needle’s angle of attack, for TurtleSkin® samples S 002-a, S 002-b, D 006-a and D 006-b, with 25G needles travelling at 13 mm/min (error bars omitted for easier reading)

3.4.3 Effect of Temperature

Variations from the standard 25°C temperature can be caused by two things. First, a microclimate can be created inside protective clothing [66]. For instance, skin temperatures of around 35°C have been recorded inside gloves during laboratory exercises simulating the effort expended by soccer goalkeepers [67]. For gloves, especially non-breathable gloves, worn continuously throughout a shift, this increase in temperature can be significant. Moreover, needlestick protective gloves can be worn in both very cold (e.g., outside in winter in Quebec) and very hot environments.

The influence of temperature on needlestick resistance was studied for four protective glove materials: neoprene, nitrile, fabric-backed nitrile and SuperFabric®. For the testing, the puncture setup shown in Figure 2 (p. 9) was placed in a thermal enclosure system positioned between the uprights of the testing machine. Measurements were taken 20 minutes after placing the sample in the oven in order to allow the temperature of the sample to stabilize.

For a 0.8 mm sheet of neoprene, tested with three-facet 23G (0.65 mm) needles, measurements were taken at temperatures between 25°C and 120°C for different needle velocities (Figure 40). This temperature range is well above this elastomer’s glass transition temperature (-50°C) [68]. A monotonic decline in maximum puncture force as a function of temperature can be seen for all needle velocities. Slight thermal softening has been reported for elastomers in this temperature range [69]. Given that needlesticks have been associated with cutting and that the cut resistance

of rubber has been shown to be proportional to the Young’s modulus of the material [59], the observed effect of temperature on the maximum puncture force for neoprene can be attributed to a change in the elasticity modulus caused by the rise in temperature.

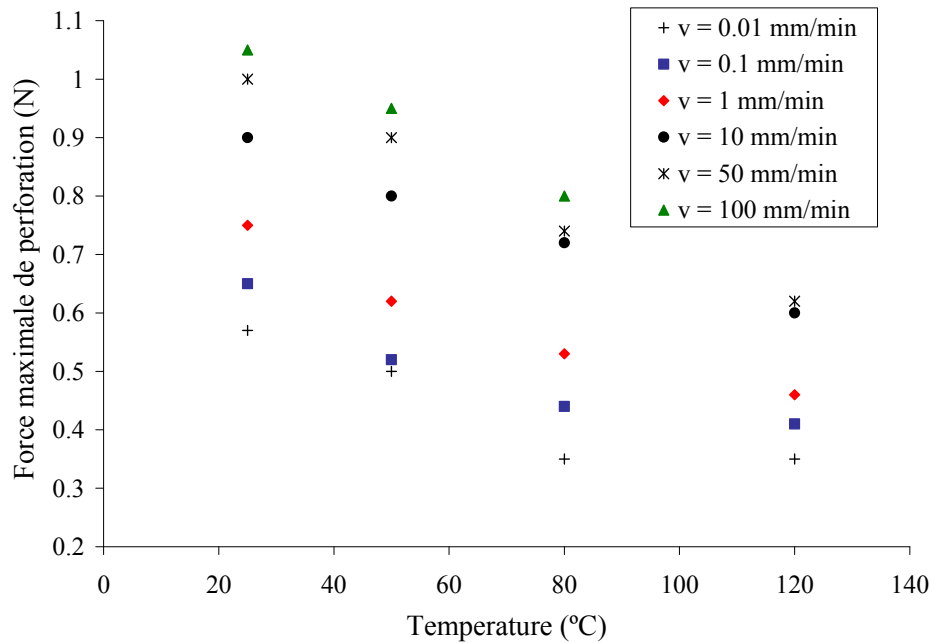


Figure 40 – Influence of temperature on maximum puncture force for a 0.8 mm sheet of neoprene, 23G needles and several needle velocity v values

To test whether neoprene’s needlestick resistance is consistent with the time-temperature superposition principle, a Williams-Landel-Ferry (WLF) transformation [70] was applied to the data in Figure 40. It was shown that fracture energy, which appears to govern the needlestick phenomenon for neoprene (see Section 3.1.3), obeys the WLF relationship [71]. The time-temperature shift factor a_T used for the transformation is provided by the WLF relationship [70]:

$$\log a_T = \frac{-8.8 (T - T_s)}{102 + T - T_s} \tag{Equation 5}$$

where T_s is a selected reference temperature, equal to 25°C. On the basis of the calculated shift factors, a master curve is obtained for the different temperature and probe velocity values (Figure 41). This shows the viscoelasticity of the needlestick mechanism in the case of neoprene. In addition, this result provides a tool for determining needlestick resistance under specific temperature and probe velocity conditions, using a master curve determined from a limited number of measurements. However, it applies only for the velocity and temperature range for which it was established and cannot be extrapolated to impact velocities unless investigation shows that the same mechanisms are involved.

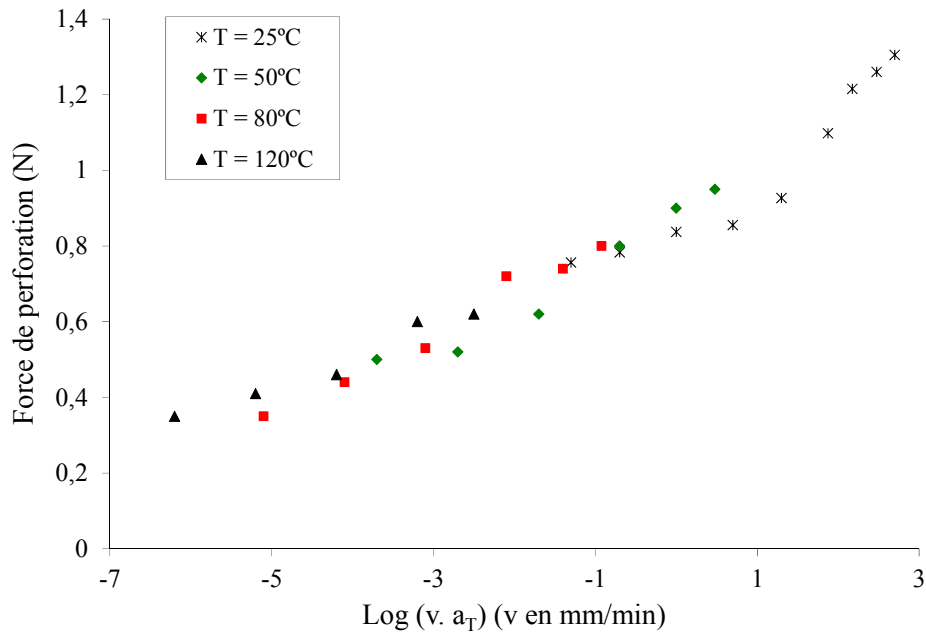


Figure 41 – Time-temperature superposition of maximum puncture force values for 0.8 mm neoprene, a 23G needle and several temperature T and probe velocity v values

For temperatures ranging between 20°C and 80°C, neoprene and nitrile behave very similarly, i.e., maximum puncture force declines very slightly (Figure 42). Measurements of the effect of temperature on maximum puncture force were also taken between 20°C and 80°C with fabric-backed nitrile (1.6 mm thick) and with a layer of SuperFabric[®] (Figure 43). No significant effect of temperature on force values was detected.

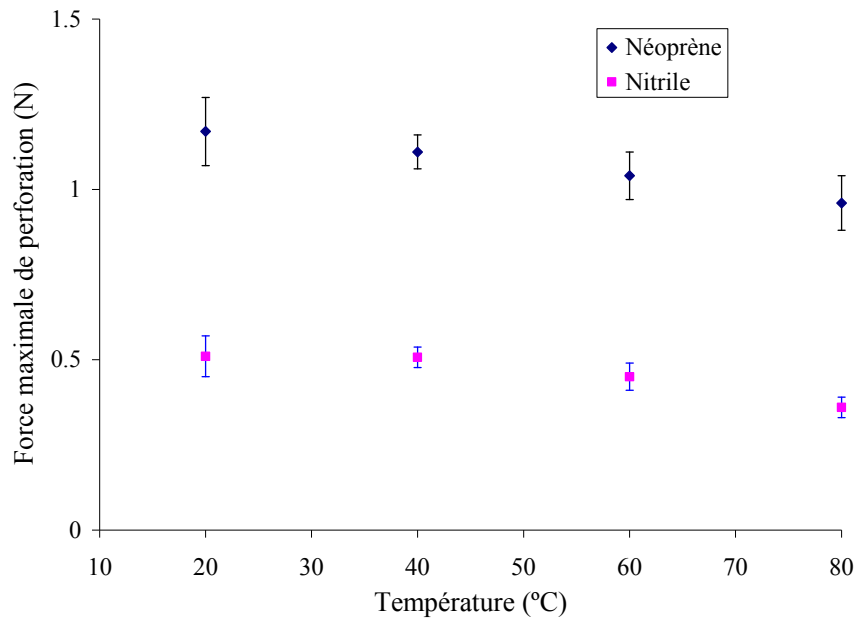


Figure 42 – Change in maximum puncture force as a function of temperature for sheets of neoprene (1.6 mm) and nitrile (0.8 mm), with a 25G needle travelling at 13 mm/min

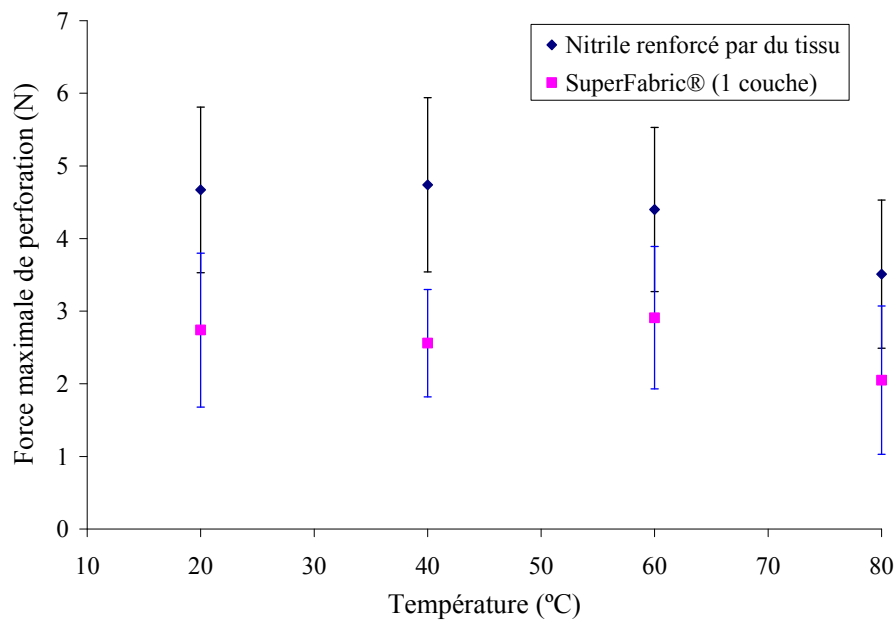


Figure 43 – Change in maximum puncture force as a function of temperature for a 1.6 mm sheet of fabric-backed nitrile and a layer of SuperFabric®, with a 25G needle travelling at 13 mm/min

With regard to needlestick protection, these results seem to show a very slight or negligible effect of temperature on maximum puncture force for all the materials examined in the temperature range relevant to the wearing of gloves to protect against mechanical hazards.

Protective gloves should be used only within the temperature range specified by the manufacturer, however. Materials generally undergo significant changes in their mechanical properties, both at low temperatures (around the glass transition temperature, for instance, for polymers) and high temperatures.

3.4.4 Effect of Humidity

The microclimate that develops inside protective clothing when it is being worn also includes high humidity levels of up to 98% [66]. In the case of firefighters' protective clothing, readings taken during training exercises have even shown that the humidity level inside clothing quickly approaches 100% as soon as a firefighter enters a burning building [72]. Some work environments, such as summer park maintenance or food preparation, also involve high rates of humidity.

To study the effect of humidity levels on the needlestick resistance of protective gloves, tests were done on samples that had been conditioned to different levels of relative humidity for 24 h at ambient temperature (25°C). The following materials were tested: a 1.6 mm sheet of neoprene, a 0.8 mm sheet of nitrile, neoprene-coated knit fabric (Scorpio[®] glove, wrist area), a 1.6 mm fabric-backed sheet of nitrile and a layer of SuperFabric[®]. Measurements were taken with three-bevel 25G (0.5 mm) needles at a probe velocity of 13 mm/min. The results are given in Figure 44 for nitrile and neoprene, and in Figure 45 for the neoprene-coated knit material, the fabric-backed nitrile and the SuperFabric[®]. In all cases, it was found that the maximum puncture force did not vary with the level of relative humidity resulting from 24 h conditioning of the samples.

For homogeneous synthetic materials such as sheets of neoprene and nitrile, this result was expected, given their low surface/volume ratio and relative waterproofness [73]. In contrast, fabric-based structures, on account of their high surface/volume ratio, can absorb more water [74].

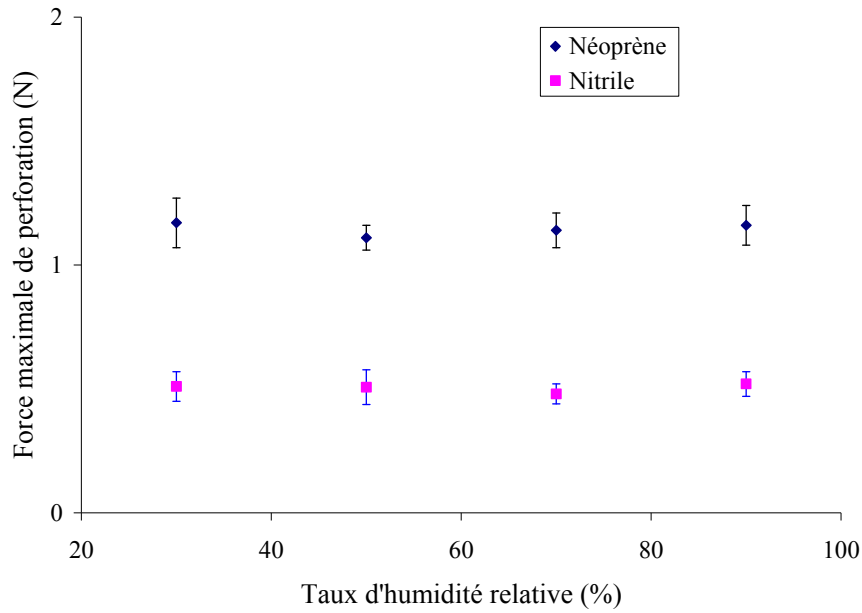


Figure 44 – Change in maximum puncture force as a function of humidity after conditioning, for a 1.6 mm sheet of neoprene and a 0.8 mm sheet of nitrile, with a 25G needle travelling at 13 mm/min

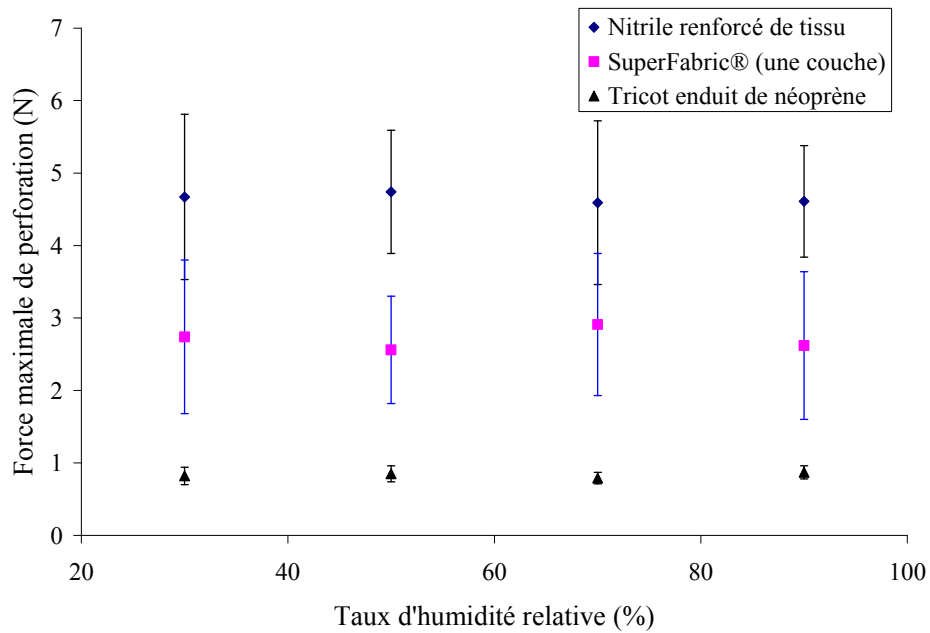


Figure 45 – Change in maximum puncture force as a function of humidity after conditioning, for a 1.6 mm fabric-backed sheet of nitrile, neoprene-coated knit material (Scorpio® glove, wrist area) and a layer of SuperFabric®, with a 25G needle travelling at 13 mm/min

3.4.5 Effect of Lubricants

When in use, gloves may come into contact with substances that can alter some of their properties. Given that needlesticks have been associated with cutting and that lubricants have been shown to have a significant effect on cut resistance [32], measurements were taken to determine the influence of lubricants on maximum puncture force of a medical needle. The tests were done on a 3.2 mm sheet of neoprene. Two types of lubricants—silicone grease and a liquid soap—were used to coat the needle being used as the probe and the membrane being tested.

Figure 46 shows the change in maximum puncture force as a function of needle diameter, with and without silicone grease lubricant. It can be seen that, for all needle diameters tested, the application of silicone grease reduces the maximum puncture force. As the needle penetrates the material, the silicone grease helps reduce the friction between the needle tip and the surfaces of the crack in the sample, which in turn reduces the maximum puncture force.

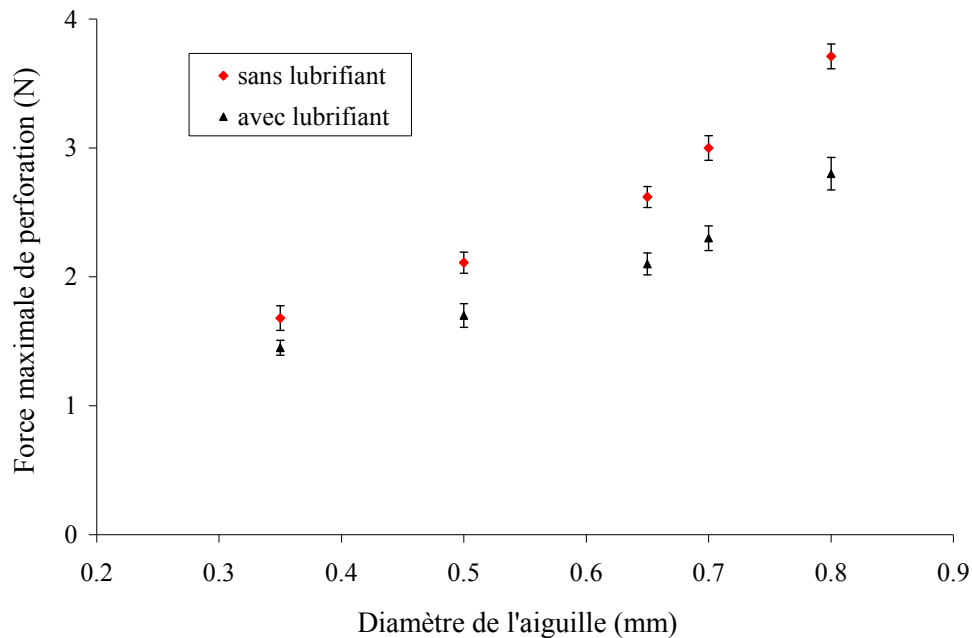


Figure 46 – Change in maximum puncture force as a function of needle diameter, with and without lubricant (silicone grease) for a 3.2 mm sheet of neoprene, with a probe velocity of 50 mm/min

When the difference in maximum puncture force attributable to applying the silicone grease is expressed as a function of needle diameter, exponential change can be seen (Figure 47). This result confirms the major role that friction plays in needlesticks. Given that the friction force is proportional to the contact surface, the relationship between the reduction in maximum puncture force and needle diameter may be due to the cylindrical shape, with elliptical edge, of the surface of the fracture made by the needle in the membrane (Figure 11, p. 21).

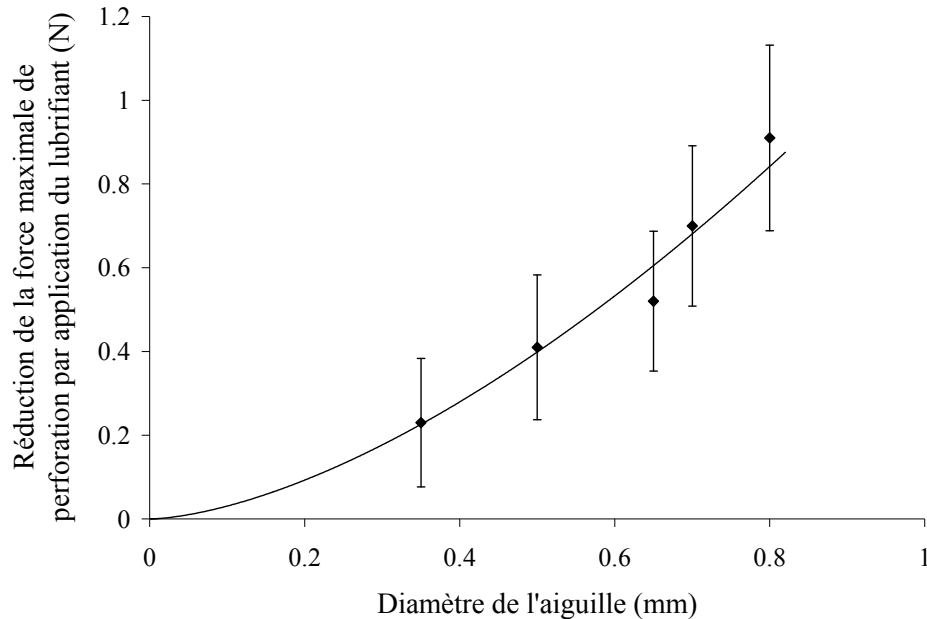


Figure 47 – Change in reduction of maximum puncture force by application of a lubricant (silicone grease) as a function of needle diameter for a 3.2 mm sheet of neoprene, with a probe velocity of 50 mm/min

In contrast, for cylindrical and conical probes, little or no change was seen in puncture force when lubricant was applied [75]. In the case of these probes, puncture occurs when the stress under the probe tip reaches the failure threshold. Friction does not affect fracture stress, nor therefore the maximum puncture force.

Testing was also done to study the effect of lubricant application on change in maximum puncture force as a function of probe velocity (Figure 48). Needlestick resistance decreases owing to the effect of lubrication with liquid soap, and the decrease is greater at higher velocities. Neoprene is a viscoelastic material: for a lower puncture probe velocity, a stable state can more easily be attained at each moment in time as the needle penetrates the membrane. This has the effect of reducing the influence of friction, and therefore of a lubricant, on needlestick resistance.

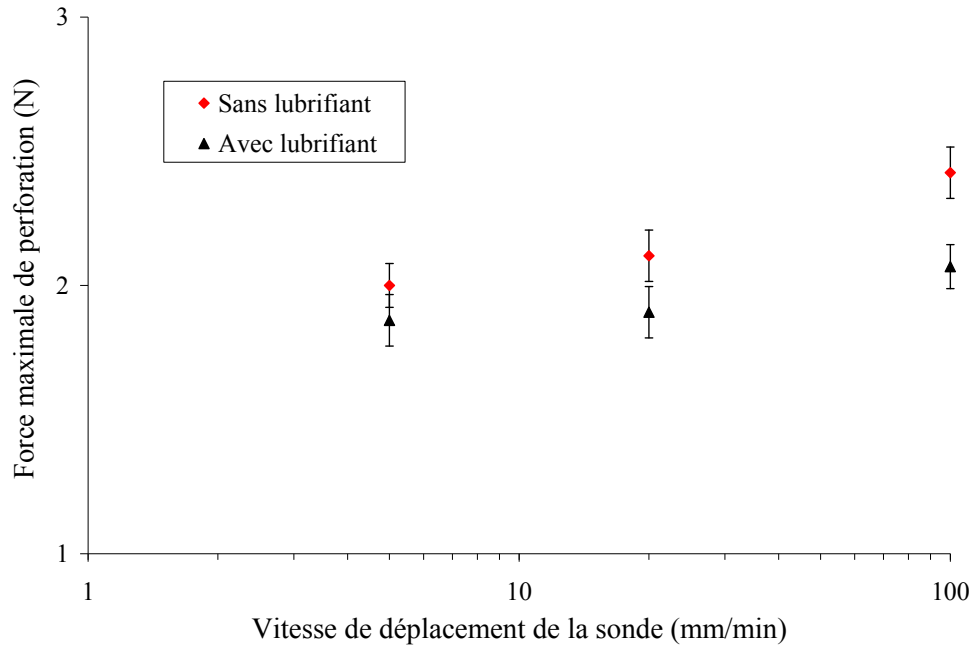


Figure 48 – Effect of liquid soap lubrication on maximum puncture force, at different probe velocities, for a 3.2 mm sheet of neoprene and 23G needles

The results show the influence of friction on the needlestick resistance of protective materials. In particular, the presence of contaminants acting as lubricants can substantially reduce needlestick resistance: the larger the needle diameter and the higher its penetration velocity, the lower the resistance.

3.5 Effect of Prestress

When worn, gloves can undergo significant deformation, especially at the joints. Figure 49 illustrates deformation, in this case around 80%, created by flexing of the hand. A system was designed (see Section 2.2.2) to apply equibiaxial stress and simulate the strain on materials when gloves are worn. The system was used to evaluate the effect of prestressing neoprene, nitrile and neoprene-coated knit fabric (Scorpio[®] glove, wrist area) on maximum puncture force. Fabric-backed sheets of nitrile and samples of SuperFabric[®] and TurtleSkin[®] could not be stretched sufficiently for testing.

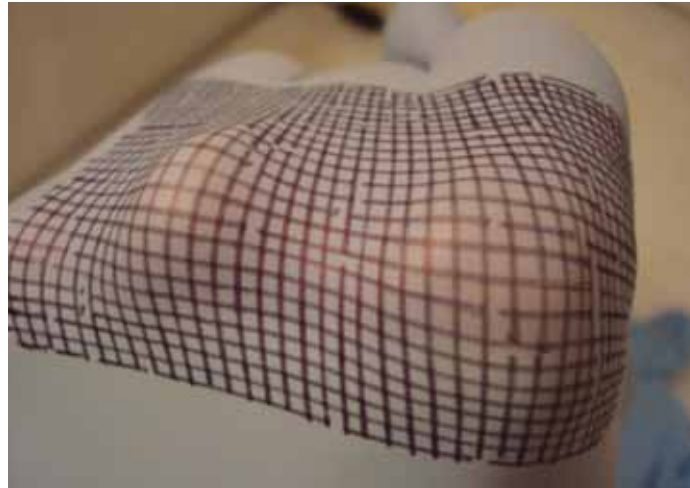


Figure 49 – Photograph of a glove under strain

Force-versus-displacement curves recorded for a 0.8 mm sheet of neoprene and three-facet 23G (0.65 mm) needles, for five different degrees of strain resulting from the applied prestress, are shown in Figure 50. The maximum puncture force and puncture probe displacement values decrease as strain rate values rise, in a manner similar to what was seen for uniaxial prestretching (see Figure 66 in Appendix C).

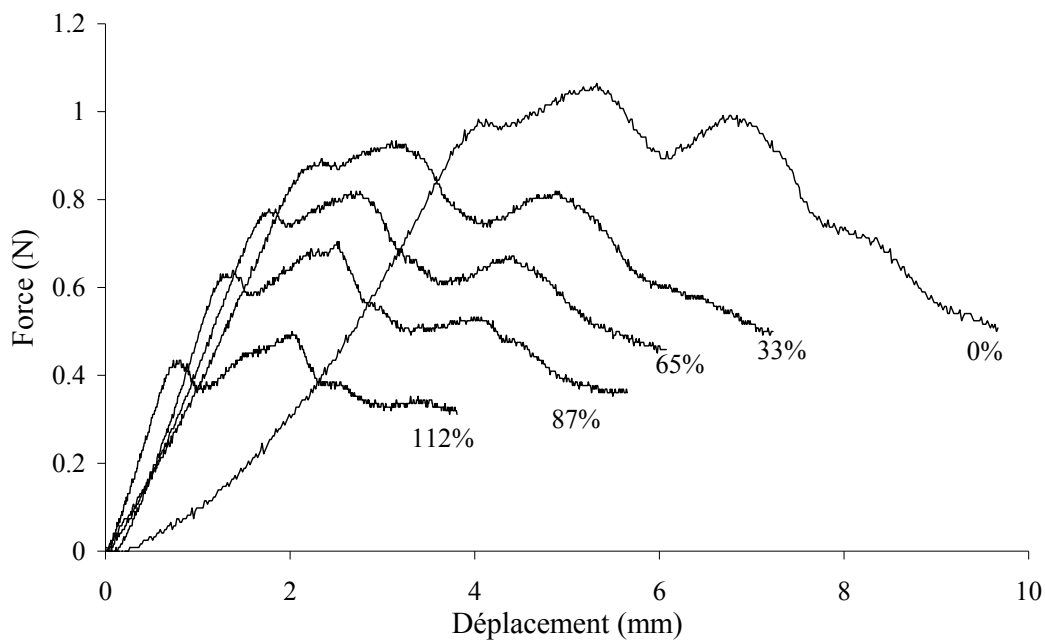


Figure 50 – Force-versus-displacement curves for different degrees of strain associated with prestress applied to a 0.8 mm sheet of neoprene, with 23G needles travelling at 50 mm/min

Change in maximum puncture force as a function of degree of strain resulting from applied prestress is shown in Figure 51 for a 1.6 mm sheet of neoprene and a 0.8 mm sheet of nitrile, with three-facet 25G (0.5 mm) needles travelling at 13 mm/min. It can be seen that maximum

puncture force declines linearly when the degree of strain resulting from the applied prestress increases between 0% and 120%. This is due to the fact that the sum of the puncture energy and the prestress-related prestretch energy remains constant, as expressed in Equation 1.

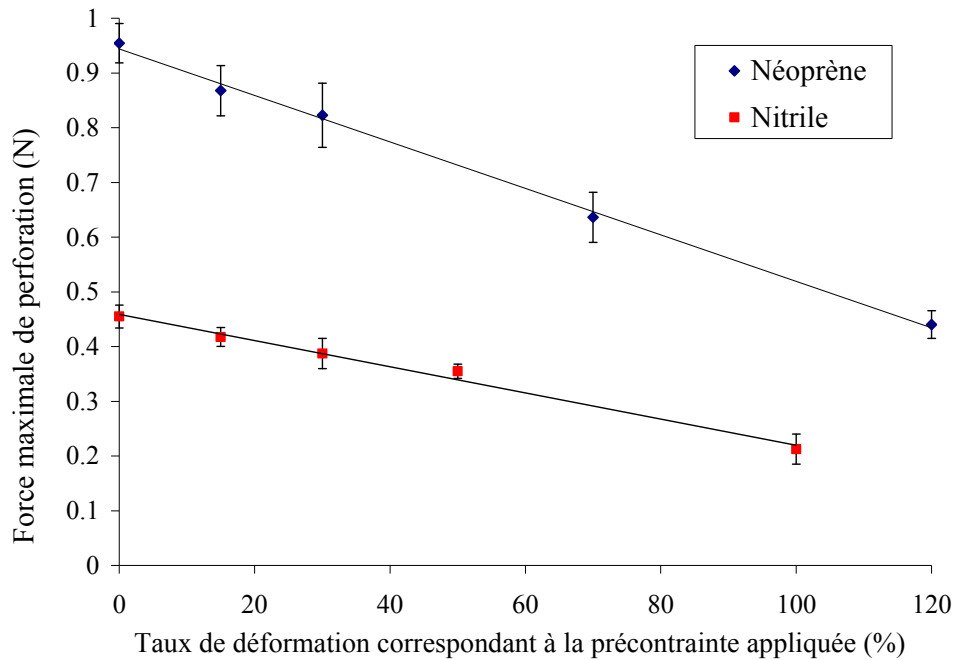


Figure 51 – Change in maximum puncture force as a function of prestress value, for a 1.6 mm sheet of neoprene and a 0.8 mm sheet of nitrile, with a 25G needle travelling at 13 mm/min

The same experiment was conducted on neoprene-coated knit cotton. In this case, the maximum strain that could be applied was 30%. Within this range, the degree of strain, and therefore the prestress, did not have any observable significant effect on maximum puncture force. The fact that this type of material was found to behave differently from the sheets of elastomer may, once again, be due to the effect of the interaction between the needle tip and the interlock knit lining.

Regarding needles protection, note that application of prestress resulting in a degree of strain of 100% reduces the maximum puncture force by half, for both neoprene and nitrile. This is an important point to take into consideration for unlined gloves.

3.6 Effect of Support Simulating a Hand

Measurements were taken to perform a preliminary assessment of whether the presence of a hand in a glove affects its needles resistance. The principle of the test setup and the rubber blocks used to simulate the hand are described in Section 2.2.3. The protective glove materials tested for needles resistance were sheets of neoprene and nitrile, neoprene-coated knit cotton (Scorpio[®] glove, wrist area) and samples of SuperFabric[®] and TurtleSkin[®].

Figure 52 shows the change in maximum puncture force as a function of the hardness of the rubber support in the case of neoprene, nitrile and neoprene-coated knit cotton. The zero-hardness point corresponds to the condition with no support, i.e., the free-form deformation configuration described in Section 2.2.1. For sheets of neoprene and nitrile, a very slight increase in maximum puncture force as a function of the hardness of the support can be seen. This behaviour is very different from what was reported for round-tip probes. In the latter case, a threefold increase in maximum puncture force can be observed for neoprene when a support of hardness 50 Shore A is used [75].

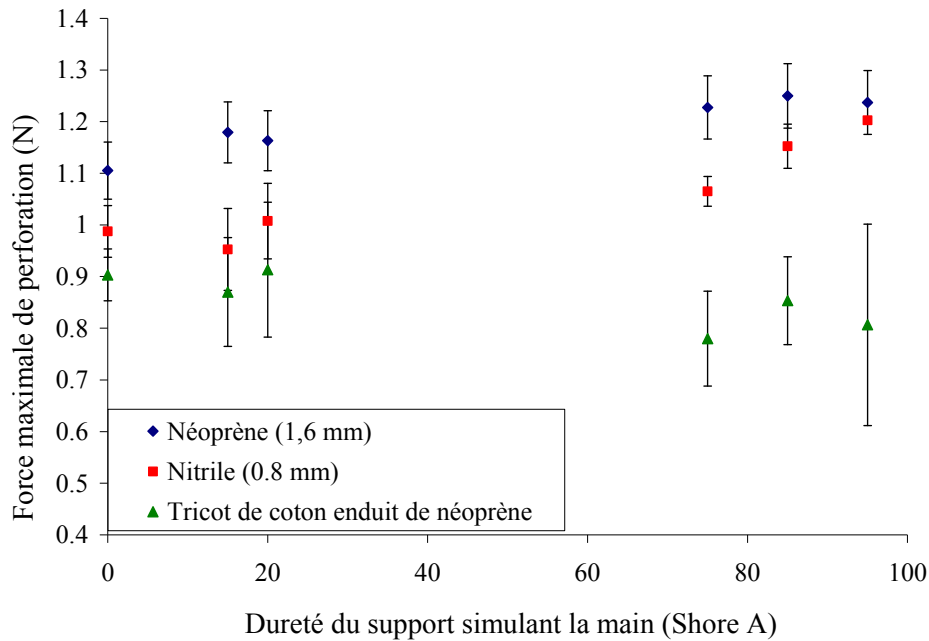


Figure 52 – Effect of hardness of rubber block simulating a hand on maximum puncture force, for a 1.6 mm sheet of neoprene, a 0.8 mm sheet of nitrile of hardness 70 Shore A, and a neoprene-coated knit cotton fabric (Scorpio[®] glove, wrist area), with 25G needles travelling at 13 mm/min

To understand this difference in behaviour, it helps to take a closer look at the mechanism associated with puncture by round-tip probes and needlesticks in the configuration with a support block (Figure 53). In the case of needlesticks (Figure 53a), the tip of the needle progressively penetrates the sample by cutting a hole in the material without causing any significant deformation. As a result, the process is virtually unaffected by the support, and the maximum puncture force varies only slightly with the hardness of the support. In contrast, in the case of round-tip probes like those used in the standard on the puncture of protective clothing, the fracture occurs suddenly, when the strain of the sample under the probe tip reaches the strain threshold. When a support is present, the fracture occurs simultaneously in the sample and the support (Figure 53b). The strain threshold to be considered thus includes a support deformation component, which has a major effect on maximum puncture force.

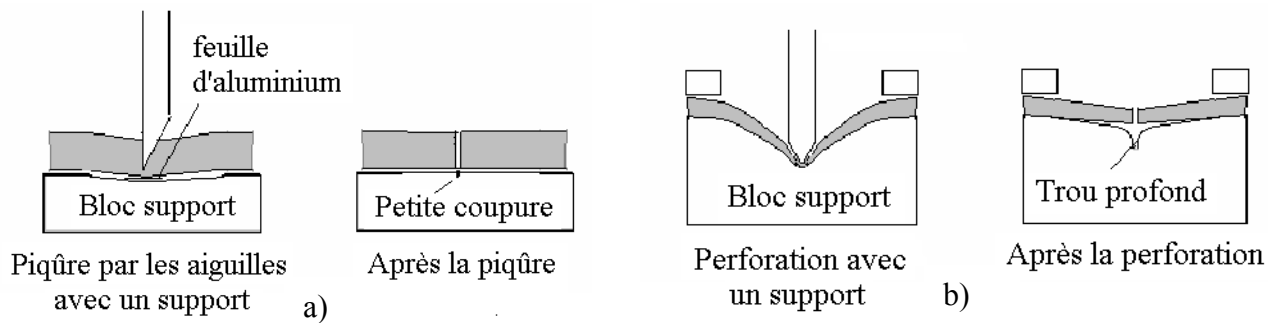


Figure 53 – Diagram showing (a) needlestick process and (b) puncture by round-tip probe, in configuration with support block

For neoprene-coated cotton (Figure 52), no significant variation in maximum force of puncture by needle in relation to hardness of support was seen. The same behaviour was found for SuperFabric[®] and the different TurtleSkin[®] samples (Figure 54). Here, too, fracture occurred without any significant deformation of the material. The influence of the support block on the maximum puncture force was therefore minimal, i.e., within measurement uncertainty.

These results would seem to indicate that, for all the materials tested, the hand-glove interface has no significant influence on needlestick resistance.

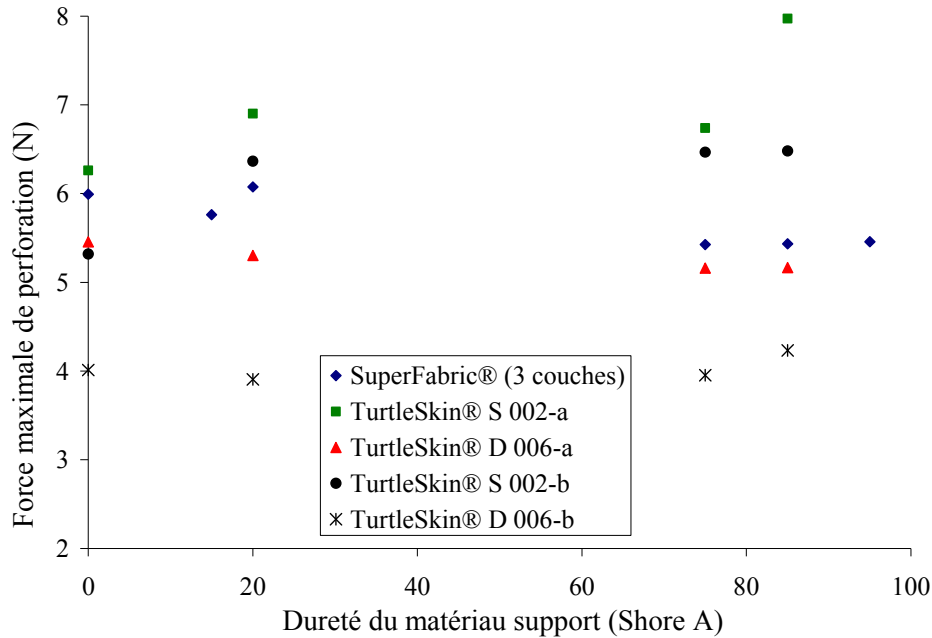


Figure 54 – Effect of hardness of rubber block simulating a hand on maximum puncture force for three layers of SuperFabric® and TurtleSkin® samples S 002-a, D 006-a, S 002-b and D 006-b, with 25G needles travelling at 13 mm/min (error bars omitted for easier reading)

3.7 Glove Performance

The protection against mechanical hazards provided by a selection of protective gloves was measured using the method developed in this project for testing needlestick resistance and the ASTM standard methods for testing puncture and cut resistance.

3.7.1 Needlestick Resistance

The 58 models of glove selected for the study were tested for needlestick resistance measurements following the method described in Section 2.2.6. The results are presented in Table 14, Appendix D. In some cases, the coefficient of variation for the maximum puncture force is very high: it is greater than 30% for 12 models and as high as 76% for one model, which reflects the heterogeneity of the materials. The models in question are made with the tiny hard plates of SuperFabric® or the woven or knit Kevlar®, Spectra® or Dyneema® yarns. Very different maximum force values were obtained, depending on the position of the needle in relation to the resisting element (plate or yarn). Figure 55 illustrates the situation with the HexArmor 8030 glove, which includes a layer of SuperFabric® and a leather palm.

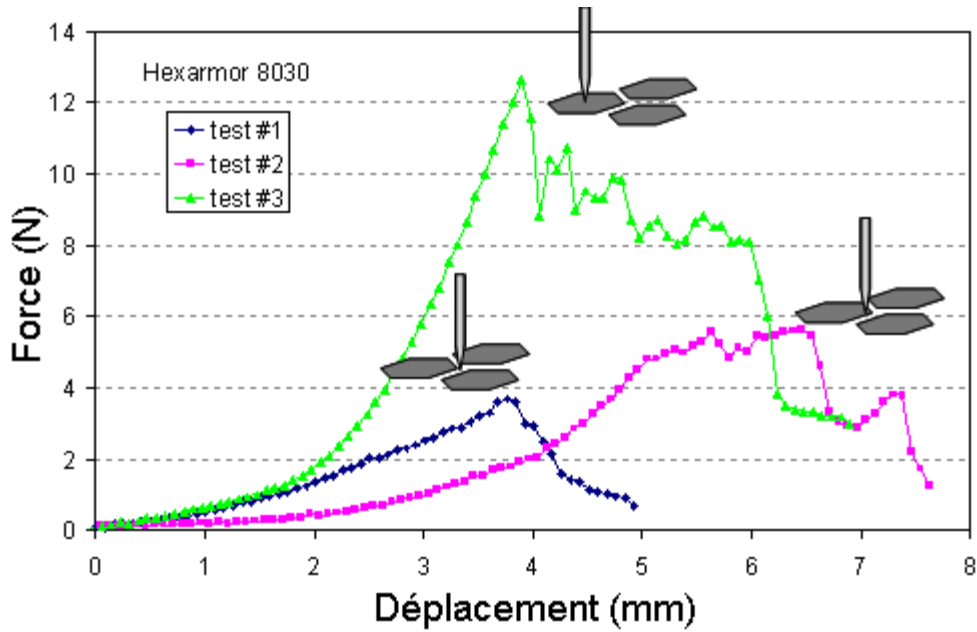


Figure 55 – Sample force-versus-displacement curves plotted from needlestick resistance values of HexArmor 8030 gloves

Four types of construction offer greater needlestick resistance than the others (Figure 56: data in Table 14, Appendix D). First there are gloves that incorporate one or more layers of SuperFabric[®]. This material, made of tiny hard plates adhering to a fabric backing, was developed to provide high protection against cuts, punctures and abrasion. Another series of high-performance gloves are based on TurtleSkin[®] technology. A very fine weave of polymer-coated aramid fibres, the material is designed to provide very good protection against cuts, punctures, abrasion and needlesticks. A third set of gloves is characterized by the overlaying of many thicknesses of a fine nylon fabric. The fourth and last type of construction offering high needlestick resistance has a fine metal mesh between the liner and the outer layer of the glove.

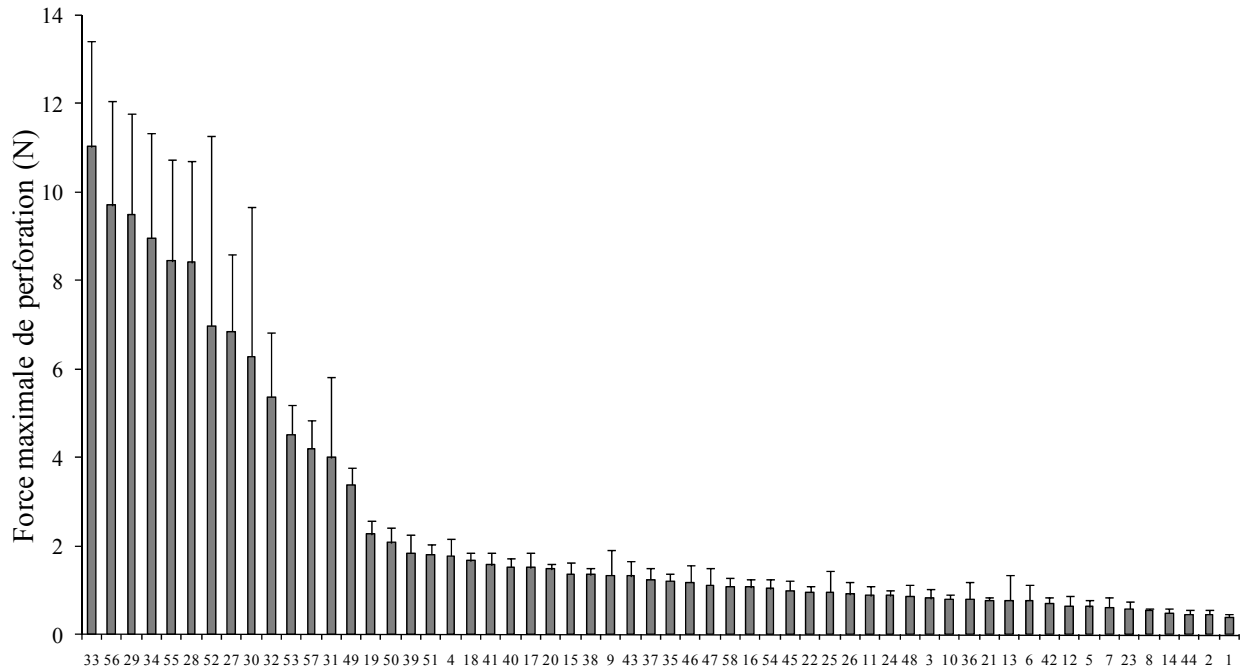


Figure 56 – Maximum puncture force measured for protective gloves, with 25G needles travelling at 500 mm/min (method described in Section 2.2.6)

3.7.2 Puncture Resistance

All 58 models of glove were also tested for puncture resistance following the method set out in ASTM Standard F1342-05 (described in Section **Erreur ! Source du renvoi introuvable.**). The results are given in Table 15, Appendix D. As in the case of needlesticks, some results have relatively high coefficients of variation, primarily owing to the heterogeneity of the materials and differences between gloves of the same model.

For some multilayer models, several distinct peaks can be seen on the force-versus-displacement curve (Figure 57). The glove represented by this curve consists of an outer layer of leather and a knit liner of Spectra[®], nylon and fibreglass. The first peak is associated with the puncture of the leather layer, while the liner’s resistance can be seen in the climb to the second peak, which reflects the position of the puncture probe in relation to the yarn of the interlock knit fabric. This illustrates one reason for the high coefficients of variation of maximum puncture force.

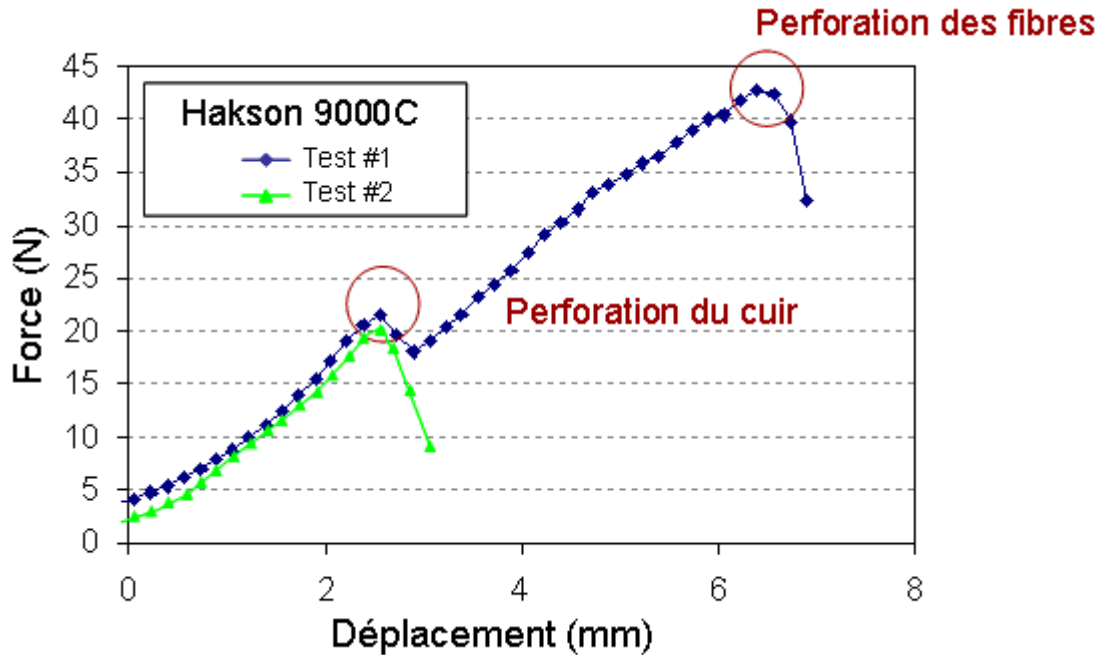


Figure 57 – Samples of force-versus-displacement curves obtained with type A puncture probe of ASTM Standard F1342-05 [34] for Hakson 9000C gloves

The results of the puncture resistance measurements are given in Figure 58. NIJ Test Protocol 99-114 [35] classifies three levels of puncture resistance: low (20 N–59 N), moderate (60 N–99 N) and high (100 N–150 N or higher). For gloves to be recognized as puncture resistant according to the NIJ protocol, they must rate high. Under the protocol, 5 models of glove rated high, 10 rated moderate and 35 rated low. Eight models were rated as offering less than low-level resistance. Note that the levels in question here are not related to needlestick resistance.

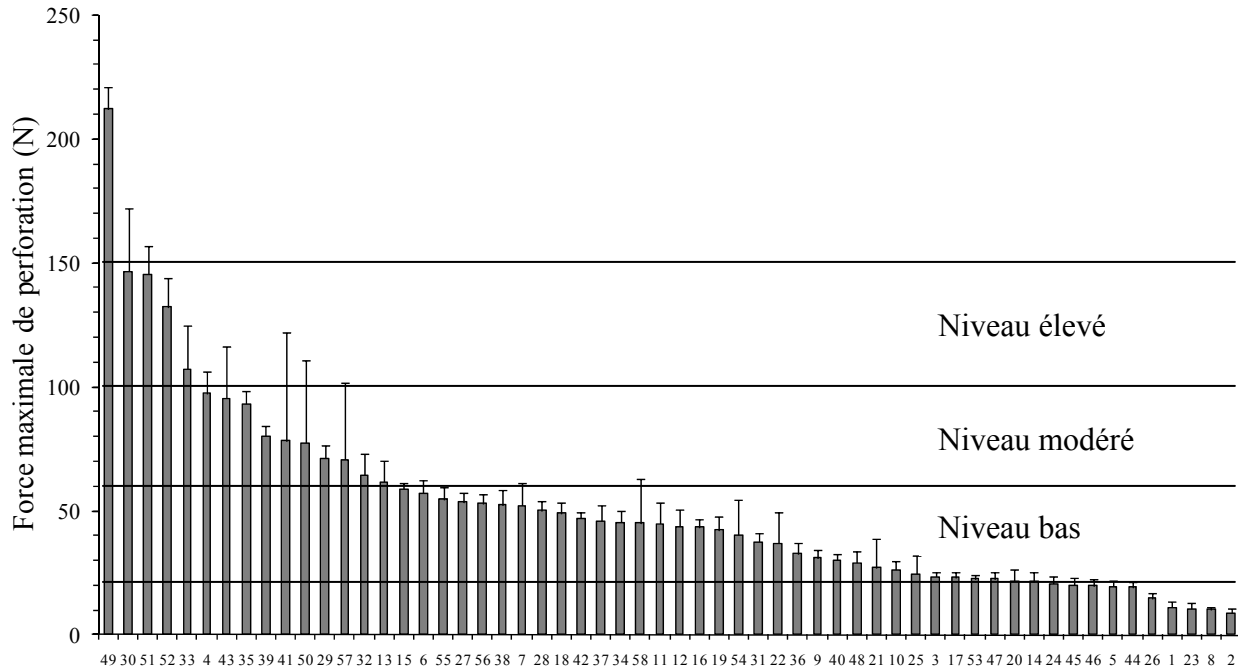


Figure 58 – Maximum puncture force measured for protective gloves, using the method described in Section 2.3, and rated according to NIJ Test Protocol 99-114

3.7.3 Cut Resistance

Cut resistance was measured (see Section 2.4 for description of procedure) for 12 models of glove offering the best puncture resistance and deemed to be the most appropriate by the occupational groups in the study. The results are set out in Table 16, Appendix D. As for puncture resistance to a standard probe or needle, some results show wide variability, as indicated by coefficients of determination (R^2) of close to 0.5. This variability is due primarily to the intrinsic lack of homogeneity of the materials, such as SuperFabric[®] and TurtleSkin[®], used to make the glove. In the case of Superior 66BRPU gloves, folds that form in some of the 12 superimposed layers of nylon create local inhomogeneity and therefore greater variability in individual measurements. For some models of glove, more individual measurements than the minimum of 15 stipulated in the standard were required in order to obtain an acceptable R^2 value, i.e., greater than or equal to 0.5.

The Superior SKLPSMT glove has fine stainless-steel mesh between the Kevlar[®] knit liner and the outer leather shell. In testing, the mesh generated accidental electrical contacts through the glove between the blade and the aluminum tape placed underneath the sample to allow electrical detection of the cut. This problem was solved by sticking electrical tape to the aluminum tape before placing the sample on it. Checks were made beforehand, and the electrical tape was found to have a negligible effect on the cut resistance measurements.

When the cut resistance measurement results for the 12 models of glove were classified according to NIJ Test Protocol 99-114 [35] (Figure 59), 10 models rated high (1,630 g–4,080 g

or more), and 2 rated moderate (600 g–1,630 g). None of the models rated low (< 600 g). The most cut-resistant glove is the one that has a fine metal mesh in the palm. The next six models have one or more layers of SuperFabric®.

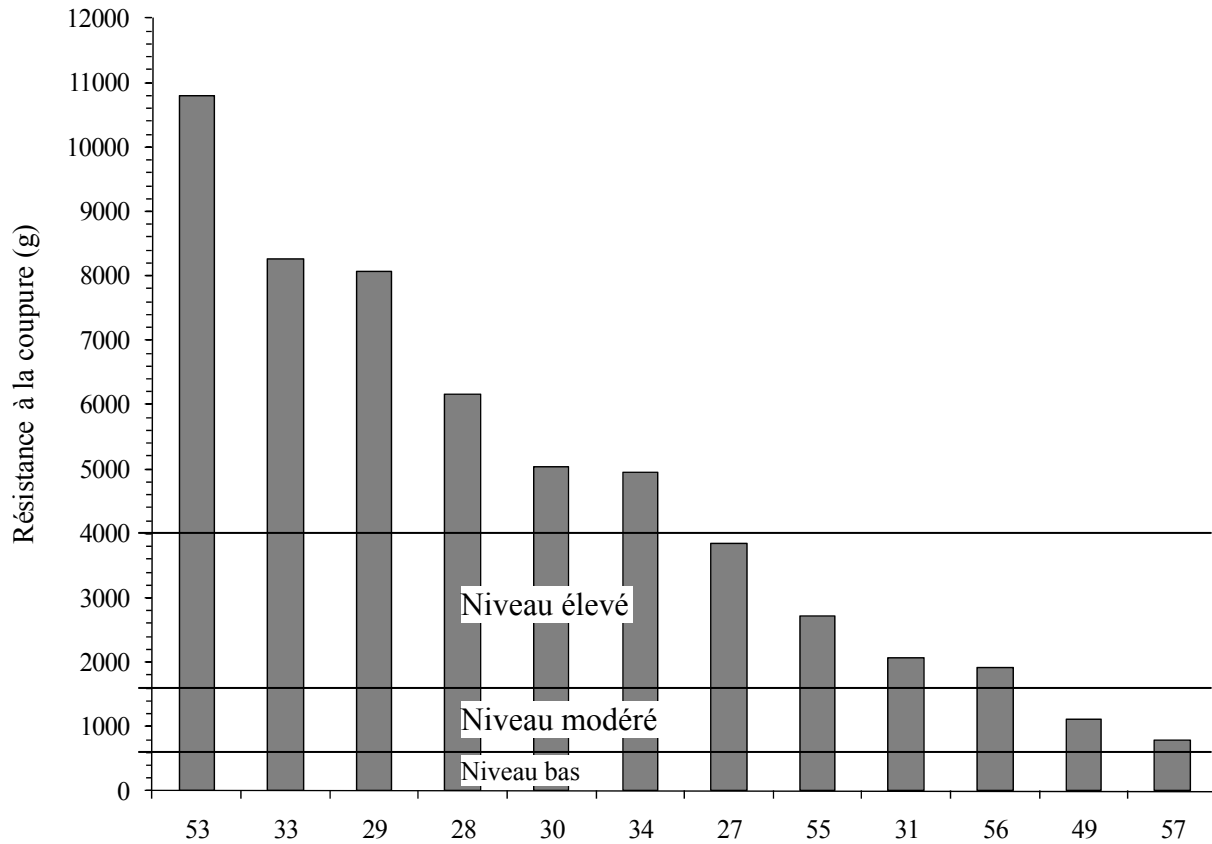


Figure 59 – Protective glove cut resistance, measured using the method described in Section 2.4, and rated according to NIJ Test Protocol 99-114

4. DISCUSSION

4.1 Comparison of Glove Resistance Measured Using Hypodermic Needle Test Method and Standard Puncture and Cutting Test Methods

The maximum puncture force values measured with 25G hypodermic needles (method described in Section 2.2.6) and those measured with probe A (ASTM Standard Test Method F1342-05) were compared for all 58 models of protective glove. The results are presented in Figure 60.

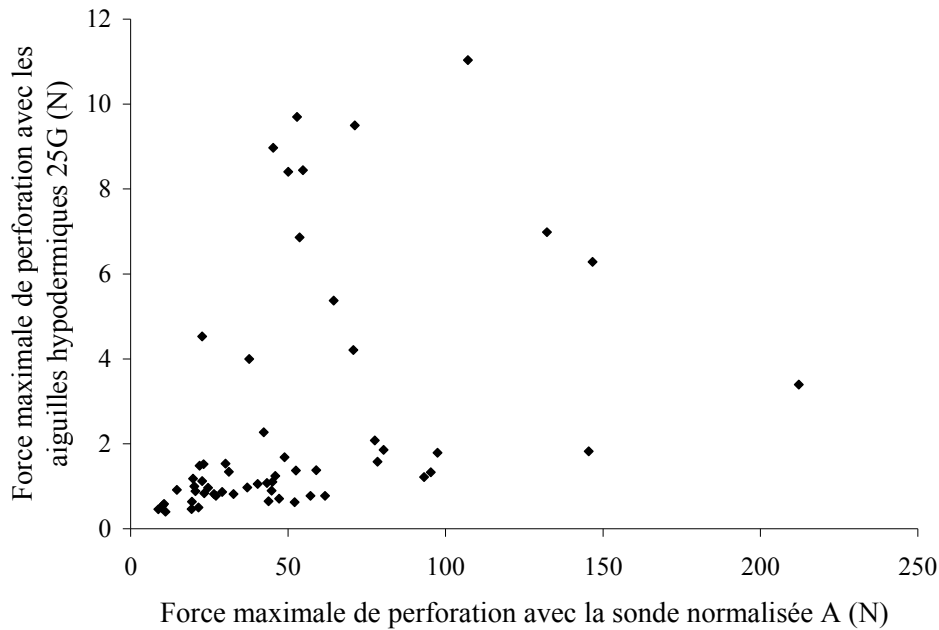


Figure 60 – Comparison of maximum puncture force values measured with 25G hypodermic needles, as described in Section 2.2.6, and those measured with probe A of ASTM Standard F1342-05, for 58 models of glove

The figure shows that there is no correlation between the measurements taken with the hypodermic needles and those taken with the standard conical-spherical probe. This result is consistent with the conclusions of the study on the mechanisms that come into play in needlesticks, presented in Section 3.1. It has been shown that needlesticks involve a significant cutting component, attributable to the cutting edge of the needle tip (and that associated with this component is a fracture energy governed by the radius of the needle tip), as well as a friction component. In contrast, puncture with a round-tip probe has been associated with the maximum degree of strain of the material.

4.2 Analysis of Behaviour of Materials with Respect to Needlesticks

All of the findings regarding the effect of the different needlestick resistance parameters studied for different protective materials are summarized in Table 9.

Table 9 – Summary of effect of parameters related to characteristics of needles and samples, experimental conditions, prestress and presence of a support simulating a hand, on maximum puncture force F for different protective materials (NT: not tested; NS: not significant; NA: not applicable)

Force F	Elastomer	Fabric-backed elastomer	Elastomer-coated knit fabric	SuperFabric [®]	TurtleSkin [®]
Needle diameter	↗	NT	↗	↗	↗
Tip angle	↗	NT	NS	NS	NT
Number of facets	↗	NT	↘	NS	NT
Size of hole of sample holder	→	→	NT	→	NT
Sample thickness	↗	NT	NT	↗	NT
Hardness of material	↗	NT	NT	NT	NT
Probe velocity	↗	NT	↗	↗	↗
Angle of attack	↘	↘	→	→	→
Temperature	↘	NS	NT	NS	NT
Humidity	→	→	→	→	NT
Lubricant	↘	NT	NT	NT	NT
Prestress	↘	NA	→	NA	NA
Support block	→	NT	→	→	→

In Table 9, an upward-pointing arrow indicates that an increase in the parameter in question is associated with an increase in maximum puncture force, a downward arrow indicates a decrease in force and a horizontal arrow indicates no effect on force. It seems that there are two major categories of behaviour. Pure elastomers and fabric-backed elastomers behave fairly similarly in relation to the different parameters studied. Their behaviour differs in some cases from that of the neoprene-coated knit fabric, SuperFabric[®] and TurtleSkin[®], especially with respect to the effect of angle of attack and number of facets. The difference may be due to the fact that, for the second category of materials, behaviour is governed by the material's textile structure, whereas the elastomer component is the dominant factor in the behaviour of the first category.

4.3 Selecting Gloves for Protection Against Needlesticks

In this project, the resistance of a series of protective gloves was measured for three types of mechanical hazards: needlesticks, puncture and cutting. This information can be useful in helping people choose gloves that offer protection against whatever potential mechanical hazards they may face. It is important to realize, however, that choosing gloves demands a compromise between protection and usability/comfort. The risk analysis that precedes glove selection must therefore identify and quantify all the hazards involved: mechanical, chemical, electrical, etc. The parameters related to usability and comfort, such as flexibility, grip, dexterity and tactile sensitivity, have a considerable impact on users' ability to perform their tasks and willingness to wear the gloves.

From the standpoint solely of needlestick resistance, four types of construction perform better than the others (see Figure 56 and Table 14, Appendix D): gloves that have one or more layers of SuperFabric[®], gloves based on TurtleSkin[®] technology, gloves made of many layers of fine nylon fabric and gloves that have fine metal mesh between an inner liner and an outer shell.

Nevertheless, good protection against needles is not sufficient. Tasks that require needlestick protection may be associated with a range of different requirements in terms of dexterity and tactile sensitivity. In some cases, such as frisking people and searching personal effects and locations, these requirements may be very high. In this connection, another study, which complements the one presented here and which concerns workplace evaluation of gloves offering needlestick protection, is presented in another report [49].

In most situations, there are not one, but several mechanical hazards: the chance of needlesticks may be combined with risks of cuts and punctures. Table 10 lists the 12 models of commercially available gloves that offer the best needlestick protection, along with their ratings for cut and puncture resistance, according to NIJ Protocol 99-114 [35].

Table 10 – Resistance to mechanical hazards for 12 models of glove. NIJ Protocol 99-114 ratings are given in parentheses.

#	Manufacturer	Model No.	Needlestick (N)	Puncture (N)	Cut (g)
33	HexArmor	9014	11.04	107 (high)	8,261 (high)
56	Warwick Mills	TWCS-003	9.70	53 (low)	1,908 (high)
29	HexArmor	7080	9.50	71 (moderate)	8,073 (high)
34	HexArmor	4041 NSR	8.97	45 (low)	4,942 (high)
55	Warwick Mills	TUS-002	8.44	55 (low)	2,717 (high)
28	HexArmor	6044	8.41	50 (low)	6,162 (high)
27	HexArmor	4042	6.86	54 (low)	3,852 (high)
30	HexArmor	8030	6.29	147 (moderate)	5,025 (high)
53	Superior	SKLPSMT	4.53	23 (low)	10,793 (high)
57	Warwick Mills	TWCS-006	4.21	71 (moderate)	800 (moderate)
31	HexArmor	9005	4.00	38 (low)	2,066 (high)
49	Superior	66BRPU	3.40	212 (high)	1,122 (moderate)

Besides offering better needlestick resistance than the other gloves tested, some models also provide high levels of puncture and cut protection. However, it is important to consider all requirements and, in particular, requirements respecting usability and comfort. Moreover, given the short-, medium- and long-term impact of wearing gloves, such as the possibility that increased fatigue might lead to musculoskeletal problems, emphasis should be placed on choosing the right level of protection, rather than trying to overprotect.

5. CONCLUSION

This study has enabled development of a method for evaluating needlestick resistance, which consists in measuring the force required to puncture a material with a hypodermic needle travelling perpendicular to a sample at a constant velocity. The sample is held between two plates with holes that allow free-form deformation of the material during the test. A new needle is used for each test.

Development of the method benefited from a number of research projects that shed light on the interaction of materials with medical needles. More specifically, it was found that the round-tip probes used in the current puncture testing standards for protective clothing do not reproduce the mechanism involved in needlestick injuries. In needlesticks, the cutting edge of the needle tip progressively penetrates the membrane, so much less force is required. This action contrasts with puncture by round-tip probe, which occurs suddenly when the degree of strain reaches the material's failure threshold. Moreover, it has been shown that the needlestick process includes significant cutting and friction components. The needlestick resistance of materials is governed by fracture energy—the value of which lies between cutting energy and tearing energy—and the diameter of the cutting edge of the needle tip.

This study saw the development of two models with concurring results for calculating the prestretch energy corresponding to a prestress force applied to eliminate friction in determining the fracture energy associated with needlesticks. The first model is based on Rivlin and Thomas's work [77] on the rupture of rubber, while the second, far simpler, consists in extending the principles of linear elastic fracture mechanics to non-linear materials.

The influence of parameters related to the needles, the material being tested and the experimental conditions was investigated using a series of protective materials: elastomers, textile/elastomer structures, and materials developed specially to provide protection against mechanical hazards, i.e., SuperFabric[®] and TurtleSkin[®]. In particular, it was shown with neoprene that variability in puncture force values associated with the dimensional tolerances of needles is governed by the needle's outer diameter at the transition between the facets. It was also observed that the wear of the cutting edge of the needle, which occurs with all materials and results in an increase in puncture force, becomes very significant in the case of materials other than pure elastomers and requires each needle to be used only once as a puncture probe. Furthermore, for all materials, greater puncture force was required for larger diameter needles and those having a larger tip angle. Regarding the effect of the number of facets, neoprene was more resistant to three-facet than single-facet needles. In contrast, the force decreased in the case of coated knit fabric because of the interaction between the needle and the interlock knit of the fabric.

The materials being tested also had an overall influence on results and were divided into two major categories: materials whose behaviour is governed by the textile liner (coated knit fabric, SuperFabric[®], TurtleSkin[®]) and those that behave like elastomers. In terms of needlestick resistance, SuperFabric[®] and TurtleSkin[®] performed far better than elastomers and coated knit fabrics.

It was shown that puncture force increases regularly with the thickness of the material. For elastomers, it was possible to associate the pattern of the change in puncture force as a function

of sample thickness with the elliptical profile of the surface of the fracture made by the needle. With respect to material hardness, an increase in force was measured for elastomers and attributed to the cutting component's contribution to the needlestick mechanism.

Regarding the influence of experimental conditions, puncture force increased with needle velocity. It was also observed that the size of the sample-holder hole does not significantly affect puncture force in the range studied. For elastomers, the effect of the needle's angle of attack is more or less equivalent to the effect of the thickness of material the needle actually penetrates. For materials whose behaviour is governed by the textile liner, angle of attack had no effect on puncture force. With respect to temperature and humidity, negligible changes in puncture force in the areas of physiological interest were recorded for all materials.

Tests were also conducted to simulate the real conditions under which gloves are used in the workplace. For instance, it was found that application of a lubricant can significantly reduce the needlestick resistance of materials. Applying a prestress typical of how gloves are deformed when worn resulted in a substantial reduction in the force needed to puncture elastomer. In contrast, a support simulating a hand in a glove had no significant effect because a needlestick is very local in nature and does not involve significant deformation of the protective material.

Resistance to puncture by gauge 25G medical needles was measured for 58 models of protective gloves following the method developed in this study. Four types of material with different structures seem to offer superior performance: (1) gloves with one or more layers of SuperFabric[®], which consists of tiny hard plates attached to a textile backing; (2) those based on TurtleSkin[®] technology, a very fine weave of aramid fibres; (3) a model containing many layers of a fine nylon fabric; and (4) another model having fine metal mesh between the liner and the outer shell. Given that in many workplace situations, workers are exposed to several mechanical hazards simultaneously, additional measurements of puncture and cut resistance under existing standards were taken to help guide users in their choice of gloves.

Lastly, the results of this project have contributed to the work of ASTM Committee F-23 on development of a new standard method for testing the needlestick resistance of protective clothing. More specifically, a close working relationship has been established with the WK15392 task group, which has been giving considerable thought to the findings of this study. This method will lead to the development of improved products by manufacturers and will also help reduce needlestick injuries and the associated potential for disease transmission.

6. RECOMMENDATIONS

Future Research

Under the standard test method now being developed by the task group of ASTM Committee F-23, it has been proposed that any one of three gauges of needle be used: 21G, 25G or 28G. However, opting for a single size of needle would have the advantage of allowing comparisons of glove resistance between models and making it easier for users to choose the best gloves for their job. In light of the results of this study, it is suggested that a 25G (0.5 mm) needle be used as a puncture probe, given that maximum puncture force changes regularly as a function of needle diameter for the materials studied. It is also one of the needle sizes most commonly found in the workplaces in question here. Finer needles, such as 28G or 29G, do not always penetrate certain types of materials. Being much shorter, they are also harder to handle. However, to determine the influence of needle diameter on the classification of needlestick resistance, a broader variety of protective glove materials should be tested.

The high end of the range of probe velocities considered in this project was limited to 500 mm/min, owing to the maximum capacity of the mechanical testing machines available. However, this value is substantially lower than the velocities at which a human hand can grab something and lower than stabbing velocities, which are between 250 and 600 m/min. To determine whether needlestick resistance values measured at 500 mm/min really tell us anything useful about actual needlestick injuries, testing should be conducted at typical hand grabbing or stabbing velocities. Such experiments will require development of an impact test bench having an energy capacity suited to the needlestick load range, i.e., much lower than traditional impact machines. Besides changing maximum puncture force values, the mechanisms involved in needlesticks may also be different in the impact velocity range because of the viscoelastic behaviour of protective glove materials.

The maximum needlestick force values recorded for the different models of protective glove turned out to be very low when compared with what is generally observed in the case of puncture by standard probe. Further progress is therefore needed in order to provide users with protective gloves that offer better needlestick resistance. The knowledge acquired in this project may help protective glove manufacturers develop materials that are more needlestick resistant. It is important to take into account the significant role played by cutting and friction in the needlestick process. It will also be necessary to ensure that this improved protection is not achieved at the expense of various usability and comfort characteristics, especially dexterity and tactile sensitivity.

For Users

Four types of structured materials were found to be more needlestick resistant than others. The first type is a model of glove sold by HexArmor that contains one or more layers of SuperFabric[®]. A second series is based on the TurtleSkin[®] technology made by Warwick Mills. Lastly, Superior has developed two types of structures that performed well in testing: one model includes many layers of a very fine nylon fabric and another incorporates a fine metal mesh.

These gloves have generally also shown good cut and puncture resistance. Choosing the best gloves for the job must also take into account the usability requirements (dexterity, tactile sensitivity, etc.) of the tasks involved.

BIBLIOGRAPHY

- 1 Commission de la santé et de la sécurité du travail (2008), Dépôt de données central et régional (DDCR), Données de 2003 à 2005 mise à jour au 1er juillet de l'année x+3, Traitement des données par l'IRSST, 23 octobre 2008, Montréal, QC.
- 2 Mackenzie, K., & Peters, M. (2000). Handedness, hand roles, and hand injuries at work. *Journal of Safety Research*, 31(4), 221-227.
- 3 Berguer, R., & Heller, P. J. (2004). Preventing sharps injuries in the operating room. *Journal of the American College of Surgeons*, 199(3), 462-467.
- 4 Jagger, J., Bentley, M. & Tereskerz, P.M. (1998). Patterns and prevention of blood exposure in operating room personnel: a multi-center study. *Advances in Exposure Prevention*, 3, 61-71.
- 5 Buster, E. H. C. J., van der Eijk, A. A., & Schalm, S. W. (2003). Doctor to patient transmission of hepatitis B virus: implications of HBV DNA levels and potential new solutions. *Antiviral research*, 60(2), 79-85.
- 6 Rabussay, D., & Korniewicz, D. M. (1997). The risks and challenges of surgical glove failure. *AORN Journal*, 66(5), 867,869-867,888.
- 7 Fry, D. E. (2005). Occupational blood-borne diseases in surgery. *American journal of surgery*, 190(2), 249-254.
- 8 Noël, L., & Bédard, A. (2005). Les risques de transmission d'infections liés à la présence de seringues et d'aiguilles à des endroits inappropriés. Institut National de Santé Publique du Québec, 16 p.
- 9 Occupational Safety and Health Administration. (2009). Bloodborne pathogens and needlestick prevention - Hazard recognition, from www.osha.gov
- 10 Dupont, M., & Thibodeau, P. (2000). Exposition au sang et aux autres liquides biologiques - Système de réponse régionale - Centres de référence Prophylaxie Post Exposition (PPE) Montréal-Centre: Rapport d'implantation d'un projet-pilote. Direction de la Santé Publique. 25 p.
- 11 Pagane, J., Chanmugam, A., Kirsch, T., & Kelen, G. D. (1996). New York City police officers incidence of transcutaneous exposures. *Occupational medicine (Oxford, England)*, 46(4), 285-288.
- 12 Hewett, D. J. (1993). Communication personnelle.
- 13 O'Leary, F. M., & Green, T. C. (2003). Community acquired needlestick injuries in non-health care workers presenting to an urban emergency department. *Emergency medicine (Fremantle, W.A.)*, 15(5-6), 434-440.
- 14 National Fire Protection Association. (2003). NFPA 1999 - Standard on protective clothing for emergency medical operations: US Standards Council.
- 15 National Institute of Justice. (2001). A comparative evaluation of protective gloves for law enforcement and corrections applications. *National Law Enforcement and Corrections Technology Center Bulletin*, October.

- 16 Krikorian, R., Lozach-Perlant, A., Ferrier-Rembert, A., Hoerner, P., Sonntag, P., Garin, D., et al. (2007). Standardization of needlestick injury and evaluation of a novel virus-inhibiting protective glove. *Journal of Hospital Infection*, 66(4), 339-345.
- 17 Korniewicz, D. M., & Rabussay, D. P. (1997). Surgical glove failures in clinical practice settings. *AORN Journal*, 66(4), 660-668.
- 18 Hansen, K. N., Korniewicz, D. M., Hexter, D. A., Kornilow, J. R., & Kelen, G. D. (1998). Loss of glove integrity during emergency department procedures. *Annals of Emergency Medicine*, 31(1), 65-72.
- 19 Manson, T. T., Bromberg, W. G., Thacker, J. G., McGregor, W., Morgan, R. F., & Edlich, R. F. (1995). A new glove puncture detection system. *The Journal of emergency medicine*, 13(3), 357-364.
- 20 Rabussay, D., & Korniewicz, D. M. (1997). Improving glove barrier effectiveness. *AORN Journal*, 66(6), 1043-1060,1063.
- 21 Tanner, J., & Parkinson, H. (2002). Double gloving to reduce surgical cross-infection. *Cochrane database of systematic reviews (Online)*(3), CD003087.
- 22 Gonzalez-Bayon, L., Gonzalez-Moreno, S., & Ortega-Perez, G. (2006). Safety considerations for operating room personnel during hyperthermic intraoperative intraperitoneal chemotherapy. *European Journal of Surgical Oncology*, 32(6), 619-624.
- 23 Avery, C. M., Gallagher, P., & Birnbaum, W. (1999). Double gloving and a glove perforation indication system during the dental treatment of HIV-positive patients: are they necessary? *British dental journal*, 186(1), 27-29.
- 24 Edlich, R. F., Wind, T. C., Heather, C. L., & Thacker, J. G. (2003). Reliability and performance of innovative surgical double-glove hole puncture indication systems. *Journal of Long-Term Effects of Medical Implants*, 13(2), 69-83.
- 25 Edlich, R. F., Wind, T. C., Hill, L. G., & Thacker, J. G. (2003). Resistance of double-glove hole puncture indication systems to surgical needle puncture. *Journal of Long-Term Effects of Medical Implants*, 13(2), 85-90.
- 26 Leslie, L. F., Woods, J. A., Thacker, J. G., Morgan, R. F., McGregor, W., & Edlich, R. F. (1996). Needle puncture resistance of surgical gloves, finger guards, and glove liners. *Journal of Biomedical Materials Research*, 33(1), 41-46.
- 27 Suttie, S. A., Robinson, S., Ashcroft, G. P., & Hutchison, J. D. (2005). Current practice in the management of high-risk orthopaedic trauma patients in Scotland. *Injury Extra*, 36(4), 59-63.
- 28 Higher Dimension Medical. SuperFabric. Retrieved 26 sept 06, 2006, from www.superfabric.com
- 29 Safety First Aid. TurtleSkin Gloves: Protection in any environment. Retrieved 15 oct 06, 2006, from www.turtleskin.com
- 30 Jackson, E. M., Wenger, M. D., Neal, J. G., Thacker, J. G., & Edlich, R. F. (1998). Inadequate standard for glove puncture resistance: allows production of gloves with limited puncture resistance. *The Journal of emergency medicine*, 16(3), 461-465.

- 31 Jagger, J., Hunt, E. H., Brand-Elnaggar, J., & Pearson, R. D. (1988). Rates of needlestick injury caused by various devices in a university hospital. *The New England journal of medicine*, 319(5), 284-288.
- 32 Vu-Khanh, T., Nga Vu, T. B., Nguyen, C. T., & Lara, J. (2005). Gants de protection: Étude sur la résistance des gants aux agresseurs mécaniques multiples. *Études et recherches /Rapport R-424*. Institut Robert-Sauvé en santé et en sécurité du travail, Montréal. 74 p.
- 33 Nguyen, C. T., Vu-Khanh, T., & Lara, J. (2005). A study on the puncture resistance of rubber materials used in protective clothing. *Journal of ASTM International*, 2(4), 245-258.
- 34 American Society for Testing and Materials. (2005). *Standard Test Method for Protective Clothing Material Resistance to Puncture (ASTM F 1342-05)*. ASTM International.
- 35 Fatah, A. A. (1999). Test protocol for comparative evaluation of protective gloves for law enforcement and corrections applications NIJ Test Protocole 99-114. National Institute of Justice, Office of Science and Technology, US Department of Justice. 9 p.
- 36 Fisher, M. D., Reddy, V. R., Williams, F. M., Lin, K. Y., Thacker, J. G., & Edlich, R. F. (1999). Biomechanical performance of powder-free examination gloves. *The Journal of emergency medicine*, 17(6), 1011-1018.
- 37 Lara, J. (1995). La résistance des gants à la coupure - Développement d'une méthode d'essai. *Études et recherches /Rapport R-103*. Institut Robert-Sauvé en santé et en sécurité du travail, Montréal. 28 p.
- 38 American Society for Testing and Materials. (2005). *Standard Test Method for Measuring Cut Resistance of Materials Used in Protective Clothing. ASTM F 1790-05*. ASTM International.
- 39 International Organization for Standardization. (1999). *Protective clothing - Mechanical properties - Determination of resistance to cutting by sharp objects. ISO 13997*.
- 40 Vu, T. B. N., Vu-Khanh, T., & Lara, J. (2005). Progress in the characterization of the cutting resistance of protective materials. *Journal of ASTM International*, 2(5), 399-413.
- 41 Vu Thi, B. N., Vu-Khanh, T., & Lara, J. (2005). Effect of friction on cut resistance of polymers. *Journal of Thermoplastic Composite Materials*, 18(1), 23-36.
- 42 Lara, J. (1992). Développement d'une méthode d'évaluation de la résistance à la perforation des gants de protection. *Études et recherches /Rapport R-059*. Institut Robert-Sauvé en santé et en sécurité du travail, Montréal. 30 p.
- 43 Nguyen, C. T., & Vu-Khanh, T. (2004). Mechanics and mechanisms of puncture of elastomer membranes. *Journal of Materials Science*, 39(24), 7361-7364.
- 44 Nguyen, C. T., Vu-Khanh, T., & Lara, J. (2004). Puncture characterization of rubber membranes. *Theoretical and Applied Fracture Mechanics*, 42(1), 25-33.
- 45 Chadwick, R. G. (2004). Comparison of nitrile and latex examination gloves. *British dental journal*, 196(11), 685-685.
- 46 Patel, H. B., Fleming, G. J. P., & Burke, F. J. T. (2004). Puncture resistance and stiffness of nitrile and latex dental examination gloves. *British dental journal*, 196(11), 695-700.

- 47 Abolhassani, N., Patel, R., & Moallem, M. (2007). Needle insertion into soft tissue: A survey. *Medical Engineering and Physics*, 29(4), 413-431.
- 48 Shergold, O. A., & Fleck, N. A. (2004). Mechanisms of deep penetration of soft solids, with application to the injection and wounding of skin. *Proceedings of the Royal Society A: Mathematical, Physical and Engineering Sciences*, 460(2050), 3037-3058.
- 49 Gauvin, C., Lara, J. (soumis, octobre 2011). Évaluation par les travailleurs de la dextérité, de la sensibilité tactile et du confort des gants résistants aux piqûres d'aiguilles. Institut Robert-Sauvé en santé et en sécurité du travail, Montréal.
- 50 Sundstrom, A., & Fatah, A. (2002). Results of comparative evaluation of protective gloves for law enforcement and corrections applications: Cut-resistance test results, Tear-resistance test results, Puncture-resistance test results, from <http://www.nlectc.org/testing/gloves.html>
- 51 Kuwahara, Y., Shima, Y., Shirayama, D., Kawai, M., Hagihara, K., Hirano, T., et al. (2008). Quantification of hardness, elasticity and viscosity of the skin of patients with systemic sclerosis using a novel sensing device (Vesmeter): a proposal for a new outcome measurement procedure. *Rheumatology (Oxford, England)*, 47(7), 1018-1024.
- 52 Annual number of syringes supplied by NASEN to their participating SEPs in 2008. J. Cronin. Communication personnelle, Janvier 2009.
- 53 Lara J., Gauvin C., Robinson D. Improvements to the ISO 13997 cut test method, Proceeding of the 4th European Conference on Protective Clothing (ECPC) and Nokobetef 9, Protective Clothing: Performance and Protection, Papendal, Arnhem, The Netherlands, June 10-12, 2009, p.28.
- 54 Lake, G. J., & Yeoh, O. H. (1978). Measurement of rubber cutting resistance in the absence of friction. *International Journal of Fracture*, 14(5), 509-526.
- 55 Lake, G. J., & Yeoh, O. H. (1987). Effect of crack tip sharpness on the strength of vulcanized rubbers. *Journal of Polymer Science, Part B (Polymer Physics)*, 25(6), 1157-1190.
- 56 Gent, A. N., Lai, S. M., Nah, C., & Wang, C. (1994). Viscoelastic effects in cutting and tearing rubber. *Rubber Chemistry and Technology*, 67(4), 610-618.
- 57 Kilwon, C., & Daeho, L. (1998). Viscoelastic effects in cutting of elastomers by a sharp object. *Journal of Polymer Science, Part B (Polymer Physics)*, 36(8), 1283-1291.
- 58 Tung Ha, A., & Toan, V.-K. (2004). Thermoxidative aging effects on mechanical performances of polychloroprene. *Journal of the Chinese Institute of Engineers*, 27(6), 753-761.
- 59 Vu Thi, B. N. (2004). Mécanique et mécanisme de la coupure des matériaux de protection. Thèse de doctorat, Université de Sherbrooke, 116 p.
- 60 Thomas, A. G. (1955). Rupture of rubber. II. The strain concentration at an incision. *Journal of Polymer Science*, 18(88), 177-188.
- 61 Lara, J., Nelisse, N. F., Cote, S., & Nelisse, H. J. (1992). Development of a method to evaluate the puncture resistance of protective clothing materials. Paper presented at the

- Symposium on Performance of Protective Clothing: Fourth Volume, Jun 18-20 1991, Montreal, Que, Can.
- 62 American Society for Testing and Materials. (2005). Standard test method for rubber property - Durometer hardness. ASTM D2240-05. ASTM International.
 - 63 McGuire, B. J., Sorrells, J. R., & Moore, J. D. (1973). Resistance of human skin to puncture and laceration. NBSIR 73-123. U.S. Department of Commerce, NTIS Springfield, VA
 - 64 Horsfall, I., Watson, C., Champion, S., Prosser, P., & Ringrose, T. (2005). The effect of knife handle shape on stabbing performance. *Applied Ergonomics*, 36(4 SPEC ISS), 505-511.
 - 65 Koralek, A.S., (2005). Communication personnelle.
 - 66 Sullivan, P. J., & Mekjavic, I. B. (1992). Temperature and humidity within the clothing microenvironment. *Aviation, space, and environmental medicine*, 63(3), 186-192.
 - 67 Purvis, A. J., & Cable, N. T. (2000). The effects of phase control materials on hand skin temperature with gloves of soccer goalkeepers. *Ergonomics*, 43(10), 1480-1488.
 - 68 Gent, A. N. (2001). *Engineering with rubber: How to design rubber components*: Hanser Publisher, Munich; HanserGardner Publications, Inc., Cincinnati.
 - 69 Burlett, D. J. (2004). Thermal techniques to study complex elastomer/filler systems. *Journal of Thermal Analysis and Calorimetry*, 75(2), 531-544.
 - 70 Williams, M. L., Landel, R. F., & Ferry, J. D. (1955). The temperature dependence of relaxation mechanisms in amorphous polymers and other glass-forming liquids. *Journal of the American Chemical Society*, 77(14), 3701-3707.
 - 71 Ha-Anh, T. (2007). Influence du vieillissement thermo-oxydatif sur les comportements mécaniques du polychloroprène. Thèse de doctorat, Université de Sherbrooke.
 - 72 Rossi, R. (2003). Fire fighting and its influence on the body. *Ergonomics*, 46(10), 1017-1033.
 - 73 Edwards, D. C. (1985). Water absorption phenomena in elastomers. *Elastomerics*, 117(10), 25-30.
 - 74 Morton, W. E., & Hearle, J. W. S. (1975). *Physical properties of textile fibers*. Manchester: The Textile Institute.
 - 75 Nguyen, C. T., Dolez, P. I., Vu-Khanh, T., Gauvin, C. & Lara, J. (sous presse). Effect of protective glove use conditions on their resistance to needle puncture. *Plastics, Rubber and Composites: Macromolecular Engineering*.
 - 76 Felbeck, D. K., & Atkins, A. G. (1996). *Strength and Fracture of Engineering Solids*. Upper Saddle River, NJ: Prentice-Hall.
 - 77 Rivlin, R. S., & Thomas, A. G. (1953). Rupture of rubber. I. Characteristic energy for tearing. *Journal of Polymer Science*, 10(3), 291-318.

- 78 Greensmith, H. W. (1963). Rupture of rubber. X. The change in stored energy on making a small cut in a test piece held in simple extension. *Journal of Applied Polymer Science*, 7(3), 993-1002.

APPENDIX A: GLOVE MODELS TESTED

Table 11 – List of 58 glove models tested

#	Manufacturer	Reference No.	Model
1	Ansell	11-500	HyFlex CR
2	Ansell	11-501	HyFlex CR + Intercept
3	Ansell	11-627	HyFlex CR2
4	Ansell	70-982	The Duke
5	Atlas	620	Vinylove
6	Atlas	KV300	
7	Atlas	KV350	
8	Best	55	Natural Latex Rubber HD
9	Best	660	CPV
10	Best	2912	Nitri Seal
11	Best	4560	Zorb IT Ultimate
12	Best	4811	Skinny Dip Aramid
13	Best	4900	Nitri Flex Aramid
14	Best	5900	Nitri Flex Ultimate
15	Best	65NFW	Original Nitty Gritty
16	Best	66NFW	Original Nitty Gritty
17	Best	6781R	Insulated Neo Grab
18	Best	68NFW	Original Nitty Gritty
19	Best	95NFW	Insulated Nitty Gritty
20	Hakson	3000C	
21	Hakson	9000C	
22	Hakson	9000G	
23	Hakson	NPG150	
24	Hatch	PPG1	
25	Hatch	SB4000	Friskmaster Max
26	Hatch	SGK100	Street Guard
27	HexArmor	4042	HiDex NSR Leather
28	HexArmor	6044	PointGuard X
29	HexArmor	7080	SharpsMaster™
30	HexArmor	8030	
31	HexArmor	9005	
32	HexArmor	9006	
33	HexArmor	9014	SharpsMaster II™
34	HexArmor	4041	HiDex NSR
35	Marigold Industrial	VHP Plus	Comacier VHP Plus
36	Marigold Industrial	PGK10	PGK10
37	Masley	Cugni-TC	
38	Masley	F1SG	
39	Masley	ICWG	
40	Masley	UA1	
41	North	62/7506	Grip N Kevlar
42	North	LA258	Nitri-Guard
43	North	NFK13	Nitri Task Plus
44	North	NFK14	Duro Task Plus

45	North	NK803	NitriKnit
46	North	T-201	Blue Tuff
47	North	T431	Rough Tuff
48	North	T65FWG	Grip Task
49	Superior	66BRPU	Heavy-Duty CrewMate™ fitters glove
50	Superior	MXBD	
51	Superior	MXBL	
52	Superior	MXSF	
53	Superior	SKLPSMT	“Triple Play” Action Steel mesh glove
54	Warwick Mills	001	NYDoCS
55	Warwick Mills	TUS-002	TurtleSkin Search TWCS-002
56	Warwick Mills	TWCS-003	TurtleSkin Special Ops
57	Warwick Mills	TWCS-006	TurtleSkin Duty
58	Warwick Mills	007	Patrol

APPENDIX B: PARAMETERS GOVERNING NEEDLESTICK MECHANISM

Figure 61 zooms in on the force-versus-displacement curve for the interval between the moment the needle begins to penetrate the material (position I on Figure 10) and the moment the tip of the needle touches the underside of the sample (position X on Figure 10). The displacement data were converted into depth values for the crack made in the material by the needle, as illustrated in the diagram beside the chart in Figure 61.

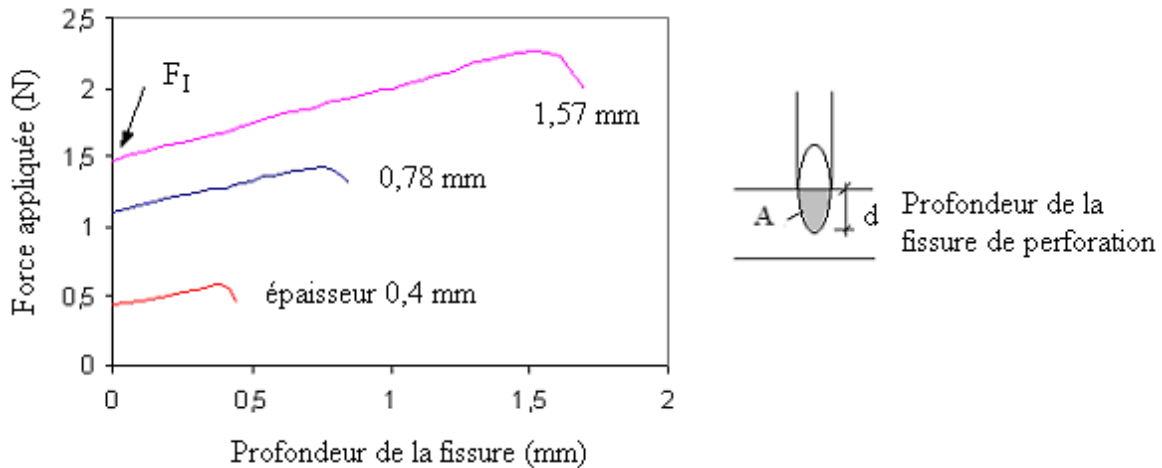


Figure 61 – Change in force applied as a function of crack depth, for three thicknesses of neoprene (0.4, 0.8 and 1.6 mm), with 25G needles travelling at 50 mm/min

It can be seen that, for neoprene, puncture force varies linearly with the depth of the crack made by the cutting edge of the needle tip. In addition, the slope of the straight line is independent of the sample thickness over the interval examined, i.e., between 0.4 and 1.6 mm. This kind of behaviour can be likened to what was reported for friction force in the neoprene cutting tests, which varied linearly as a function of sample thickness [32].

The change in force corresponding to the initiation of the crack, that is, at position I, as a function of the thickness of the neoprene membrane tested, is shown in Figure 62. It can be seen that the force increases with sample thickness. This result indicates that even if, at the time of initiation, only the surface of the sample is penetrated, the local deformation of the sample under the tip of the needle must reach a certain critical value for the crack to be made. For thicker samples, a greater force is required to reach the same level of deformation.

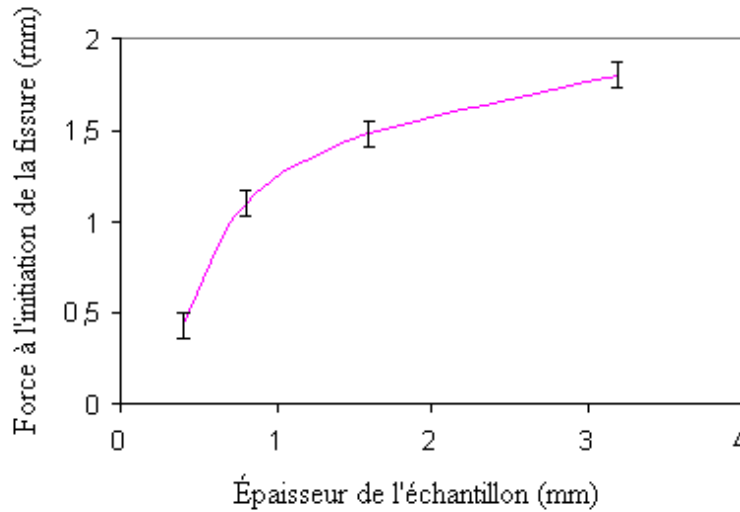


Figure 62 – Change in force required to initiate crack (position I in Figure 10, p. 20) as a function of neoprene thickness, with 25G needles travelling at 50 mm/min

Given the fact that the tips of hypodermic needles have cutting edges and that penetration has been seen to be a gradual phenomenon, needlestick has been associated with a cutting process [32,33]. In the literature, cutting has been related to a material's fracture energy [55,57]. Similarly, the energy balance principles described by fracture mechanics can be applied to calculate the energy required to make a new fracture surface, that is, fracture energy G_s [76]:

$$G_s = -\left(\frac{\partial U}{\partial A}\right) \approx -\frac{\Delta U}{\Delta A} \quad \text{Equation 6}$$

where ΔU is the change in strain energy corresponding to the change in fracture surface ΔA . In the case of needlesticks, the fracture surface created in the material is elliptical (Figure 11, p. 21).

In practice, ΔU can be measured using force-versus-displacement curves: when the puncture has reached a certain depth in the sample, corresponding to fracture surface A_i , the needle is withdrawn so as to produce a return curve. Figure 63 illustrates how the change in strain energy ΔU is calculating by subtracting the energy released corresponding to the different depths of penetration of the needle. The changes in strain energy $-\Delta U_{ij}$ corresponding to the changes in the fracture surface ΔA_{ij} are therefore given by:

$$-\Delta U_{ij} = U_i - U_j \quad \Delta A_{ij} = A_i - A_j \quad \text{Equation 7}$$

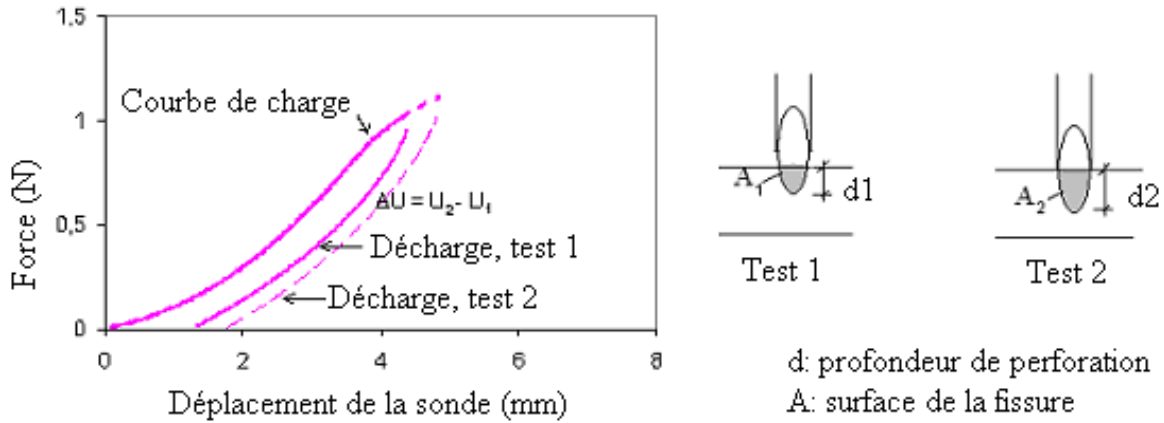


Figure 63 – Method of determining change in strain energy corresponding to different needlestick depths

Tests using this method were conducted with the same sample and the same needle (to limit variability due to the probe and the material) for different penetration depths. They yielded different values of the energy released: $-U_1, -U_2, \dots$ corresponding to different fracture surface values, A_1, A_2, \dots , measured by optical microscope (see Figure 11, p. 21). Figure 64 shows the change in puncture energy G_s measured as a function of crack depth, for different thicknesses of neoprene. The results suggest a slight increase in G_s with depth of penetration, i.e., as the crack propagates. By analogy with what has been observed with elastomer cut resistance [41], this increase may be due to friction between the needle and the surface of the crack made in the material.

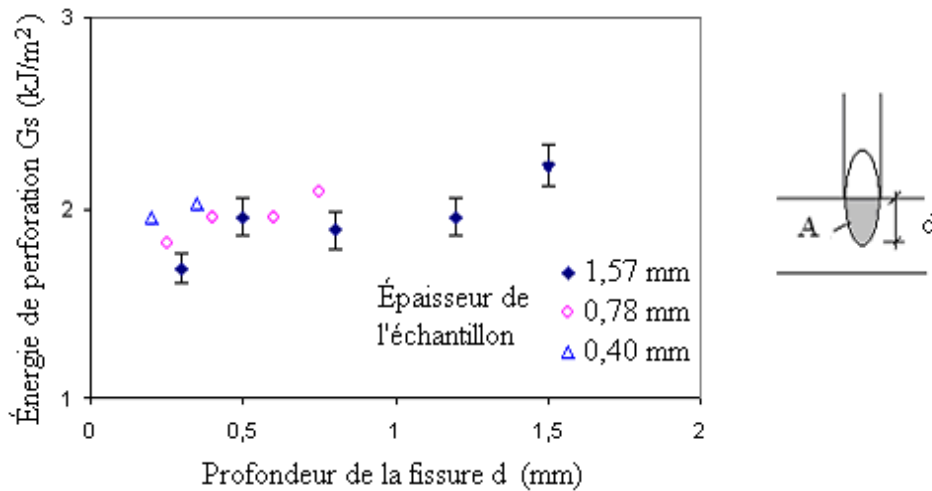


Figure 64 – Change in puncture energy as a function of crack depth, for three thicknesses of neoprene, with a 23G needle travelling at 50 mm/min

A first approximation of the fracture energy at the moment the needle initiates the crack can be obtained by extrapolating to zero penetration depth $d = 0$, puncture energies G_s shown in Figure 64. Table 12 presents the results of such an extrapolation for three gauges (diameters) of three-facet needle [28G (0.35 mm), 25G (0.50 mm) and 23G (0.65 mm)] and two thicknesses of

neoprene (0.40 and 1.6 mm). The results seem to suggest a constant value of the fracture energy at crack initiation. However, the possibility that friction may make a contribution, as has been reported for cutting [41], cannot be ignored and must be taken into consideration.

Table 12 – Needlestick fracture energy extrapolated for three gauges (diameters) of three-facet needle (23G, 25G and 28G) and two thicknesses of neoprene (0.4 and 1.6 mm), with a probe velocity of 50 mm/min, standard deviation in parentheses

Extrapolated fracture energy G_s (kJ/m ²)		Needle gauge (diameter)		
		28G (0.35 mm)	25G (0.50 mm)	23G (0.65 mm)
Neoprene thickness	0.4 mm	1.7 (0.3)	1.9 (0.4)	1.8 (0.3)
	1.6 mm	1.8 (0.3)	1.7 (0.2)	1.7 (0.4)

To determine the contribution of friction to the needlestick process and to puncture energy, a lubricant (BP™) was sprayed onto the needles before they were used as puncture probes. Table 13 shows the results in terms of extrapolated fracture energy for three gauges of three-facet needle, both with and without lubricant, and for two elastomers: 1.6 mm neoprene and 0.8 mm nitrile (samples from a nitrile glove). Use of lubricant reduced the fracture energy values, confirming the hypothesis that friction contributes to the needlestick process. However, the rise in fracture energy values as a function of needle diameter for nitrile shows that the use of lubricant does not appear to eliminate the effect of friction completely.

Table 13 – Needlestick fracture energy extrapolated for three gauges (diameters) of three-facet needle (23G, 25G and 28G), both with and without lubricant, and two elastomers (1.6 mm neoprene and 0.8 mm nitrile glove), with a probe velocity of 50 mm/min, standard deviation in parentheses

Extrapolated fracture energy G_s (kJ/m ²)		Needle gauge (diameter)		
		28G (0.35 mm)	25G (0.50 mm)	23G (0.65 mm)
Neoprene (1.6 mm)	Without lubricant	1.8 (0.3)	1.7 (0.2)	1.7 (0.4)
	With lubricant	1.6 (0.2)	1.6 (0.3)	1.5 (0.3)
Nitrile glove (0.8 mm)	Without lubricant	3.8 (0.7)	4.1 (0.6)	4.2 (0.8)
	With lubricant	3.6 (0.6)	3.7 (0.5)	4.0 (0.7)

APPENDIX C: CALCULATION OF NEEDLESTICK FRACTURE ENERGY

This appendix provides detailed information about the procedure and calculations for determining the fracture energy associated with the needlestick process, using the prestretching technique.

C.1 Principle of Approach

The setup devised to prestretch the samples is shown in the diagram in Figure 65. The sample is prestretched lengthwise, and the puncture force is applied through the thickness, i.e., perpendicular to the prestretching. As Lake and Yeoh [54,55] note, this configuration may end up producing an out-of-plane effect. However, given that the puncture forces are more than an order of magnitude weaker than the prestress values corresponding to the applied prestretching, this effect can only be minor.

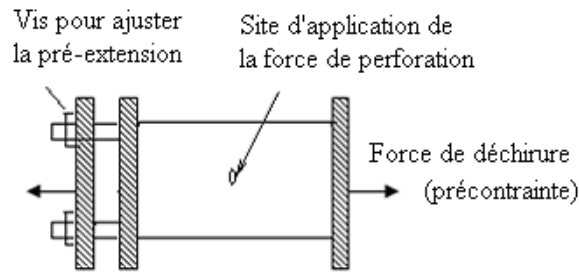


Figure 65 – Sample-holder setup devised for prestretching samples in preparation for needlesticks

Figure 66 shows how various degrees of prestretching affect the change in the needle’s puncture force as a function of its vertical displacement. While the general shape of the force-versus-displacement curve is the same, the maximum puncture force values and the probe displacement values at puncture decline as prestretch values increase. In addition, the shoulder in the right part of the curve, which is associated with the point where the crack is initiated in the material, is amplified by prestretching.

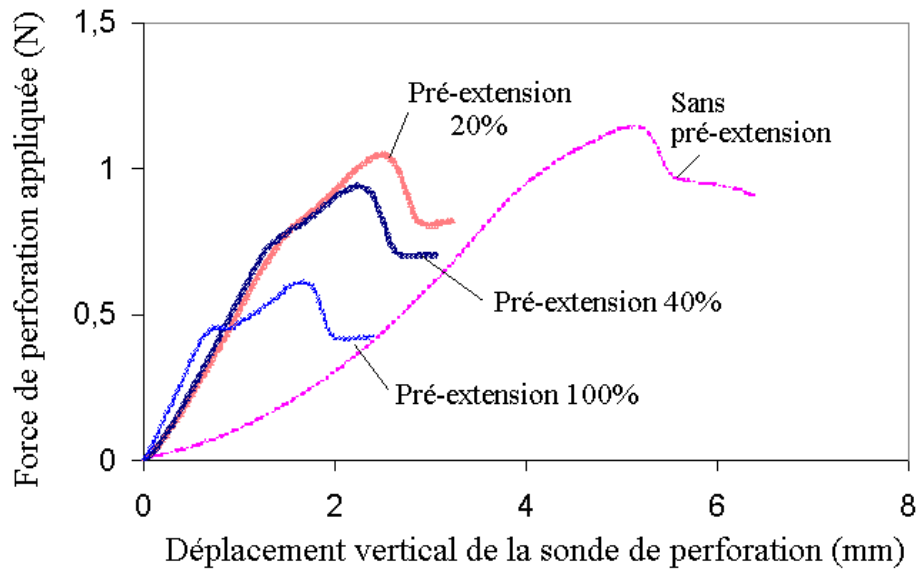


Figure 66 – Typical force-versus-displacement curves for different degrees of prestretching applied to neoprene, for 23G needles travelling at 50 mm/min

Using the technique developed in this project for calculating the fracture energy associated with punctures (described in Appendix B), the puncture energies present in the case of prestretching were calculated. Figure 67 shows the variation in the puncture energy values obtained using this technique as a function of crack depth, for different degrees of prestretching applied to a 1.6 mm sheet of neoprene punctured with three-facet 23G (0.65 mm) medical needles. The increase in puncture energy with crack depth, which was seen in samples not prestretched and which was attributed to the effect of friction between the needle and the material fracture surface (Figure 64), disappears with prestretching of more than 20%. The method used seems to eliminate the friction component in the process. However, determining needlesstick fracture energy requires knowing the energy associated with the applied prestretching. The determination of the applied prestretching is described in the next section.

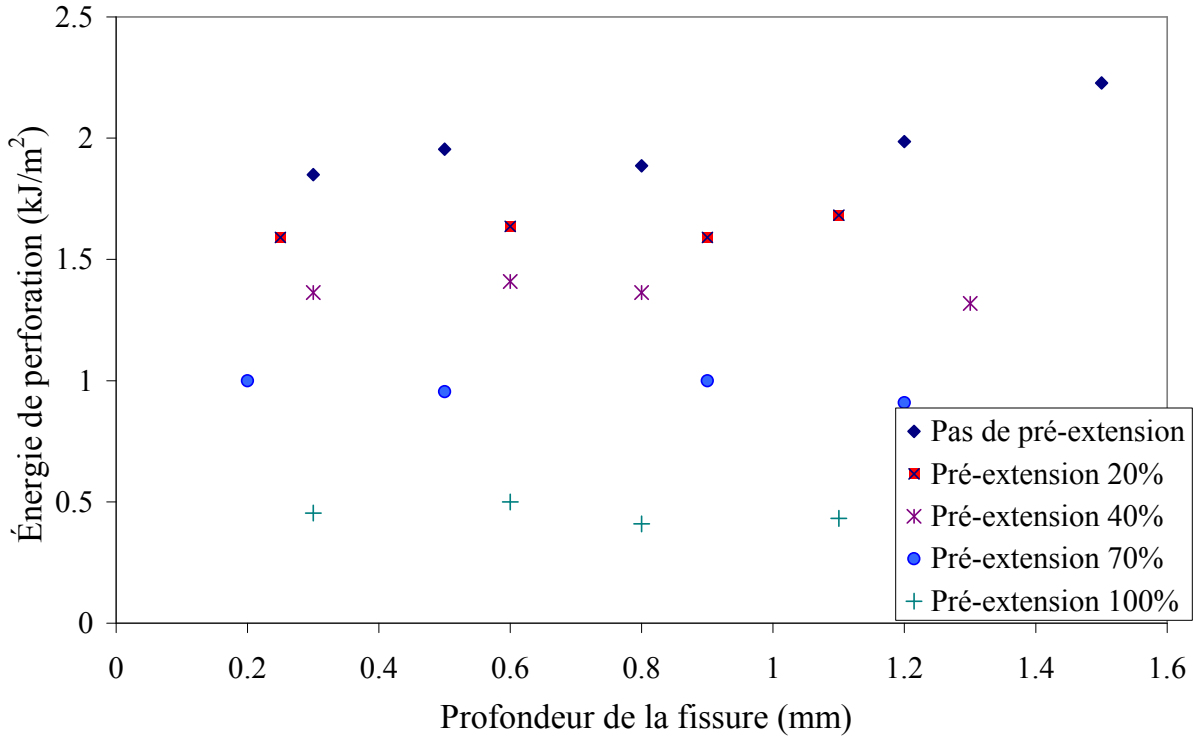


Figure 67 – Change in puncture energy as a function of crack depth, for different degrees of prestretching applied to a 1.6 mm sheet of neoprene, with 23G needles travelling at 50 mm/min

C.2 Calculation of Prestretch Energy

For the purposes of calculating the prestretch energy for the configuration shown in Figure 65, a theoretical model was developed on the basis of Rivlin and Thomas’s work on cutting [77]. They have shown that when a small cut is made in a test piece stretched in simple extension (Figure 68a), the change in total energy stored in the test piece is given by

$$W_t - W = \beta c^2 t S_e \tag{Equation 8}$$

where W_t and W are the total amounts of energy stored respectively before and after the cut is made. The quantities $2c$ and t are, respectively, the length of the cut and the thickness of the test piece measured in the unstrained state (Figure 68a). S_e is the stored energy density corresponding to the extension λ in the simple extension region, and β is a numerical factor that varies with λ .

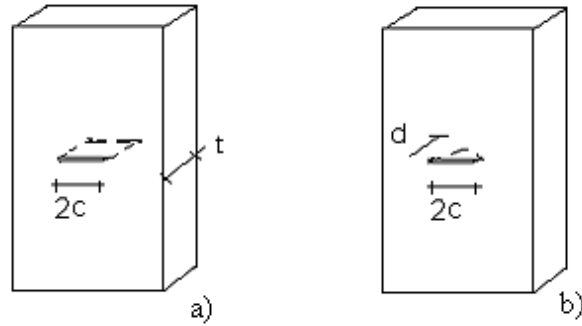


Figure 68 – Cut geometries (a) corresponding to the description of Rivlin and Thomas, (b) corresponding to needlestick

Considering the elliptical shape of the cut in the case of needlesticks, the surface of which is given by $A = \pi \cdot dc/2$ (Figure 68b) and the fact that the cut does not go all the way through the sample, Equation 8 becomes

$$W_t - W = \beta d^2 c S_e = \frac{4\beta A^2 S_e}{\pi^2 c} \quad \text{Equation 9}$$

As a result, prestretch energy T can be expressed by the following relationship:

$$T = -\left(\frac{\partial W}{\partial A}\right) = \frac{4}{\pi} \beta d S_e \quad \text{Equation 10}$$

Rivlin and Thomas [77] and Greensmith [78] have shown that the change in the value of the elastically stored energy density S_e , following the making of the cut, is minor (a few percent). Consequently, S_e can be expressed as a function of λ according to the following relationship [77]:

$$S_e = C_1 \left(\lambda^2 + \frac{2}{\lambda} - 3 \right) + C_2 \left(\frac{1}{\lambda^2} + 2\lambda - 3 \right) \quad \text{Equation 11}$$

where C_1 and C_2 are Mooney-Rivlin coefficients determined from tensile tests, and λ is the extension of the prestrained sample.

They also determined that the numerical factor β declines from a value of 3 at low extension to a value close to 2 for an extension $\lambda = 3$. The function corresponding to the numerical factor $\beta(\lambda)$ can be calculated using the method developed by Greensmith [78], which is based on measurement of the elastic properties of rubber. Based on Equation 9, β is given by the formula

$$\beta = \frac{W_t - W}{d^2 c S_e} \quad \text{Equation 12}$$

In the case of a partial precut made by a medical needle in a sample stretched in simple extension, the change in total energy of the sample is expressed by

$$W_t - W = \int_{l_0}^l (F_t - F) dl \tag{Equation 13}$$

where F_t and F are respectively the forces acting on the sample without and with a precut of length $2c$ and depth d .

The stored energy density S_e can be obtained by [77]

$$S_e = \int_1^\lambda (F_t / A_0) d\lambda \tag{Equation 14}$$

By expressing Equation 13 as a function of extension $\lambda = l/l_0$, and by combining it with Equations 12 and 14, the following formula is obtained for the function corresponding to numerical factor β :

$$\beta(\lambda) = \frac{\int_1^\lambda [l_0(F_t - F) / d^2 c] d\lambda}{\int_1^\lambda (F_t / A_0) d\lambda} \tag{Equation 15}$$

The values $[l_0(F_t - F)/d^2 c]$ and $[l_0(F_t)/A_0]$ can be read from the force-versus-displacement curves measured with and without a precut in the sample. Taking the values of the function $\beta(\lambda)$ calculated using the method described above and the Mooney-Rivlin coefficient values obtained from the tensile tests, the prestretch energy can be calculated using Equation 10. Figure 69 shows the change in prestretch energy as a function of the extension calculated for a 1.6 mm sheet of neoprene.

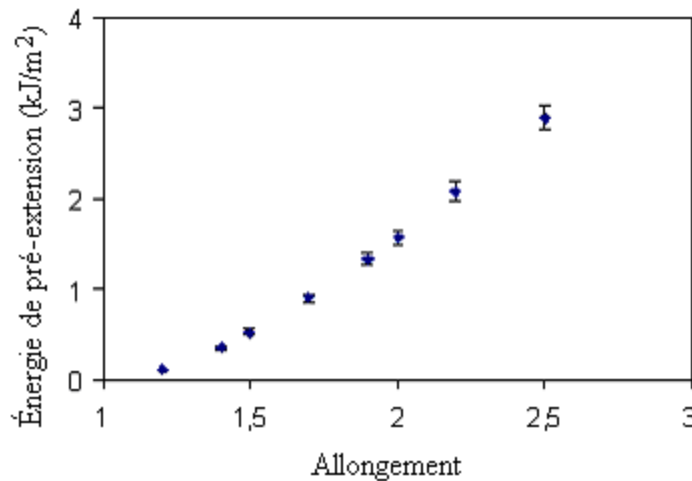


Figure 69 – Change in prestretch energy T as a function of extension, for a 1.6 mm sheet of neoprene ($C_1 = 172$ kPa, $C_2 = 443$ kPa), calculated using Equation 10

To test the accuracy of the calculation of prestretch energy T described above, an alternative method was developed by applying the principles of linear elastic fracture mechanics (LEFM) to rubber while taking into account its non-linear stress-strain behaviour. More specifically, the

technique involves (1) replacing the stored energy density $\sigma^2/2E$ in LEFM with $S_e(\lambda)$ given by Equation 11, and (2) using the expressions $c = c_0/\lambda^{1/2}$ and $d = d_0/\lambda^{1/2}$ respectively for the length and depth of the crack (c_0 and d_0 corresponding to the unstrained state) in order to take into account the narrowing of the crack with extension λ .

For an elliptical crack in the case of rubber and for configuration $d > c$, the stress intensity factor K in LEFM is given by [76]

$$K = 1.12 \frac{\sigma}{\Phi} \sqrt{\pi d^2 / c} \quad \text{Equation 16}$$

with Φ a numerical factor given by the following relationship:

$$\Phi = \frac{3\pi}{8} + \frac{\pi d^2}{8 c^2} \quad \text{Equation 17}$$

The expression for the prestretch energy provided by LEFM, in the case of rubber, is therefore

$$T = \frac{K^2}{E} = Y \frac{\sigma^2}{E} \frac{d^2}{c} = \frac{2Y S_e}{\lambda^{1/2}} \frac{d^2}{c} \quad \text{Equation 18}$$

with Y a geometric factor ($Y = 1.254\pi/\Phi^2$) [76].

The results obtained for prestretch energy as a function of the extension applied by the prestretch using the two methods—that is, the formalism of Rivlin and Thomas (Equation 10) and the extension of LEFM principles to rubber (Equation 18)—are compared in Figure 70 for a 1.6 mm thick sheet of neoprene. It can be seen that, even if the calculation in Equation 18 is relatively simple, it shows good agreement with the more complex method based on the formalism of Rivlin and Thomas.

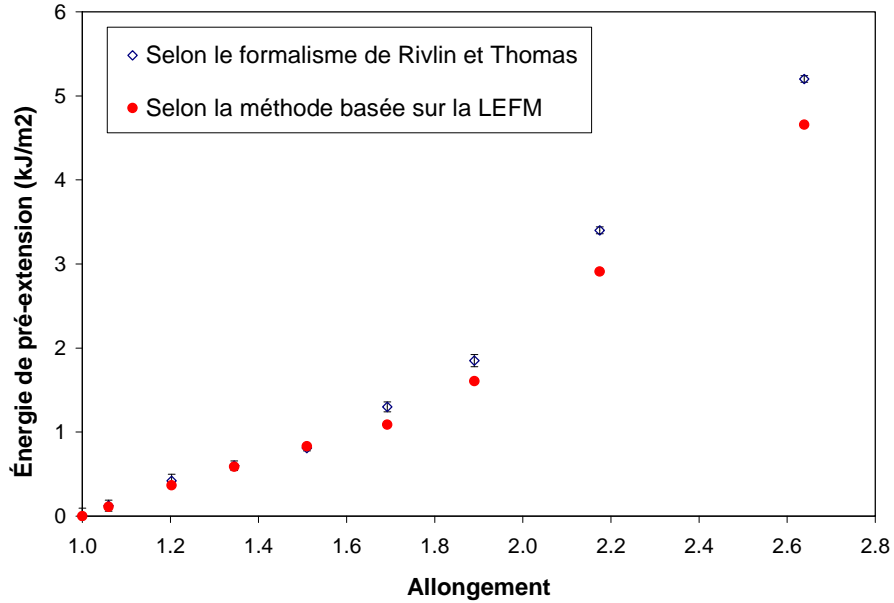


Figure 70 – Comparison of calculations of prestretch energy using Equation 10 (method based on formalism of Rivlin and Thomas) and Equation 18 (extension of LEFM to rubber), for a 1.6 mm sheet of neoprene

C.3 Needlestick Fracture Energy

Using the methods described in Appendix B and Section C.2 to calculate the prestretch energy corresponding to the different applied prestretch values, the Figure 67 data for neoprene have been expressed in terms of change in puncture energy as a function of prestretch energy (Figure 71). A linear section can be seen at low values of T , corresponding to a constant value of total energy G consistent with Equation 1. In contrast, at higher values of prestretch energy T , the puncture only initiates the crack, which then propagates solely from the effect of the prestretch energy. In this case, the contribution of the puncture is marginal. These results indicate that the same principle used by Lake and Yeoh in the case of cuts also applies to needlesticks. As a result, needlestick fracture energy can be determined by extrapolating the linear part of the curve in Figure 71 at a prestretch energy T of zero.

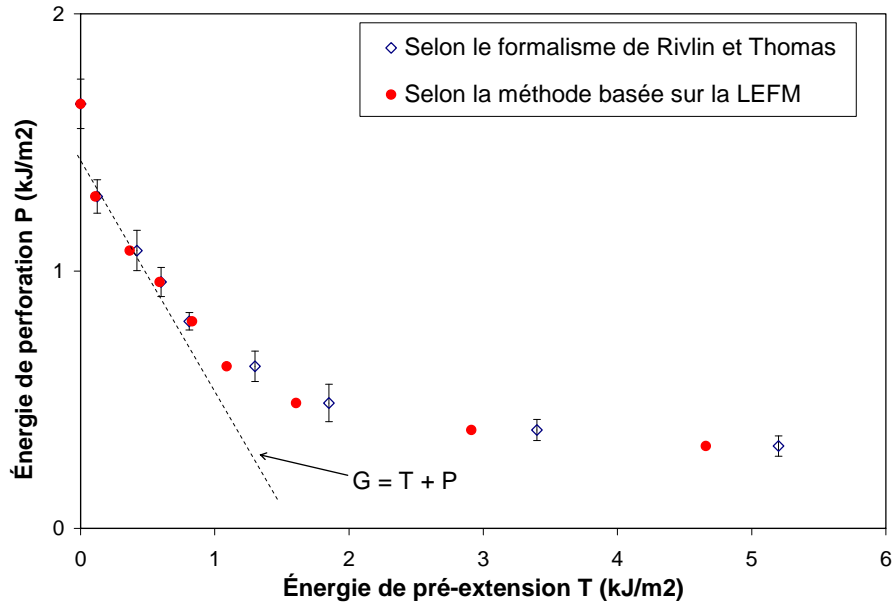


Figure 71 – Change in puncture energy as a function of prestretch energy calculated using Equation 10 (method based on formalism of Rivlin and Thomas) and Equation 18 (extension of LEFM to rubber), for a 1.6 mm sheet of neoprene punctured by 23G medical needles travelling at 50 mm/min

To verify that all friction was eliminated through the use of the prestretch technique, tests were conducted by combining prestretching with the application of a lubricant to the needle surface. Figure 72 shows the change in puncture energy as a function of prestretch energy in the case of nitrile, with and without application of lubricant to the needle. On the linear section of the curve and for high prestretch energy values, the experimental points are virtually superimposed on one another, which indicates that the lubricant does not reduce friction any further. In contrast, where prestretch energy is zero or very low, a difference between experimental results can be seen. The difference is due to the fact that, in these cases, the prestretch is not sufficient to eliminate all effects of friction between the needle and the fracture surface. This result shows that the prestretch technique totally eliminated the contribution of friction when determining needlestick fracture energy.

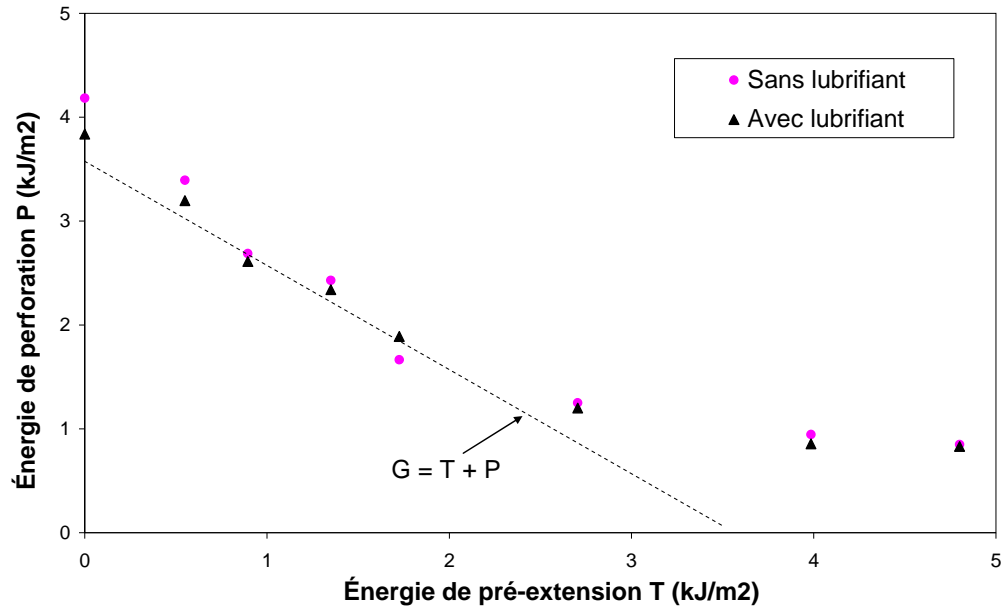


Figure 72 – Change in puncture energy as a function of prestretch energy, for 0.8 mm nitrile punctured by 23G medical needles, with and without lubricant, travelling at 50 mm/min

APPENDIX D: GLOVE TEST RESULTS

Table 14 – Results of testing of protective glove needlestick resistance, using method described in Section 2.2.6

#	Manufacturer	Ref. No.	Number of tests	Max. puncture force (N)	SD (N)	Coefficient of variation (%)
1	Ansell	11-500	6	0.40	0.07	18
2	Ansell	11-501	7	0.46	0.10	22
3	Ansell	11-627	7	0.83	0.20	24
4	Ansell	70-982	7	1.79	0.37	21
5	Atlas	620	4	0.64	0.16	26
6	Atlas	KV300	5	0.77	0.35	45
7	Atlas	KV350	5	0.63	0.23	36
8	Best	55	7	0.55	0.06	11
9	Best	660	7	1.34	0.59	44
10	Best	2912	7	0.82	0.09	12
11	Best	4560	7	0.89	0.22	24
12	Best	4811	7	0.65	0.22	34
13	Best	4900	8	0.77	0.58	76
14	Best	5900	7	0.50	0.09	18
15	Best	65NFW	7	1.38	0.25	18
16	Best	66NFW	7	1.08	0.17	16
17	Best	6781R	7	1.52	0.34	23
18	Best	68NFW	7	1.68	0.18	11
19	Best	95NFW	7	2.27	0.31	14
20	Hakson	3000C	7	1.48	0.13	9
21	Hakson	9000C	7	0.78	0.08	10
22	Hakson	9000G	7	0.97	0.14	15
23	Hakson	NPG150	7	0.58	0.16	27
24	Hatch	PPG1	7	0.88	0.14	16
25	Hatch	SB4000	10	0.96	0.50	51
26	Hatch	SGK100	10	0.92	0.26	29
27	HexArmor	4042	11	6.86	1.74	25
28	HexArmor	6044	10	8.41	2.30	27
29	HexArmor	7080	10	9.50	2.29	24
30	HexArmor	8030	10	6.29	3.38	54
31	HexArmor	9005	10	4.00	1.83	46
32	HexArmor	9006	5	5.38	1.47	27
33	HexArmor	9014	10	11.04	2.37	21
34	HexArmor	4041	10	8.97	2.37	26
35	Marigold Industrial	VHP Plus	5	1.22	0.18	15
36	Marigold Industrial	PGK10	7	0.82	0.37	45
37	Masley	Cugni-TC	7	1.25	0.26	21
38	Masley	F1SG	7	1.37	0.14	10

#	Manufacturer	Ref. No.	Number of tests	Max. puncture force (N)	SD (N)	Coefficient of variation (%)
39	Masley	ICWG	7	1.86	0.41	22
40	Masley	UA1	7	1.53	0.21	14
41	North	62/7506	7	1.58	0.26	17
42	North	LA258	7	0.71	0.14	20
43	North	NFK13	8	1.33	0.35	26
44	North	NFK14	7	0.46	0.12	25
45	North	NK803	7	1.00	0.22	22
46	North	T-201	7	1.18	0.40	34
47	North	T431	7	1.12	0.39	34
48	North	T65FWG	7	0.87	0.26	29
49	Superior	66BRPU	10	3.40	0.38	11
50	Superior	MXBD	10	2.08	0.34	17
51	Superior	MXBL	10	1.82	0.24	13
52	Superior	MXSF	10	6.98	4.27	61
53	Superior	SKLPSMT	10	4.53	0.65	14
54	Warwick Mills	001	10	1.05	0.21	20
55	Warwick Mills	TUS-002	10	8.44	2.29	27
56	Warwick Mills	TWCS-003	10	9.70	2.37	24
57	Warwick Mills	TWCS-006	12	4.21	0.64	15
58	Warwick Mills	007	10	1.10	0.20	18

Table 15 – Results of testing of protective glove puncture resistance, using method described in Section 2.3

#	Manufacturer	Ref. No.	Number of tests	Max. puncture force (N)	SD (N)	Coefficient of variation (%)
1	Ansell	11-500	10	11.11	2.11	19
2	Ansell	11-501	10	8.79	1.62	18
3	Ansell	11-627	10	23.35	1.81	8
4	Ansell	70-982	10	97.45	8.63	9
5	Atlas	620	5	19.44	2.48	13
6	Atlas	KV300	5	57.15	5.53	10
7	Atlas	KV350	5	52.06	9.39	18
8	Best	55	10	10.20	0.77	8
9	Best	660	10	31.19	3.30	11
10	Best	2912	10	26.42	3.59	14
11	Best	4560	10	44.78	8.41	19
12	Best	4811	10	43.78	7.09	16
13	Best	4900	10	61.72	8.63	14
14	Best	5900	10	21.51	3.73	17
15	Best	65NFW	10	58.92	2.62	4
16	Best	66NFW	10	43.32	3.36	8
17	Best	6781R	10	23.14	2.28	10
18	Best	68NFW	10	48.92	4.49	9
19	Best	95NFW	10	42.26	5.70	13
20	Hakson	3000C	10	21.89	4.71	21
21	Hakson	9000C	10	27.03	11.96	44
22	Hakson	9000G	10	37.03	12.55	34
23	Hakson	NPG150	10	10.61	2.11	20
24	Hatch	PPG1	10	20.59	2.79	14
25	Hatch	SB4000	11	24.57	7.64	31
26	Hatch	SGK100	11	14.63	2.44	17
27	HexArmor	4042	10	53.66	3.87	7
28	HexArmor	6044	10	50.07	3.92	8
29	HexArmor	7080	10	71.18	5.49	8
30	HexArmor	8030	10	146.68	25.23	17
31	HexArmor	9005	10	37.65	3.66	10
32	HexArmor	9006	10	64.50	8.75	14
33	HexArmor	9014	10	107.12	17.48	16
34	HexArmor	4041	10	45.27	4.83	11
35	Marigold Industrial	VHP Plus	10	93.19	5.08	5
36	Marigold Industrial	PGK10	10	32.67	4.70	14
37	Masley	Cugni-TC	10	45.92	6.45	14
38	Masley	F1SG	9	52.43	5.98	11
39	Masley	ICWG	7	80.31	3.78	5
40	Masley	UA1	10	30.12	2.63	9

#	Manufacturer	Ref. No.	Number of tests	Max. puncture force (N)	SD (N)	Coefficient of variation (%)
41	North	62/7506	10	78.40	43.50	55
42	North	LA258	10	47.13	2.09	4
43	North	NFK13	10	95.34	21.12	22
44	North	NFK14	10	19.39	2.02	10
45	North	NK803	10	20.17	2.79	14
46	North	T-201	11	19.79	2.56	13
47	North	T431	10	22.71	2.43	11
48	North	T65FWG	10	29.04	4.54	16
49	Superior	66BRPU	10	212.18	9.02	4
50	Superior	MXBD	12	77.51	33.38	43
51	Superior	MXBL	10	145.48	11.61	8
52	Superior	MXSF	10	132.19	11.98	9
53	Superior	SKLPSMT	10	22.71	1.66	7
54	Warwick Mills	001	10	40.31	14.26	35
55	Warwick Mills	TUS-002	10	54.69	4.79	9
56	Warwick Mills	TWCS-003	10	52.85	3.92	7
57	Warwick Mills	TWCS-006	10	70.76	30.83	44
58	Warwick Mills	007	10	44.99	17.98	40

Table 16 – Results of testing of protective glove cut resistance, using method described in Section 2.4

#	Manufacturer	Ref. No.	Cutting force (g)	R ²
27	HexArmor	4042	3,852	0.71
28	HexArmor	6044	6,162	0.47
29	HexArmor	7080	8,073	0.54
30	HexArmor	8030	5,025	0.77
31	HexArmor	9005	2,066	0.48
33	HexArmor	9014	8,260	0.92
34	HexArmor	4041	4,942	0.78
49	Superior	66BRPU	1,122	0.85
53	Superior	SKLPSMT	10,793	0.54
55	Warwick Mills	TUS-002	2,717	0.64
56	Warwick Mills	TWCS-003	1,908	0.55
57	Warwick Mills	TWCS-006	800	0.52